Modified virus as a vaccine against EBV infection

2018

Dwain George van Zyl

Dissertation
submitted to the
Combined Faculties for Natural Sciences and for Mathematics
of the Ruperto-Carola University of Heidelberg, Germany
for the degree of
Doctor of Natural Sciences

presented by

Dwain George van Zyl, M.Sc.

Born in: Kempton Park, South Africa

Oral Examination:_____

Title:

Modified virus as a vaccine against EBV infection

Referees: Prof. Dr.Dr. Henri-Jacques Delecluse
Prof. Dr. Martin Müller

“Dancing in all its forms cannot be excluded from the curriculum of all noble education; dancing with the feet, with ideas, with words, and, need I add that one must also be able to dance with the pen?”
- **Friedrich Nietzsche**, *Twilight of the Idols*

Corrigendum

Dwain George van Zyl:
Modified virus as a vaccine against EBV infection
PhD Thesis, Ruperto-Carola University of Heidelberg, 2018

Last updated: November, 5th 2018.

Acknowledgements

This section has been modified.

Chapter 3: Results

The Figure 3:20 (Page 63) contains errors. The corrected figure is shown below.

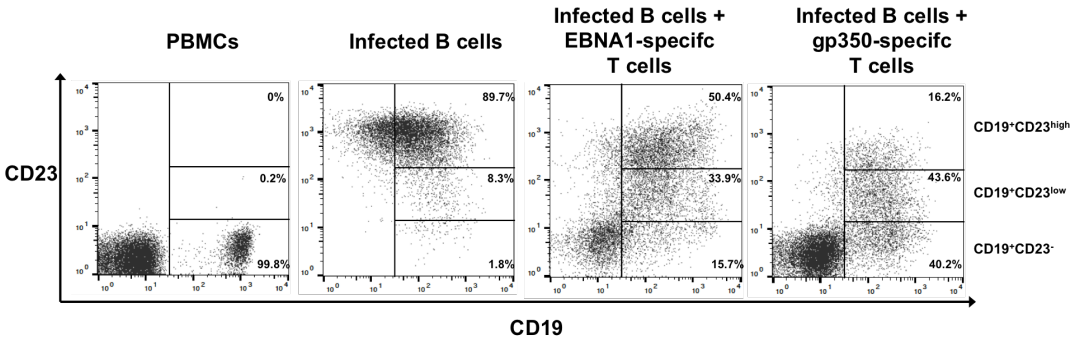

Table of Contents

Summary

The Epstein-Barr virus (EBV) is a γ-herpesvirus that establishes lifelong infection in the majority of the human population. Whilst EBV infection is asymptomatic in most cases, the global disease burden of EBV is substantial. EBV is the primary cause of infectious mononucleosis and approximately 200,000 cases of EBV-associated malignancies are annually diagnosed. EBV has multifaceted life cycle that comprises lytic replication and latency, with the establishment of latency enabling lifelong EBV carriage. The majority of EBV vaccine candidates have previously focused on the major glycoprotein gp350. However, the interrogation of a gp350 vaccine in a phase II clinical trial showed that it was unable to prevent EBV infection. Our laboratory has recently developed a vaccine candidate in the form of defective EBV particles. These defective particles lack viral DNA, are non-infectious and are composed of several dozen EBV lytic proteins. In the present work, the antigenic spectrum of defective EBV particles was enlarged to include immunodominant latent proteins. The introduction of latent proteins into the defective particles enabled the stimulation of several lytic protein- and latent protein-specific $CD4^+$ T cells. Polyclonal T cells specific for the modified particles were shown to be far superior to gp350-specific T cells at controlling EBV-infected B cells *ex vivo*. Furthermore, the modified particles afforded significant protection against EBV-infection in humanised mice. This suggests that EBV vaccines can be enhanced through the inclusion of additional antigens. By incorporating the most immunodominant EBV antigens into defective particles, it would prime the immune system against EBV antigens that are expressed at all stages of viral infection and in all EBV-associated malignancies. Such a multipronged approach is likely increase the possibility of achieving sterile immunity after prophylactic vaccination.

Zusammenfasung

Das Epstein-Barr-Virus (EBV) ist ein Gammaherpesvirus, mit dem die Mehrheit der Bevölkerung latent infiziert ist. Obwohl die EBV Infektion in den meisten Fällen asymptomatisch verläuft ist die globale Gesamtbelastung durch das Virus erheblich. Durch die Erstinfektion mit EBV wird das Krankheitsbild der infektiösen Mononukleose hervorgerufen. Darüber hinaus verursacht das Virus 200000 EBV-assoziierte Krebsfälle jährlich. Der Lebenszyklus von EBV ist facettenreich und umfasst die lytische Vermehrung und die Latenz, welche zur Ausbildung einer lebenslangen latenten Infektion führt. Mehrheitlich konzentrierten sich Vakzinierungen bisher auf das Glykoprotein gp350. Phase II Studien zeigten jedoch, dass eine Vakzinierung gegen dieses Protein nicht gegen eine EBV Infektion schützen kann. In unserem Labor wurde ein Vakzinekanditat entwickelt, der auf defekten Viruspartikeln beruht. Diese defekten Viruspartikel tragen keine virale DNA mehr und sind nicht infektiös, tragen jedoch einige duzend lytischer Proteine. In der dargelegten Arbeit wurde das virale Proteinspektrum um immundominante latente Proteine erweitert. Das Einführen dieser latenten Proteine in die defekten EBV Partikel ermöglichte die Stimulation von spezifisch gegen diese Proteine gerichteten CD4+ T Zellen. Die Kontrolle EBV infizierter B Zellen ex vivo war durch polyklonale T Zellen, die gegen die modifizierten Partikel gerichtet waren, deutlich den herkömmlichen gp350 spezifischen T Zellen überlegen. Darüber hinaus erzielten die modifizierten Partikel signifikanten Schutz gegen eine EBV-Infektion im Modell der humanisierten Maus. Die Ergebnisse lassen darauf schließen, dass die Vakzinierung gegen EBV durch die Integration latenter Proteine deutlich verbessert werden kann. Durch die Integration der immunodominanten EBV Antigene kann eine Immunantwort hervorgerufen werden, die gegen EBV Proteine gerichtet ist, die sich in jedem Stadium der Infektion sowie EBV-assoziierten Malignomen zu finden ist. Dieser Vakzinierungsansatz erhöht die Wahrscheinlichkeit eine sterile Immunität gegen EBV nach Impfung zu entwickeln.

Acknowledgements

I would like to thank my supervisor Prof. Dr. Dr. Henri-Jacques Delecluse for giving me the opportunity to pursue a PhD in his laboratory. His support over the last four years has been invaluable. He always made himself promptly available upon request, a true luxury during one's PhD.

Next, I would to thank Prof. Dr. Martin Müller and Prof. Dr. Josef Mautner for being part of my Thesis Advisory Committee. Their advice during the first three years of my PhD certainly helped me to focus on the most important scientific questions.

I additionally have to thank Prof. Dr. Josef Mautner for the countless times he supplied me with important reagents and T-cell clones. He also taught me to culture T cells, which was an enjoyable and fruitful experience.

I would like to thank Angelika Schmidt-Zitouni, the administrative superwoman of the F100 group. Her supportive and good-hearted nature helped me remain positive on even the toughest days. Additionally, I also have to thank all the members of the F100 laboratory, past and present, which helped me along this demanding journey. I would certainly not have made it without their scientific and moral support. They enabled me to enjoy this journey, not simply survive it. A special mention has to be made to Viktor Schneidt who walked this journey alongside me from the day one.

Next, I would like to thank my friends. They have been my 'substitute family' during my time in Heidelberg. My interactions with my friends enabled me to learn from life while I was learning in the lab. I have certainly changed a lot over the last few years due to their influence.

A special thank you has to be made to the DKFZ for being such an awesome organisation. By being under its umbrella, and that of the Helmholtz International Graduate School for Cancer Research, it has placed many opportunities at my fingertips. As a foreign student, I especially have to mention Mrs. Heike Langlotz. The service she consistently provided was exceptional and always reminded me I was at a world-class institution. I am proud to be a part of such an amazing organisation, filled with so many great people.

I would also like to thank the German Cancer Aid (Deutsche Krebshilfe) for their financial support during my PhD.

Lastly, I have to thank my family and loved ones. Their unwavering support and love is the greatest consolation in this life. I dedicate this thesis to them.

List of Abbreviations

aa	amino acid
BAC	bacterial artificial chromosome
BART	BamHI fragment A rightward transcript
BCR	B-cell receptor
BL	Burkitt lymphoma
CD	cluster of differentiation
CDS	coding DNA sequence
cHL	classical Hodgkin's lymphoma
Co-IP	Co-immunoprecipitation
Cp	C promoter
DNA	Deoxyribonucleic acid
ds	double-stranded
E	early lytic gene
EBER1	Epstein-Barr virus-encoded small RNA 1
EBER2	Epstein-Barr virus-encoded small RNA 2
eBL	endemic Burkitt's lymphoma
EBNA	Epstein-Barr nuclear antigen
EBV	Epstein-Barr Virus
EM	Electron microscopy
FBS	fetal bovine serum
fwd	forward
GC	germinal center
HCMV	human cytomegalovirus
HCV	hepatitis C virus
HHV	Human herpesvirus
HL	Hodgkin's lymphoma
HRS	Hodgkin and Reed/Sternberg
HSP	heat shock protein
HST	hematopoietic stem cell transplant (HST
IE	Immediate Early lytic gene
IM	Infectious mononucleosis
KSHV	Kaposi's sarcoma-associated herpesvirus
L	late lytic gene
LCL	lymphblastoid cell lines
LCV	LymphocryptoviruS
LD	lymphocyte depletion
LMP	latent membrane protein
LP	lymphocyte predominance
LTP	Large tegument protein
MC	mixed cellularity

MCP	major capsid protein
MHV	Murine gammaherpesvirus
MTP	Major tegument protein
NPC	nasopharyngeal carcinoma
NS	nodular sclerosis
nt	nucleotide
ORF	open reading frame
OriLyt	origin of lytic replication
OriP	origin of plasmid replication
PBMC	peripheral blood mononuclear cells
PTLD	Post-transplant lymphoproliferative disorder
RGD	Arginine-glycine-aspartate motif
sBL	sporadic Burkitt lymphoma
SCP	Small capsid protein
SOT	solid organ transplant
TNF	Tumor Necrosis factor
TR	terminal repeat
ZRE	BZLF1 responsive elements

1. Introduction

1.1. The Epstein-Barr Virus

The Epstein-Barr Virus (EBV) is a member of the *Herpesviridae*, a family known to possess a large DNA genome. This diverse family of viruses infect many mammals and vertebrates and, rarely, invertebrates [1-3]. Despite the genetic variation within the *Herpesviridae*, it is clear that herpesviruses from mammals and birds are more closely related; i.e. there is clear evidence that they share a common ancestor [1].

The *Herpesviridae* were initially divided into the *Alpha-*, *Beta-* and *Gammaherpesvirinae* following observations made about their biological properties. However, this subfamily classification has since been refined through the use of molecular phylogenetics [4]. EBV, also known as human herpes virus 4, has been placed into the gammaherpesvirus subfamily. The gammaherpesviruses, which branched off from the other herpesviruses around 200 million years ago, are typified by their lymphotropism and neoplastic associations [4]. Furthermore, EBV is the type species of the gamma-1 herpesviruses, a genus that is also know as the Lymphocrytoviruses (LCVs). Members of this genus are known to exclusively infect primates and EBV is the only member of this genus that infects humans [5]. In humans, EBV is transmitted orally and preferentially infects B cells. EBV can also infect epithelial cells, but it is the colonisation of the B cell pool that enables EBV to be acquired as a lifelong infection [6].

1.1.1. The structure of EBV virions

One of the defining features of the herpesviruses is their structure (Fig. 1.1). Just like other herpesviruses, EBV is rather large in size (~180 nm) and complex in structure [3, 7]. EBV virions contain more than 40 different proteins [8]. At the core of EBV virions is a highly ordered T=16 icosahedral capsid, containing a linear dsDNA genome (~170 kb). Immediately

outside of the capsid is a protein matrix that has been termed the tegument. The outermost structure of the EBV virions is the glycoprotein-rich envelope [2].

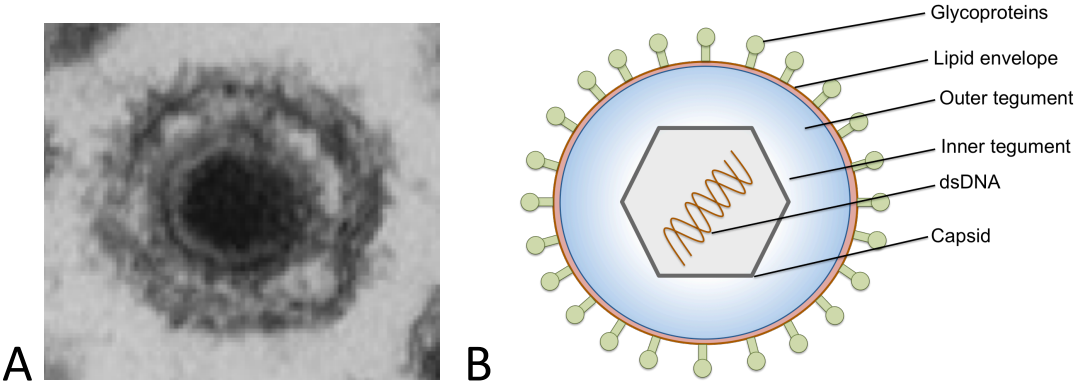

Figure 1.1: The structure of EBV. An electron micrograph (left) and a schematic representation (right) of EBV virions are shown. The electron micrograph was taken of B95-8 EBV particles pelleted from the supernatant of induced producer cells. The schematic representation of an EBV virion highlights the classic structural features of herpesviruses. The linear dsDNA genome is packaged within an icosahedral capsid. Beyond the capsid is a protein matrix that is divided into the inner and outer tegument. The tegument is enclosed with a lipid bilayer rich in glycoproteins. The electron micrograph was taken from Pavlova *et al.*, 2013 [9].

1.1.1.1. The EBV capsid

The icosahedral capsid of herpesviruses is formed through the assembly of 150 hexamers and 12 pentamers; i.e. 162 capsomeres in total are required [10]. The capsomeres, which are composed of the major capsid protein (MCP) (BcLF1), are linked to each other through a heterotrimeric triplex structure. The triplex structure is composed of triplex protein α (BORF1) and a homodimer of triplex protein β (BDLF1) [10, 11]. The structural details of EBV icosahedral facets can be seen in Figure 1.2. In total, there are 320 triplex structures per capsid and one triplex structure is found at the interface of three capsomeres. Furthermore, there is the small capsid protein (SCP), encoded by BFRF3, which interacts with the MCP. The role of the SCP has been shown to be indispensible for gammaherpesvirus capsid assembly, but this is not the case for alphaherpesviruses [11, 12]. In the case of gammaherpesviruses SCP has been suggested to crosslink neighbouring MCPs to ensure capsid stabilisation [12].

Lastly, there are the scaffold protein (BdRF1) and maturation protease (BVRF2) that are also required for capsid assembly. However, these proteins are more likely to play a role in assembly and maturation of the icosahedral capsid rather than being integral structural units [8, 11].

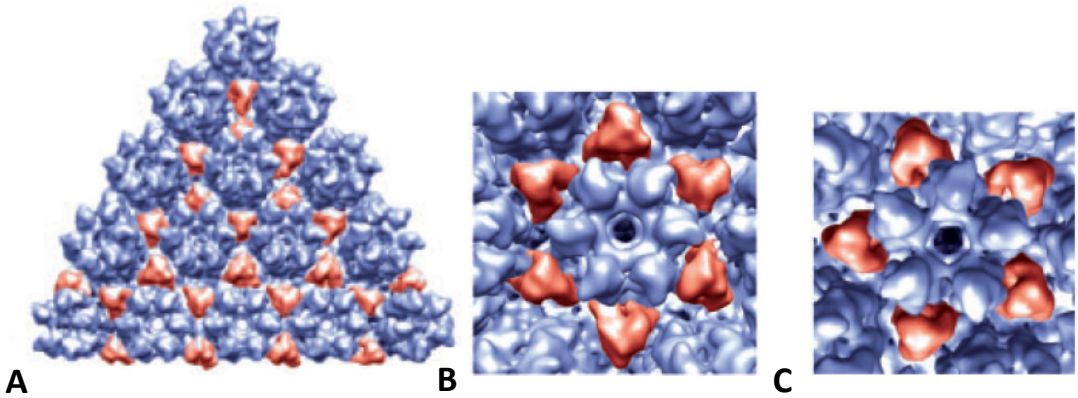

Figure 1.2: Structural details of EBV icosahedral capsids. The 3D-structure was derived from cryo-EM images that were taken of sucrose gradient-purified EBV capsids. (A) A single EBV facet showing hexamers (blue) and pentamers (blue) and triplex structures (red). Pentamers are found exclusively at the vertices of facets. (B) The view of a hexamer (blue) interacting with six different triplex structures (red). (C) The view of a pentamer (blue) interacting with interacting with 5 different triplex structures (red). The figure was taken from Germi *et al.*, 2012 [10].

1.1.1.2. The EBV Tegument

The tegument is the protein layer that is sandwiched between the capsid and viral envelope. The tegument of mature virions can be between 15 nm and 50 nm thick and is divided into the inner and outer tegument. The inner tegument proteins engage in strong interactions with the capsid, while those in the outer tegument associate loosely with the viral envelope [13]. The tegument was initially thought to be an amorphous protein layer; however, recent studies have shown the tegument of herpesviruses to be an organised structure [14-17]. Two of these studies involved the Human Herpesvirus-8 (HHV-8) and Murine herpesvirus-68 (MHV-68), both gammaherpesviruses and close relatives of EBV [16, 18]. These studies allow inferences to be made with regard to the organisation of EBV tegument. This is important as

gammaherpesviruses encode tegument proteins that are not found in other herpesvirus subfamilies [19].

The tegument of HHV-8, also known as Kaposi's sarcoma-associated herpesvirus (KSHV), has been studied through cryo-Electron Microscopy [18]. This revealed that ORF19 and ORF32, homologues of EBV BVRF1 and BGLF1 respectively, form a complex that simultaneously interacts with capsid pentamers and nearby triplex structures. This interaction is thought to act as an anchoring site to which other tegument proteins can attach (Fig. 1.3). In another study, the large tegument protein (LTP) of HHV-8 was also found to interact with the capsid [16]. Through the use of yeast two-hybrid and coimmunoprecipitation (co-IP) assays the LTP, a homologue of EBV BPLF1, was shown to interact with the MCP, triplex α and triplex β proteins. Furthermore, the LTP was also found to interact with itself and with a large variety of tegument proteins (e.g. ORF33/BGLF2, ORF45/BKRF4 ORF63/BOLF1, and ORF75/BNRF1) and membrane proteins (e.g. gM, gB and gH) (Fig. 1.3). This finding suggests that the LTP could act as a scaffold for other tegument proteins. Furthermore, the ability of the LTP to interact with the capsid and tegument suggest that it could play an important role in capsid positioning prior to envelopment [16, 20].

BLRF2 is another tegument protein that has been found to interact strongly with the capsid. Hence, BLRF2 has also been implicated as an anchor for other tegument proteins. This reasoning has been strengthened by the observation that BLRF1/ORF52 from EBV, KSHV and MHV-68 interacts with 13 viral proteins [19]. One of these interaction partners is the major tegument protein (MTP) [21] (Fig. 1.3). The EBV MTP, encoded by BNRF1, has been found to play an important role during infection. Specifically, BNRF1 has been found to be required for the transfer of virions from the endosomal compartment to the nucleus [22]. In this manner, capsid-binding tegument proteins enable virion cargo to be delivered to newly infected cells [19].

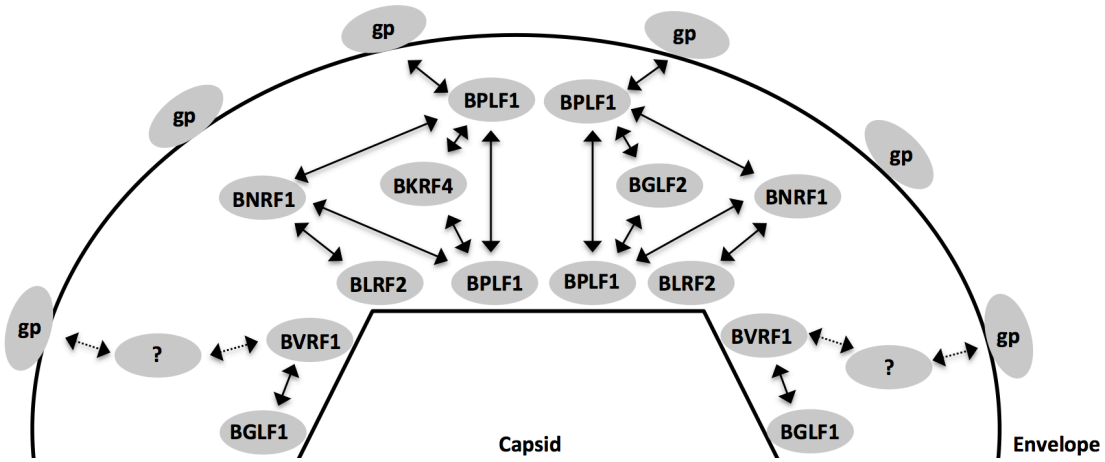

Figure 1.3: An overview of EBV tegument organisation. Confirmed interactions (solid arrows) and hypothetical interactions (dotted arrow) are indicated. Unknown infraction partners have been signified with a question mark (?). Whilst specific envelope glycoproteins (gp) are not exemplified, BPLF1 is known to interact with gB, gM and gH.

Tegument proteins that interact strongly with the capsid have also been shown to be important for viral egress. BLRF2/ORF52 enables the transport of mature virions from the nucleus to the extracellular space [23]. An ORF52 deletion mutant of MHV68 was shown to produce mature capsids that contained some inner tegument and lacked outer tegument. These capsids failed to form mature virions and accumulated within the cytoplasm [24]. Another tegument protein, ORF45, a homologue of EBV BKRF4, has also been implicated in the transport of capsid during viral lytic replication [25]. ORF45 was found to interact with KIF3A, a subunit of kinesin-2. The ORF45-KIF3A interaction enables the transport of capsids along microtubules and mediates viral egress.

Lastly, it is important to note that host cellular proteins (e.g. actin, cofilin, tubulin and HSP70) have also been found to be abundant components of the EBV tegument [8]. The occurrence of host protein within enveloped viruses have been well documented in recent years [26]. However, the exact role of these host proteins, if any, has not been well defined. In the case of EBV, it is hypothesised that host proteins are accumulated during morphogenesis, and that they potentially play a role in virion stability and/or ingress [8].

1.1.1.3. The EBV Envelope

EBV encodes an impressively high number of envelope glycoproteins. In total, 11 glycoproteins have been found to associate with the viral envelope [8]. Glycoproteins were amongst the first proteins to be studied after EBV was discovered in 1964. The envelope glycoproteins of EBV can be divided into two groups, those that are involved in the assembly of virions and those that are responsible for virus entry and spread [27].

The most abundant glycoprotein in the EBV envelope is gp350/gp220 (BLLF1). BLLF1 encodes two alternatively spliced forms that have a mass of approximately 350 and 220 kDa [28]. It is known that gp350 is a 907 residue glycoprotein that has a short cytoplasmic tail (18 aa) at its C-terminus and a large extracellular ectodomain (860 aa) at its N-terminus. The ligand-binding domain of gp350 has been shown to comprise the first 470 aa [29]. The principle function of gp350 is the attachment of EBV to B cells. The classical ligand partner of gp350 on B cells is CD21. It is known that gp350 binds with high affinity (10^{-8}M) to a protein surface within short consensus repeats (SCR) 1 and 2 of CD21 [28]. Additionally, gp350 has been shown to interact with CD35 in B cells [30-32]. When it comes to the attachment of EBV to epithelial cells it is known that gp350 does not play a role. EBV has recently been shown to interact with Ephrin receptor A (EphA2) expressed on epithelial cells through the use of gH/gL [33, 34]. Furthermore, the glycoprotein BMRF2 has been hypothesised to interact with integrins expressed on epithelial cells through the use its arginine-glycine-alanine (RGD) motif [35, 36].

Once EBV attaches to host cells there are several events that occur in order for membrane fusion to occur. There are in total at least four glycoproteins that are required for membrane fusion to occur once virions bind to host cells, *viz*. gH (gp85), gL (gp25), gp42 and gB (gp110) (Fig. 1.4). Of these glycoproteins, it is gH, gL and gB that form the core fusion machinery; with gH and gL playing a mediatory role and gB executing the fusion of the viral and host

membranes. The importance of gB in membrane fusion was first shown through the use of a gB deletion mutant [37]. Mutant virions were able to bind to cells and enter endosomes, but were unable to carry to out fusion. Once virions bind to host cells, the gH/gL-HLA class II complex undergoes conformational changes, mediated by gp42, to bring apposing membranes in close proximity. Furthermore, these conformational changes enable gH/gL to be positioned such that gB can be activated and initiate membrane fusion [38].

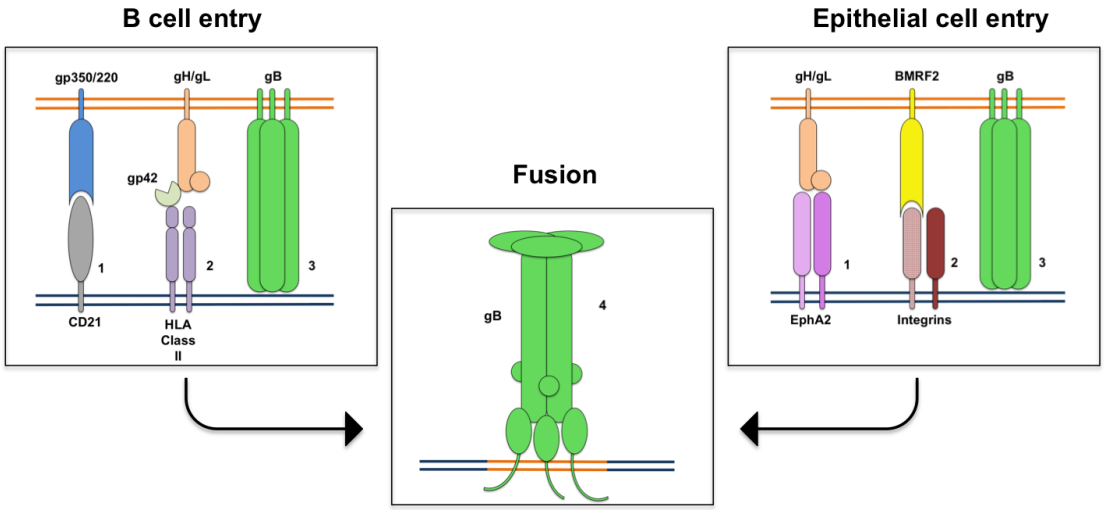

Figure 1.4: Attachment and fusion of EBV with host cells. The viral membrane is represented in orange while the host cell membrane is represented in dark blue. For B cell entry, the attachment of virus occurs through the gp350-CD21 interaction (1). The gp42 protein, which associates with gH/gL via a high affinity interaction, interacts with human leukocyte antigen (HLA) class II (2). This triggers membrane fusion through the action of gH/gL and gB (3). The capsid of EBV is delivered into the cytoplasm after the viral envelope fuses with the membrane of endosomes (4). For epithelial cell entry, the attachment of virus is mediated through the interaction of gH/gL with Ephrin receptor (EphA2) (1) and BMRF2 with integrins (α3β1, α5β1 or αvβ1) (2). Membrane fusion is triggered via the action of gB (3) and the EBV capsid is directly delivered in the cytoplasm of epithelial cells (4). This image was adapted from Longnecker *et al*., 2013 [39].

The EBV glycoproteins that are responsible for virus assembly have not been extensively studied. However, glycoproteins gM and gN have been implicated in exocytosis. For herpesviruses, the release of virions requires that tegumented capsids move from the cytoplasm into the secretory compartment [27]. gM is a large multispan membrane protein, while gN is a small single-pass glycoprotein. These glycoproteins associate with one another to carry out their effector functions. Deletion of gN was shown to reduce the occurrence of

mature gM [40]. The lack of gN-gM was found have a deleterious effect on virion production; i.e. many virions were found to be incompletely enveloped. Additionally, virions that were successfully enveloped were trapped in vesicles.

1.1.2. The Genome structure of the EBV

The linear-double stranded DNA genome found in EBV capsids is approximately 172 kb in size and contains at least 86 open reading frames [41, 42] (Fig. 1.5). The linear genome is flanked on either side by terminal repeats, which mediate circularisation to form episomes within the nuclei of infected cells [43]. The circular form of EBV, prevalent during viral latency, is maintained through the origin of plasmid replication (oriP). Conversely, lytic replication is initiated from the origin of lytic replication (orilyt) and yields head-to-tail concatemers [44]. The unique long region of the EBV genome encodes nine latent proteins and several non-coding RNAs. The latent proteins encoded by this region include the Epstein-Barr nuclear antigen 1 (EBNA1), EBNA2, EBNA3A, EBNA3B, EBNA3C, EBNA-LP, latent membrane protein 1 (LMP1), LMP2A and LMP2B. The non-coding RNAs include the Epstein-Barr virus-encoded small RNA 1 (EBER1) and 2 (EBER2), BART-derived microRNAs (miRNAs-BARTs) and BHRF1 microRNAs (miRNAs-BHRF1) [42].

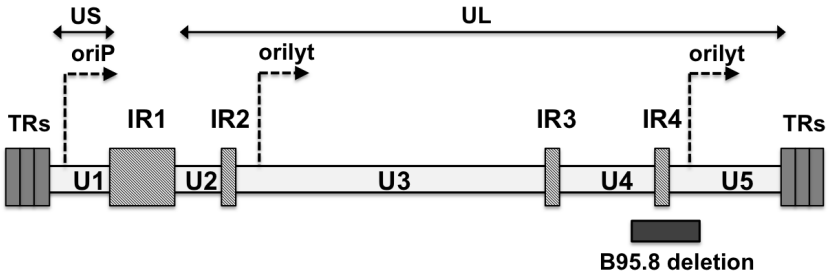

Figure 1.5: Organisation of the linear EBV genome. The linear genome is flanked by 0.5 kb terminal direct repeats (TRs) and contains four internal repeat sequences (IRs). The unique short sequence (US) region comprises the unique sequence domain 1 (U1). The unique long sequences (UL) spans the region containing U2 to U5. The origin of replication during latency (oriP) contains *cis*-acting elements that ensure that episome maintenance occurs. The synthesis of EBV DNA during lytic replication is initiated from the origins of lytic replication (orilyt). An 11.8 kb deletion within the B95-8 strain, the first herpesvirus to have its genome sequenced [41], is shown. The image was adapted from Longnecker *et al*., 2013 [39].

1.1.3. The EBV life cycle

1.1.3.1. Latency

The ability to establish latency in B cells is an essential characteristic of EBV. It is the colonisation of the memory B cell pool that enables EBV to be carried lifelong [45]. During the early stages of primary infection EBV infects B cells found at oropharyngeal mucosa [46]. Once EBV infects naïve B cell, there are a host of events that lead to the establishment of true latency in memory B cells (Fig. 1.6). EBV-infected B cells display different patterns of antigen expression, and depending on the antigens expressed, cells can be classified as having one of four latency programs [45, 47]. There are potentially 6 nuclear proteins (EBNA-1, -2, -3A, - 3B, -3C and -LP) and two membrane proteins (LMP1 and LMP2) that can be expressed during latency.

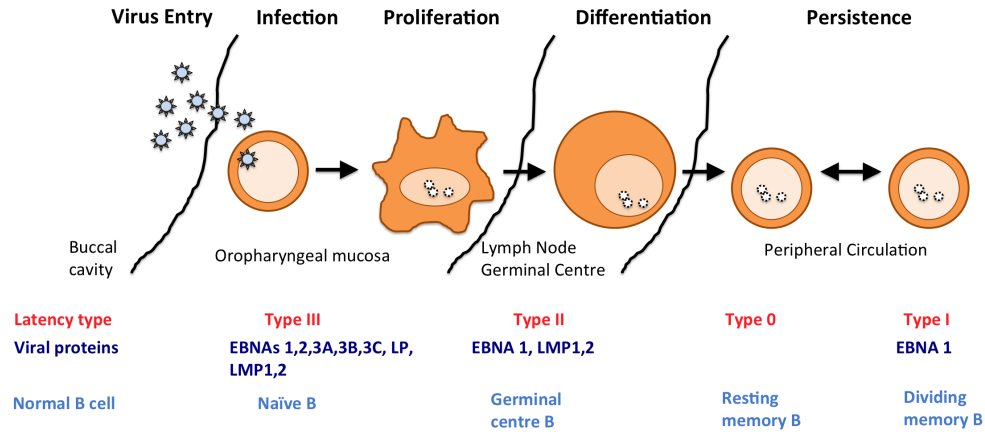

Figure 1.6: The latency programs in EBV-infected B cells. In the first stage of infection EBV infects host squamous epithelial cells and B cells in the oropharynx. In these cells the virus undergoes lytic replication and this leads to a rise of virus levels locally [45]. Infected naïve B cells display type III latency and are characterised as being activated. The activated B cells proliferate and ensure that the number of EBV infected cells rise. Some of these B cells enter the germinal centres of secondary lymphoid tissues and display type II latency [47]. These B cells eventually differentiate into memory cells B cells and exit the germinal centres. Infected memory B cells circulate freely and display either type I or type 0 latency. Since memory B cells express a limited number of antigens, they are not efficiently recognised by immune cells [47]. When memory EBV-infected B cells are activated they can differentiate into plasma cells and this can lead to lytic replication [48]. It is important to note that irrespective of the type of latency, all EBV-infected cells express EBV-encoded small RNAs (EBERs) [47]. This image was adapted from Heslop, 2009 [47].

Several of the above mentioned latent proteins have crucial roles in B cell survival, some of which will be considered here. EBNA1 is expressed during all forms of latency, except for type 0, and is a DNA-binding phosphoprotein that is necessary for viral genome replication and maintenance [46]. EBNA1 interacts simultaneously with the oriP of the EBV genome and host chromosomes, ensuring that the EBV genome is tethered to the host chromosome during mitosis [49]. EBNA2 is one of the first viral genes to be transcribed after infection, and once translated, it is able to act as a transactivator of several viral (e.g. LMP1, LMP2A and LMP2B) and host proteins (e.g. CD23 and CD21) [39, 50]. The EBNA3 family of proteins, which came about through gene duplication [51], act as transcriptional regulators [52]. All members of the EBNA3 family interact with the DNA-binding transcription factor RBPJ. Interestingly, EBNA2 also interacts with this transcription factor and it is suggested that members of the EBNA3 family act as coactivators of EBNA2 [53]. Furthermore, EBNA3A and EBNA3C inhibit pro-apoptotic signals from BIM and the tumour suppressor p16INK4A [54]. LMP1 is a multispan membrane protein that behaves like a constitutively active tumour necrosis factor (TNF) receptor. The signals generated by LMP1 are very similar to that of CD40. LMP1 also upregulates several B activation markers in infected cells (viz. CD21, CD23, CD30 and CD40) and antiapoptotic markers (e.g. Bcl2 and A20) [55]. LMP2 is also a multispan membrane protein that plays an important role in B cell survival and proliferation. However, LMP2 can be transcribed from two promoters to give rise to LMP2A or LMP2B [56]. LMP2A and LMP2B are very similar except that LMP2B lacks a tyrosine kinase signalling domain. The presence of this domain enables LMP2A to mimic B cell receptor (BCR) signals [39].

1.1.3.2. Lytic replication

While latency is important for EBV to survive within infected individuals, it is lytic replication that ensures that EBV is transmitted from one host to another [57]. Contrary to latency, characterised by the expression of a small subset of genes, lytic replication involves the

expression of around 80 viral genes [58]. The exact mechanism that leads latently infected cells to undergo reactivation *in vivo* is not well understood. However, it is know that lytic replication occurs in memory B cells associated with the oropharyngeal mucosa [59, 60].

During lytic replication a cascade of viral gene expression occurs that results in the production of immediate-early (IE), early (E) and late (L) gene products. This cascade is chiefly mediated by the activities of BZLF1; a DNA-binding, d-zip transcription factor [61-63]. BZLF1 interacts with multiple BZLF1 responsive elements (ZRE) in the promoters of viral and cellular genes and the EBV orilyt [58, 63, 64].

During lytic replication the EBV genome is replicated by a rolling circle mechanism and results in the generation of large head-to-tail concatemers [60, 65]. In order for this process to be initiated several viral proteins are required; viz. DNA polymerase catalytic domain (BALF1), polymerase-associated processivity factor (BMRF1), single strand DNA-binding protein (BALF2), primase (BBLF4) and helicase/primase-associated protein (BBLF2/3) [65, 66]. Subsequent to DNA replication, the concatemers are cleaved within the TRs by a terminase complex (BALF3, BGRF1/BDRF1 and BFRF1A) to yield individual genomes that are packaged into viral capsids [9, 67, 68].

1.2. EBV-associated diseases and malignancies

Infection of human hosts by EBV is exceptionally common. Around 95% of the human population is EBV seropositive once they reach adulthood [69]. In the majority of cases, EBV is acquired early in life and infection is asymptomatic [69, 70]. However, when EBV is acquired during adolescence it can lead to the development of infectious mononucleosis (IM), a disease that is usually self-limiting [70]. During the acute phase of IM patients develop cervical lymphadenopathy, fever and pharyngitis. Subsequently, a small proportion of patients (10-20%) experience fatigue and malaise that lasts for 2-6 months [69, 71, 72]. In addition to IM, for which there are at least 125,000 new cases each year in the USA, there is

also a wide range of malignancies that are associated with EBV. Every year around 200,000 new cases of EBV-associated malignancies are diagnosed worldwide [73]. Furthermore, EBV is also considered to be an important factor in the development of Multiple Sclerosis [72].

1.2.1. EBV-associated diseases in Immunocompromised Individuals

There are several EBV-related lymphoproliferative disorders that can occur in individuals with genetic or acquired immunosuppression [74]. In these individuals, their immune system fails to prevent transformation of EBV-infected cells [75].

A classic example of this is post-transplant lymphoproliferative disorder (PTLD), a heterogeneous group of lymphoproliferative diseases, often malignant, that involves lymphoid or plasmacytic proliferations [76, 77]. Since transplant patients are subjected to pharmacological immunosuppression, it is possible for EBV-positive cells to survive and proliferate despite the fact that they display type III latency [76]. PTLD occurs in patients that that have received a solid organ transplant (SOT) or hematopoietic stem cell transplant (HST). There are a several factors that influence ones likelihood of developing PTLD. One major factor is the serostatus of patients prior to receiving the transplant. Patients that experience primary infection during or after transplantation have a significantly higher risk than those that are already EBV positive prior to transplantation [77, 78]. Primary infection can occur via the normal route or EBV can be acquired from the tissues/cells of the seropositive donor. Another major risk factor is the level of immunosuppression received. Patients receiving higher levels of immunosuppressive drugs are more likely to develop PTLD. This is one of the reasons why a reduction in immunosuppression is a common treatment option for PTLD. Other treatment options include low-dose chemotherapy, adoptive immunotherapy and the use of the monoclonal anti-CD20 (also known as rituximab) [78].

1.2.2. EBV-associated malignancies in Immunocompetent Individuals

1.2.2.1. Burkitt lymphoma

The history of EBV and Burkitt lymphoma is irrevocably intertwined. It was almost 60 years ago when Dennis Burkitt described tumours found in the jaws of equatorial African children [79]. Cell lines established from Burkitt lymphoma (BL) biopsies were analysed through electron microscopy (EM) by Epstein *et al*., 1964 [80] to reveal the presence of the EBV particles.

The clinical variant first described by Dennis Burkitt is now known as endemic BL (eBL). This variant occurs frequently in children from equatorial Africa and Papa New Guinea and displays type I latency [74]. Incidentally, the regions affected by eBL are also affected by the malarial parasite *Plasmodium falciparum*. This led to a hypothesis that coinfection with EBV and *P.falciparum* promotes the development of eBL [81]. It is thought that infection with *P.falciparum* causes latently infected B cells to expand and undergo reactivation. Furthermore, *P.falciparum* infection is also hypothesised to negatively affect EBV-specific T-cells, enabling EBV-infected B cells to proliferate [77].

In addition to eBL, there are two other clinical variants know as sporadic BL (sBL) and HIV-associated BL [81]. Both of these variants do not associate with EBV to the same extent as eBL, where nearly every malignant cell is EBV-positive. However, irrespective of the clinical variant displayed, all BLs are known to involve reciprocal chromosome translocations between the c-MYC locus on chromosome 8 with immunoglobulin heavy or light chain loci on chromosome 14, 2 or 22 [82-84].

1.2.2.2. Hodgkin lymphoma

Hodgkin lymphoma is a malignancy in which a small number of neoplastic Hodgkin Reed-Sternberg (HRS) cells, displaying type II latency, are surrounded by an inflammatory

infiltrate; comprised of granulocytes, lymphocytes, plasma cells and histiocytes [74, 81, 85]. Hodgkin lymphoma can either be defined as classical Hodgkin lymphoma (cHL) or nodular lymphocyte-predominant lymphoma (NLPHL). Of these two groups, EBV has a stronger association with cHL [86]. cHL most commonly affects the lymph nodes, spleen, bone marrow and liver. In these tissues, less than 1% cellularity is due to the HRS cells. The majority of proliferations in the affected tissues are due to the inflammatory cells [74]. Upon histological analysis, cHL can be further classified into lymphocyte predominance (LP), nodular sclerosis (NS), mixed cellularity (MC) and lymphocyte depletion (LD) subtypes [77]. Of these subtypes EBV associates more frequently with MC and LD than with NS and LP [81].

The origin of HL has been a topic of intense debate [77]. However, it is now widely accepted that in the majority of cases HRS cells are germinal centre (GC) B cells. Through analysing the immunoglobulin genes of HRS cells, it was found that they had undergone somatic hypermutation (SHM). These mutations were found to prevent HRS cells from expressing a functional BCR [74, 77]. Usually, GC B cells that lack a BCR die by apoptosis. However, the expression of LMP2, which can mimic BCR signals, enables the HRS cells to survive [85].

1.2.2.3. Nasopharyngeal Carcinoma

Nasopharyngeal carcinoma (NPC) is an epithelial malignancy that occurs sporadically worldwide, but is far more prevalent in Southern China and Southeast Asia [42, 87, 88]. In Southern China NPC is the third most common diagnosed cancer and it can affect up to 50 persons per 100 000 [89]. NPC can be divided into three types based on histological inspection; i.e. keratinising squamous cell carcinoma (type I), differentiated non-keratinising squamous cell carcinoma (type I) and undifferentiated non-keratinising squamous cell carcinoma [90]. The non-keratinising types are very common and account for more than 80% of NPC cases worldwide. Importantly, these two are almost always EBV positive [74, 90].

EBV-positive NPC cells display gene expression that is intermediate between what has been observed for BL (latency I) and HL (latency II). NPC cells always express EBNA1 and EBERs, however, in around 50% of cases LMP1 and LMP2 proteins can also be detected [74, 89]. EBNA1 is known to be required for EBV episome maintenance, but in the case of NPC, EBNA1 has also been shown to promote cell survival and proliferation [91]. Furthermore, EBNA1 expression has also been shown to contribute to tumorigenicity and metastasis [90, 91]. LMP1 and LMP2A expression in NPC has been shown to induce epithelial-mesenchymal transition (EMT) through the action of Snail and Twist; both of which negatively regulate epithelial cadherin (E-cadherin) [92, 93].

NPC differs from other head and neck cancers in terms of its unusually high propensity to metastasise and in terms of the treatment modalities used, i.e. radiotherapy, in combination with chemotherapy, is preferentially used for treatment rather than surgery [94, 95]. This is due to the increased sensitivity of NPC to radiotherapy and chemotherapy [95]. However, since patients are usually diagnosed at an advanced stage, it is common for patients to experience relapse after treatment. Additionally, the occurrence of secondary malignancies after treatment is common [89]. Considering these issues collectively, and the high association rates with EBV, there is a keen interest in developing therapeutic and prophylactic vaccines that specifically target EBV components [96].

1.3. Immune responses against EBV

1.3.1. Innate Immune Responses

The innate immune response provides the first line of defence against pathogens. Components of innate immunity exist prior to pathogen exposure and are able to respond within minutes of infection [97]. Traditionally, the innate immune system is thought to provide defence prior to the activities of the adaptive immune system. However, in recent years new evidence has emerged that suggests that the innate immune system modifies and

regulates the adaptive immune response [98]. Furthermore, components of the innate immune have also been found to exhibit memory-like features [99].

In the case of EBV, the innate immune response has been found to play an important role in managing infection [100, 101]. During the early phase of infection, the innate immune system recognises EBV pathogen-associated molecular patters (PAMPs) through pattern recognition receptors (PRR) [45, 100]. Several APCs express Toll-like receptors (TLR), a specific class of PRRs, which are able to recognise different components of EBV. Plasmacytoid dendritic cells (pDCs), B cells and monocytes express an endosomal receptor, known as TLR9, which allows them to recognise the unmethylated DNA of incoming virions [45, 102]. Activation of TLR9 stimulates NFκB to induce the production pro-inflammatory cytokines [98]. TLR3, another endosomal receptor, is expressed by conventional dendritic cells (cDCs) and enables the recognition of hairpin structures of EBERs. EBERs interact with the EBER-binding protein known as La, and when released from dead cells, can be taken up and recognised by cDCs. Additionally, EBERs can also be recognised by the intracellular PAMP known as retinoic acid-inducible gene 1 (RIG-1) [102]. In addition to being sensed by intracellular TLRs, EBV can also be recognised by a TLR expressed on the surface of immune cells. Specifically, TLR2 is expressed on the surface of monocytes and its interaction with EBV leads to the release of monocyte chemotactic protein 1 (MCP-1) [103].

Natural killer (NK) cells are known to be an important component of the innate immune system that enables protection against viruses and cancer [101]. In the case of EBV, NK cells are the main effector cells of the innate immune response [97]. NK cells carry out their effector functions through the secretion of cytokines, mediating the activity of other immune cells, or through cytotoxic activity [104]. In humans, there are two NK cell subsets that are responsible for carrying out these functions. The $CD56^{bright}CD16^{-}KIR^{-}$ subset is less mature and is commonly found within lymphoid organs. These cells are responsible for

secreting IFN-γ, tumour necrosis factor and granulocyte-macrophage colony-stimulating factor (GMSF). In contrast, the $CD56^{dim}CD16^{+}KIR^{+}$ subset is more differentiated and is commonly found within the blood. These cells contain preformed perforin and granzymes and are poised to release them upon stimulation [45, 104, 105]. The activities of NK cells in conjunction with APCs are summarised in Fig. 1.7.

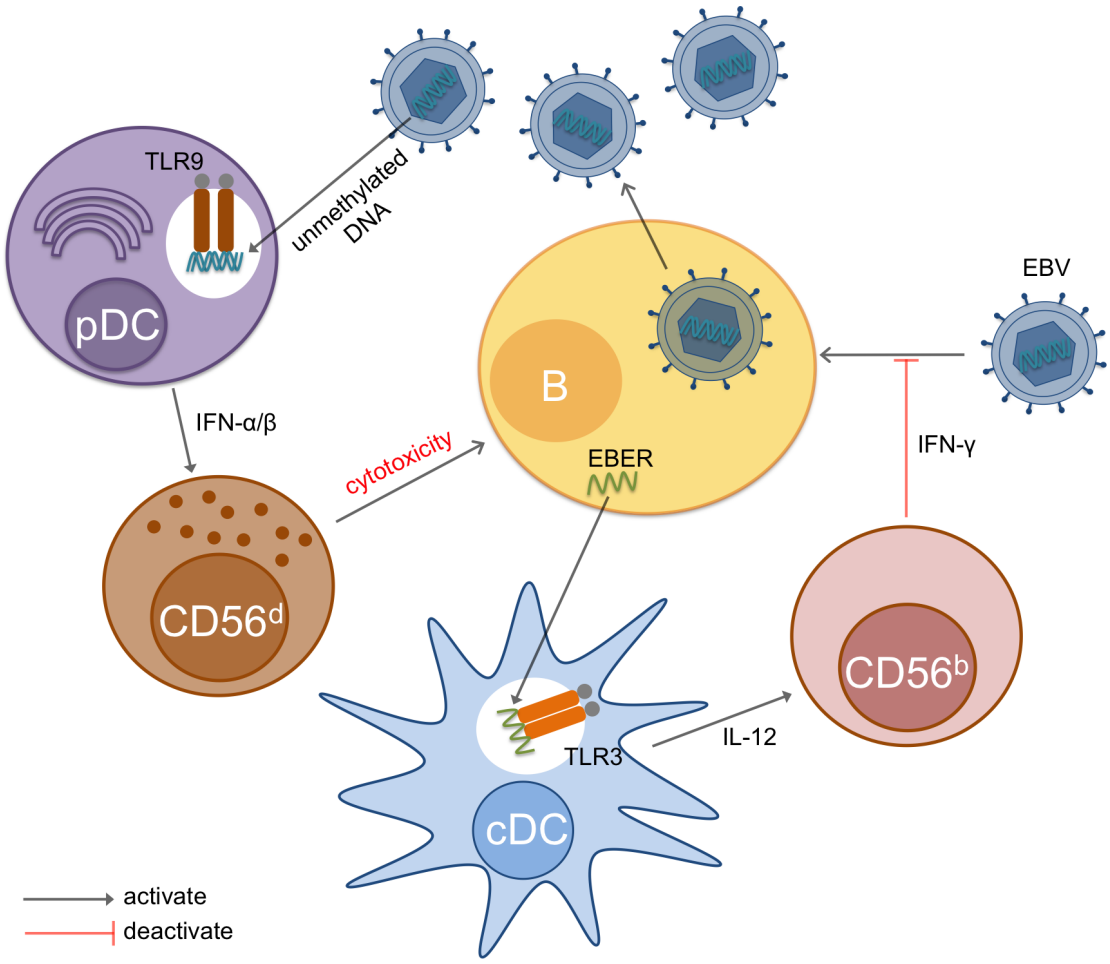

Figure 1.7: An overview of the innate immune response against EBV. EBERs are expressed within infected B cells. Upon cell death EBERs, along with their binding partner La, are released and taken up by cDCs. The endosomal TLR3 becomes activated by the EBERs and results in the release of IL-12 [102]. $CD56^{bright}CD16^{-}KIR^{-}$ NK cells ($CD56^{b}$) in turn secrete IFN-γ and restrict B cell infection [100]. Furthermore, IFN-γ is also known to limit B cell transformation [45]. Unmethylated DNA within EBV particles is able to stimulate TLR9 in pCDs. This results in the secretion of IFN-α/β and the concomitant activation of $CD56^{dim}CD16^{+}KIR^{+}$ NK cells (CD56a). These cells destroy EBV infected cells through the release of cytotoxic molecules [102].

1.3.2. Adaptive Immune Responses

1.3.2.1. Antibody Response

Lytic and latent antigens are both targeted by the antibodies of infected hosts [106] (Fig. 1.8). Viral capsid antigen (VCA)-specific IgM is one of the first antibodies that can be detected after the onset of IM [75]. The VCA-IgM response last for 2-3 months and this enables it to be used as an indicator of primary infection [107]. Conversely, VCA-IgG is not very useful for the diagnosis of IM. VCA-IgG appears several weeks after the onset of symptoms and persists lifelong [106]. EBNA1-IgG appears in the blood of most individuals three months after primary infection, but once they appear they can be detected lifelong [75].

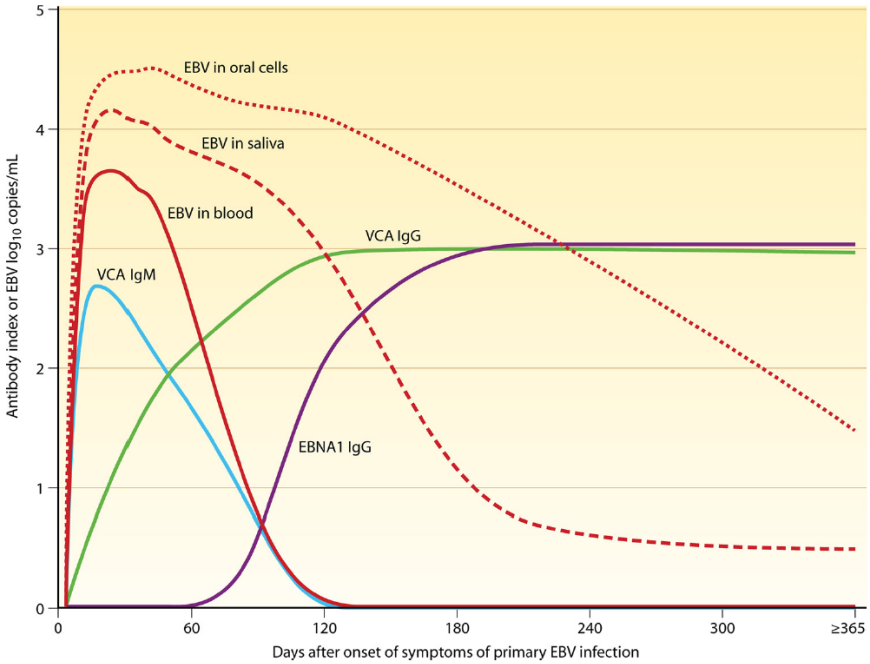

Figure 1.8: EBV load and EBV-specific antibodies during symptomatic primary EBV infection. During the initial phase of primary infection, the level of EBV is relatively high within the oral cavity. For this reason, EBV can usually be detected in the oral cavity with quantitative PCR before it detected in the blood. Moreover, EBV is cleared much faster from the blood than in the oral compartment. Shedding of virions from the oral cavity generally persists for several months after primary infection. However, shedding can also occur sporadically in healthy carriers. VCA-IgM and VCA-IgG levels rise during the early stages of primary infection, while EBNA1-IgG is only detected months later. This figure was taken from Odumade *et al.*, 2011 [75].

1.3.2.2. Cellular immune response

The activities of $CD4^+$ and $CD8^+$ T cells are fundamental to the control of acute and persistent EBV infection [108]. Both $CD8^+$ and $CD4^+$ T-cell populations have been studied in the context of IM (Fig. 9A), with the former receiving more attention thus far. During the acute phase of IM there is a dramatic expansion of the $CD8^+$ compartment. The large majority of the expanded $CD8^+$ T cells are virus-specific [45, 105, 109]. The $CD4^+$ compartment expands significantly less when compared to the $CD8^+$ compartment. However, when specificities against individual epitopes are considered collectively, they comprise a much larger proportion of the total T-cell pool [45, 110]. Despite this discrepancy between the $CD8^+$ and $CD4^+$ responses to EBV infection, it is thought that both $CD8^+$ and $CD4^+$ T cells are required to control EBV infection. Immunocompromised transplant patients suffering from PTLD are usually treated with preparations containing $CD4^+$ and $CD8^+$ components [108]. Furthermore, better clinical outcomes are observed when the T-cell preparations have broader specificity and when they contain higher proportions of $CD4^+$ T cells [111, 112].

The response of healthy seropositive individuals has also been studied with regards to their immunodominance hierarchies (Fig. 9B). Unsurprisingly, memory responses in healthy individuals reflect the immunodominance hierarchies observed in IM patients. Memory $CD8^+$ T cells respond readily to lytic cycle antigens. In particular, the $CD8^+$ memory response shows a marked hierarchy towards IE and E antigens [110]. In addition to lytic proteins, $CD8^+$ T cells from healthy donors also respond frequently to members of the EBNA3 family [113]. Memory $CD4^+$ T cells respond broadly to lytic and latent antigens. $CD4^+$ responses against lytic cycle antigens (e.g. gp110 (BALF) and gp350 (BLLF1)) can frequently be detected, while $CD8^+$ responses against these antigens are rarely detected [108, 110]. Interestingly, work by Adhikary *et al*., 2006 [108] have shown that gp350- and gp110-specific $CD4^+$ T cells are

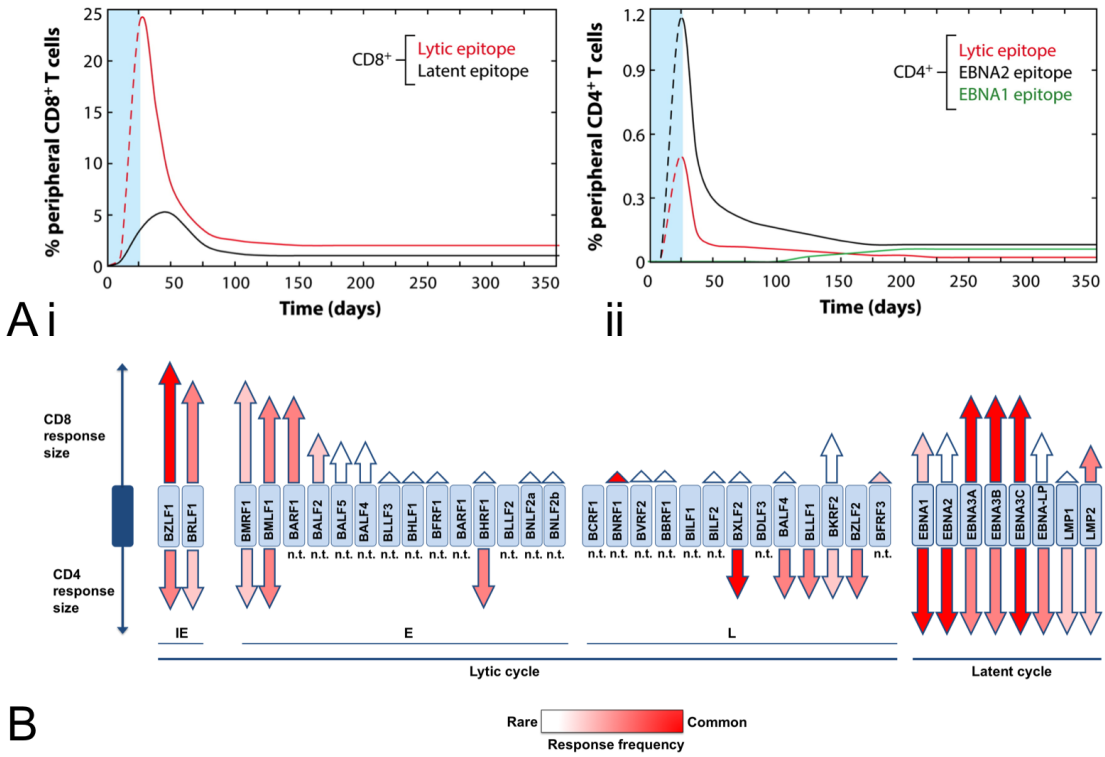

Figure 1.9: Cellular immune responses to EBV. (A) Response kinetics during primary symptomatic EBV infection. The blue shaded area represents the first 4-6 weeks after primary infection. During this time signs and symptoms are apparent but it is difficult to perform detailed diagnostics. Dotted lines during this period signify uncertainty about a particular parameter. (i) $CD8^+$ T cells specific against lytic antigens expand massively during the initial phase of IM. Conversely, $CD8^+$ T cells specific against latent antigens are far less abundant. As signs and symptoms disappear, the number of $CD8^+$ T cells specific for latent and lytic antigens in blood decreases. This observation is more pronounced for lytic antigen-specific $CD8^+$ T cells. (ii) EBV-specific $CD4^+$ T cells are significantly less numerous compared to EBV-specific $CD8^+$ T cells. Furthermore, $CD4^+$ responses decline much faster than $CD8^+$ responses. Latent epitope-specific responses are usually more dominant than those of lytic antigen-specific responses. Unique amongst latent epitope $CD4^+$ T-cell responses, EBNA1-specific $CD4^+$ T cells only appear months after IM. (B) EBV antigens recognised by memory $CD4^+$ and $CD8^+$ T cells. Healthy seropositive donors contain T cells that are specific against latent and immediate-early (IE), early (E) and late (L) antigens. The data displayed was obtained primarily through IFN-γ ELISPOT analysis of $CD4^+$ or $CD8^+$ depleted PBMCs. The frequency and intensity of each response is illustrated. 'Not tested' (n.t.) is indicated for antigens that were not analysed. The image was adapted from Hislop *et al*., 2007 [110] and Taylor *et al*., 2015 [45].

cytotoxic in character; i.e. they control the outgrowth of EBV-infected cells through the release of granzyme B and perforin. $CD4^+$ cytolytic T-cell (CTL) responses are known to occur when individuals suffer from chronic viral infections. $CD4^+$ CTLs have also been reported to

respond to human cytomegalovirus (HCMV), hepatitis virus, and human immunodeficiency virus 1 infections [114]. Responses of $CD4^+$ T cells to latent proteins have been well studied and healthy donors have been found to respond frequently to a number of latent proteins [110, 115]. Many individuals develop $CD4^+$ T-cell responses against latent antigens despite the fact that latent antigens are endogenously derived. It is thought that DCs or B cells take up latent antigens released from infected cells and present them on MHC class II molecules [115]. In the case of EBNA1, there is a more intriguing explanation for the development of $CD4^+$ T-cell responses. Loading of cytosolic EBNA1 peptides onto MHC class II molecules have been shown to occur after autophagy. Specifically, EBNA1 is taken-up by autophagocytic vesicles, transported to lysosomes, processed and loaded onto MHC class II molecules. Considering that EBNA1 is expressed during almost all forms of latency (*viz*. type I, II and III), it might suggest an important role for EBNA1-specific $CD4^+$ T cells in healthy hosts [116].

1.3.3. Immune Evasion

EBV has evolved a plethora of immune evasion mechanisms that target innate and adaptive immune components [117]. In fact, EBV encodes a lytic cycle protein that is capable of targeting the innate, $CD4^+$ and $CD8^+$ responses. This protein is an alkaline exonuclease (BGLF5) that has RNase activity [118]. The RNase activity of BGLF5 enables it to mediate host shutoff; i.e. destabilise host cell mRNA such that host protein synthesis is down regulated [119]. Some of the genes that are targeted in this manner include those that encode TLR2, TLR9, HLA I and HLA II molecules. Two additional proteins are produced during lytic replication that contributes to immune evasion; *viz*. BNLF2a and BCRF1 [120]. BCRF1 is a viral homologue of the anti-inflammatory IL-10, which is known to negatively affect the priming of $CD4^+$ cells and their effector functions [117]. BNLF2a is a protein that has been found to integrate into ER membranes and interfere with the TAP transporter associated with HLA class I presentation [110].

EBV also encodes immune evasion proteins that form part of virions. The major tegument protein BNRF1 and the large tegument protein BPLF1 have both been identified as having immune evasive properties [121, 122]. BNRF1 has been shown to disrupt the functioning of promyelocytic leukemia nuclear bodies (PML-NBs). PML-NBs carry out antiviral activities by suppressing the expression of viral DNA [123]. The disruption of PML-NBs by BNRF1 ensures the occurrence of viral latency and cellular immortalisation post-infection [124]. BPLF1 is a deubiquitinase (DUB) and it uses this activity to interfere with intermediates of TLR signaling pathways. By interfering with TLR signaling, BPLF1 is able to inhibit the production of cytokines in the presence of TLR stimulation [117].

1.4. Vaccination against EBV

The first virus that was shown to be oncogenic in humans is EBV [48]. Subsequent to this paradigm-shifting discovery, vaccination against EBV has been touted as a possible means of limiting EBV-associated diseases and cancers. Epstein and Achong suggested vaccination against EBV as early as 1973 [125]. Unfortunately, despite decades of research, no EBV vaccine has made it onto the market.

The struggle towards a prophylactic vaccine is not exclusive to EBV, but it has also been the case for the majority of human herpesviruses. The only human herpesvirus for which there is currently a licensed vaccine is the varicella-zoster virus (VZV). VZV, also known as human herpesvirus 3 (HHV-3), is an alphaherpesvirus that is responsible for the development of varicella (or chickenpox) and zoster (or shingles) [126, 127]. Varicella is a self-limiting disease that occurs during primary infection, usually in childhood, and is characterised by a diffuse vesicular rash [127, 128]. As with EBV, VZV establishes a life-long latent infection subsequent to primary infection [126]. VZV is able to reactivate, usually in older individuals or the immunocompromised, and results in a painful vesicular rash that can be followed by post-herpetic neuralgia (PHN) [129]. Vaccines have been developed that prevent varicella and

zoster. Both vaccines are based on the live attenuated Oka strain that was first isolated in Japan [126]. The only difference between the two is that the zoster vaccine is given at a dose 14 times higher than the varicella vaccine [130]. Once individuals are vaccinated, the attenuated Oka strain is able to carry out latent infection in a similar fashion to wild-type VZV strains [126]. Furthermore, vaccinated individuals are not protected from subsequent VZV infection [131]. Despite the inability to achieve sterile immunity, vaccination still manages to prevent up to 85% of varicella cases and 69.8% of zoster cases [127].

Vaccination against herpesviruses has also successfully been carried out in animals. An excellent example is that Marek's disease (MD), a lymphoproliferative disease that afflicts poultry. MD is caused by the highly oncogenic alphaherpesvirus know as Marek's disease virus (MDV) or Gallid herpesvirus 2 (GaHV-2) [132, 133]. Fowls that acquire MD suffer from paralysis, blindness and develop lymphomas within visceral organs [132]. As with VZV, vaccination against MDV is achieved through the use of a live attenuated vaccine. The most widely used vaccine is a high passage clone of the CVI988 strain that was first used in the Netherlands [134, 135]. Vaccinated fowls are protected from mortality and the development of MD. Vaccination against MD was the first instance in which a cancer was prevented through the use of antiviral vaccination. It is important to note that vaccination against MD does not prevent infection with MDV [135].

The majority of prophylactic EBV vaccines that have been investigated have targeted the envelope glycoprotein gp350 [131, 136]. This glycoprotein was selected due to its abundance within viral membranes and the membranes of infected cells. Furthermore, gp350 is a frequent target of neutralising antibodies [73]. gp350 based vaccines initially showed great promise when tested in non-human primates; i.e. cotton-top tamarins [137, 138], common marmosets [139]and rhesus macaques [140]. In all of these studies, vaccination was shown to offer some form of protection, e.g. a reduction in seroconversion,

EBV viral load or the development of lymphomas. In contrast, results obtained from a handful of clinical trials in humans have been less impressive. The largest of these was a phase II, double-blind, randomised, placebo controlled trial [71]. In total, 181 EBV negative young adults (aged 16 to 25) were given three doses of a recombinant gp350 vaccine or the placebo. The vaccine was well tolerated and almost all vaccinated individuals (99%) developed anti-gp350 responses. Nineteen months after vaccination, it was established that the vaccine did not protect individuals from EBV infection. However, it was found that vaccination greatly reduced the incidence (78%) of IM over a 2-year observation period.

Our group recently developed a vaccine candidate in the form of EBV virus-like particles and light particles (VLPs/LPs), herein referred to as DNA-free EBV ($_{DF}$EBV) [9]. Deletion of the BFLF1/BFRF1A-coding sequence from wtEBV (B95-8 strain) produced a mutant incapable of packaging viral genomes. Since BFRF1A is an integral part of the terminase complex, a collection of proteins that cleave DNA concatemers into individual genomes prior to packaging into capsids, its deletion prevented packaging of viral DNA. Importantly, the mutant EBV particles were shown to be as immunogenic as wtEBV, with both tegument- and envelope-specific T cells being stimulated by $_{DF}$EBV. Whilst the absence of DNA rendered $_{DF}$EBV non-infectious, the deletion of gp110 has recently been shown necessary to abrogate the toxic potential of EBV structural proteins [141]. This suggests that deletion of gp110 is necessary for $_{DF}$EBV to be considered as a suitable prophylactic vaccine candidate.

2. Aims and objectives

$_{DF}$EBV that lacks gp110, hereafter simply referred to as $_{DF}$EBV, is highly immunogenic, devoid of viral DNA, incapable of infection and non-toxic [9, 141]. Whilst these characteristics indicate that $_{DF}$EBV has potential as a prophylactic vaccine candidate, it is completely devoid of latent proteins. Latency is a major aspect of the EBV life cycle, and vaccination with lytic/structural proteins would not afford protection if a subset of infected cells are left untargeted and latency is established.

To address the aforementioned shortcoming of $_{DF}$EBV, the primary aim of the present thesis was to enlarge the antigenic spectrum of $_{DF}$EBV to include latent proteins. Ideally, the incorporated latent proteins should not compromise the antigenicity of preexisting structural proteins. Thus, enabling the stimulation of latent protein- and structural protein-specific T cells (Fig. 2.1). A secondary aim of this thesis was to extensively examine the antigenicity of $_{DF}$EBV containing latent proteins. The following objectives were established to determine whether $_{DF}$EBV containing latent protein moieties has potential as a prophylactic vaccine candidate:

(i) Design a strategy to introduce latent antigens into $_{DF}$EBV.

(ii) Develop a method of quantifying $_{DF}$EBV.

(iii) Comprehensively interrogate the antigenicity of $_{DF}$EBV containing latent antigens *in vitro* and *ex vivo*.

(iv) Evaluate the performance of $_{DF}$EBV containing latent antigens in an *in vivo* model.

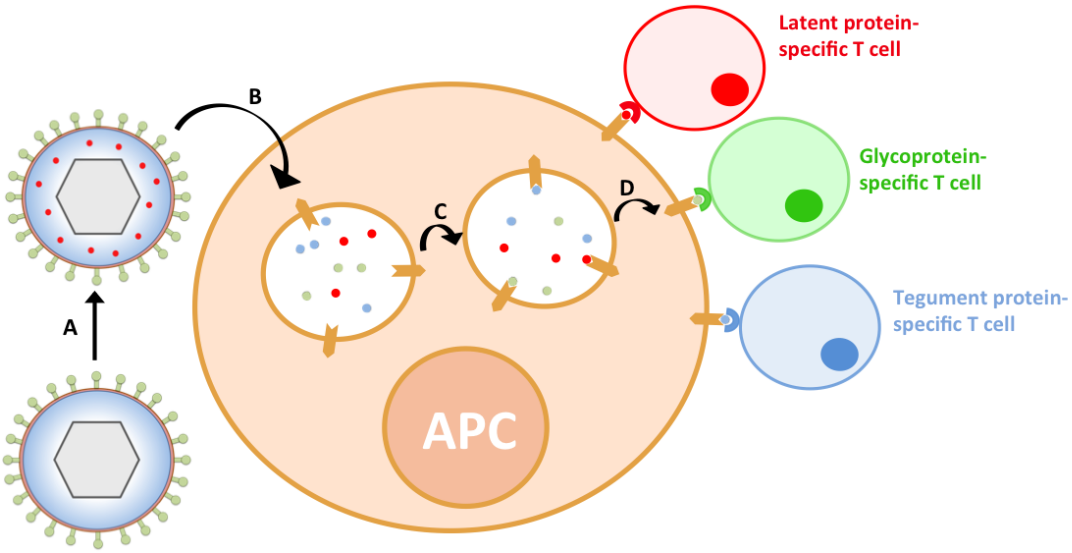

Figure 2.1: The introduction of latent proteins into $_{DF}$EBV is proposed to enlarge its antigenic spectrum. (A) Enlarging the antigenic spectrum of $_{DF}$EBV to include latent proteins (solid red dots). (B) Modified $_{DF}$EBV binds to antigen presenting cells (APCs) that express CD21 and is taken up via receptor-mediated endocytosis. Alternatively, modified $_{DF}$EBV is phagocytosed by phagocytic APCs. Particles are degraded in endolysosomes/phagolysosomes to release peptides from multiple structural proteins (e.g. membrane proteins (solid green dots), capsid proteins (not shown) and tegument proteins (solid blue dots). (C) Epitopes from various proteins are loaded onto MHC class II molecules. (D) Epitope-loaded MHC class II molecules are transported to the surface of the APC and engage the TCRs of T cells. Structural proteins and latent proteins can prime different T-cell clones.

3. Results

3.1. Enlarging the antigenic spectrum of wtEBV with latent proteins

3.1.1. Constructing EBV mutants containing BNRF1-latent protein fusions

To determine the possibility of introducing latent proteins into $_{DF}$EBV, we opted to first modify wtEBV. Since wtEBV can be accurately quantified with real-time qPCR, it enables the antigenicity of modified particles to be accurately assessed; i.e. reliably relate antigenicity to virus titre. In order to introduce latent proteins into viral particles, the major tegument protein BNRF1 was utilised. Since, BNRF1 is abundant within virions and is highly immunogenic [8, 9, 22], it implied that latent proteins could be incorporated into virions by fusing them to BNRF1. Thus, the BNRF1 ORF was modified with galK recombination to accommodate latent-protein coding sequences. The 5' region of the BNRF1 ORF was specifically modified because it is not conserved amongst γ-herpesviruses and has not been ascribed a function (Fig. 3.1A). BNRF1 is member of the family of viral proteins known as viral phosphoribosylformylglycineamide amidotransferases (vFGARATs) [123]. Members of this protein family have conserved FGAM and GAT1 domains towards their C-terminus. Hence, it was rationalised that modification of the 5' region of BNRF1 is unlikely to influence packaging of BNRF1-fusion proteins into virions.

Galk recombination was performed on wtEBV bacterial artificial chromosome (BAC) DNA to generate a BNRF1-EBNA3C gene fusion. Since, is EBNA3C is a highly immunogenic protein [115] that is expressed during latency type III [142], it is a promising vaccine candidate. Details regarding galK recombination are described in section 5.2.10. The first step in galK recombination was the insertion of the galK cassette into the target site, in this case, the 5' region of the BNRF1 ORF1. In a second step, the galK cassette was replaced with a 150 bp fragment encoding the 5H11 epitope from EBNA3C. Figure 3.1B illustrates the BNRF1 ORF before and after galK recombination.

Once a BAC mutant was generated in *E.coli,* it was introduced into mammalian 293 cells to generate producer cells upon hygromycin selection. The EBV-EC3 (150 bp) BAC DNA contained within 293 producer cells was rescued in *E.coli* and analysed through restriction

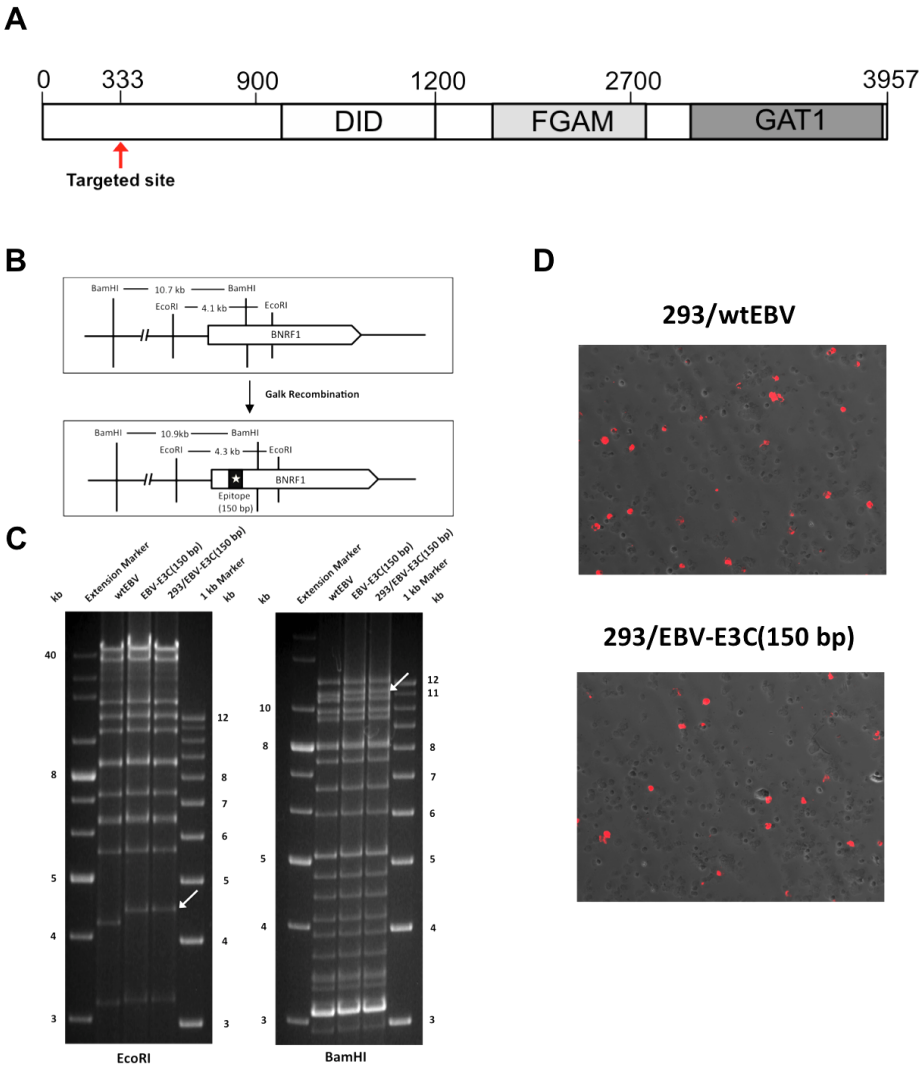

Figure 3.1: Construction of EBV BAC DNA encoding a BNRF1-EBNA3C fusion protein. (A) The structure of the BNRF1 ORF. Domains conserved amongst vFGARATs (FGAM and GAT1) are highlighted in dark grey, while the functional Daxx-interaction domain (DID) interaction domain is shown in dark grey. (B) Galk recombination was carried out with a 150 bp fragment encoding the 5H11 epitope of EBNA3C. The schematic indicates *Eco*RI and *Bam*HI restriction sites before and after recombination, as are the sizes of the fragments generated by these enzymes. (C) Recombinant BAC DNA from *E.coli* and 293 producer cells were analysed via restriction digestion. *Eco*RI and *Bam*HI was selected to interrogate the integrity of EBV-E3C (150 bp). White arrows emphasise DNA fragments that are different between wtEBV DNA (B95-8) and DNA modified with galK recombination. (D) The BNRF1-latent protein fusion does not influence lytic replication in 293 producer cells. Producer cells were transfected with the lytic cycle transactivator BZLF1 and were analysed for the expression of the late lytic gene product gp350. Induced 293 producer cells were stained with and analysed with α-gp350 and α-mouse IgG-Cy3 antibodies immunofluorescence.

digestion (Fig. 3.1C). Digestion of BAC DNA with *Eco*RI and *Bam*HI confirmed that the DNA contained within producer cells was the same as the DNA constructed with galK recombination in *E.coli*. Furthermore, restriction digestion also showed that BAC DNA modified through galK recombination displayed the appropriate digestion pattern. Digestion of EBV-E3C (150 bp) BAC DNA with *Eco*RI and *Bam*HI respectively showed that recombination gave rise to 4.3 kb and ~10.9 kb fragments as expected. Lastly, DNA sequencing was carried out to confirm that the BNRF1-latent protein gene fusion was correctly constructed.

Next, the newly generated 293/EBV-EC3 (150 bp) producer cell line was analysed for its ability to support lytic replication and produce modified virions. A plasmid encoding the lytic cycle transactivator BZLF1 was transfected into producer cells and they were analysed with immunofluorescence for the expression of the late lytic protein gp350 (Fig. 3.1D). This showed that the 293/EBV-EC3 (150 bp) cell line gave a similar percentage of gp350-positive cells as the 293/wtEBV producer cell line. Furthermore, qPCR analysis of supernatants from the 293/EBV-EC3 (150 bp) producer cells frequently gave titers in the range of 1×10^7 genome equivalents (geq)/mL (data not shown), which is similar to 293/wtEBV producer cells. These results indicate that BNRF1 can be modified to contain latent antigens without influencing lytic replication in producer cells.

3.1.2. The antigenicity of EBV mutants containing BNRF1-latent protein fusions

The next step was to test the antigenicity of the EBV-E3C (150 bp) virus. To this end, T cells specific for BNRF1 and EBNA3C were used. Autologous lymphoblastoid cell lines (LCLs), which served as antigen-presenting cells (APCs), were pulsed with increasing amounts (geq) of wtEBV and EBV-E3C (150 bp). Concurrently, LCLs were pulsed with peptide (BNRF1 VSD epitope or EBNA3C 5H11 epitope) or medium only, which respectively served as positive and negative controls. The pulsed LCLs were then cocultured with HLA-matched $CD4^+$ T cells that

were specific for BNRF1 VSD or EBNA3C 5H11 epitopes and T-cell activation was determined by quantifying IFN-γ in cell culture supernatants (Fig. 3.2). This revealed that LCLs pulsed with EBV-E3C (150 bp) and wtEBV were recognised to the same degree by BNRF1 VSD-specific $CD4^+$ T cells. This indicates that BNRF1 contained within the EBV-E3C (150 bp) virus is as antigenic as that of wtEBV. This implies that modification of BNRF1 to contain latent antigen does not influence the antigenicity of BNRF1. Furthermore, the T-cell responses that

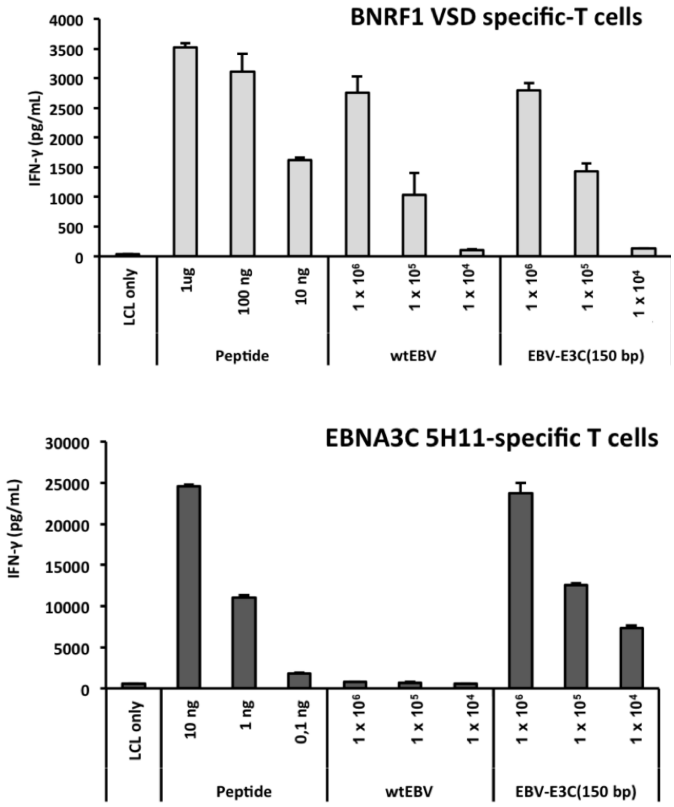

Figure 3.2: EBV virions containing BNRF1-EBNA3C fusion proteins are recognised by EBNA3C-specific $CD4^+$ T cells. The antigenicity of EBV-E3C (150 bp) and wtEBV were concurrently tested against BNRF1 VSD- and EBNA3C 5H11-specific T cells. LCLs were pulsed with 1 x 10^4, 1 x 10^5 and 1 x 10^6 genome equivalents (geq) or peptide controls (pg to µg quantities) and then cocultured with the relevant $CD4^+$ T cells. The degree of T-cell activation was determined by measuring IFN-γ release with ELISA. The data shown in each graph represents triplicate values and error bars indicate standard deviation. Each graph is a representative experiment of at least three.

were generated corresponded to the amount of virus applied. The antigenicity of the EBV-E3C (150 bp) virus was further confirmed through a T-cell activation assay with the EBNA3C 5H11-specific $CD4^+$ T-cell clone. LCLs pulsed with the EBV-E3C (150 bp) virus was well

recognised by the EBNA3C 5H11-specific $CD4^+$ T cells, whilst LCLs pulsed with wtEBV was unrecognised. This confirms that the antigenic spectrum of wtEBV could be enlarged through the construction of BNRF1-latent proteins fusions.

To confirm that the antigenicity of supernatants containing EBV-E3C (150 bp) was exclusively due to BNRF1-EBNA3C fusion proteins contained within viruses, a control experiment was performed with the 72A1 neutralising antibody [143]. Specifically, EBV-E3C (150 bp) and wtEBV supernatants were preincubated with neutralising antibody and used in T-cell antigen

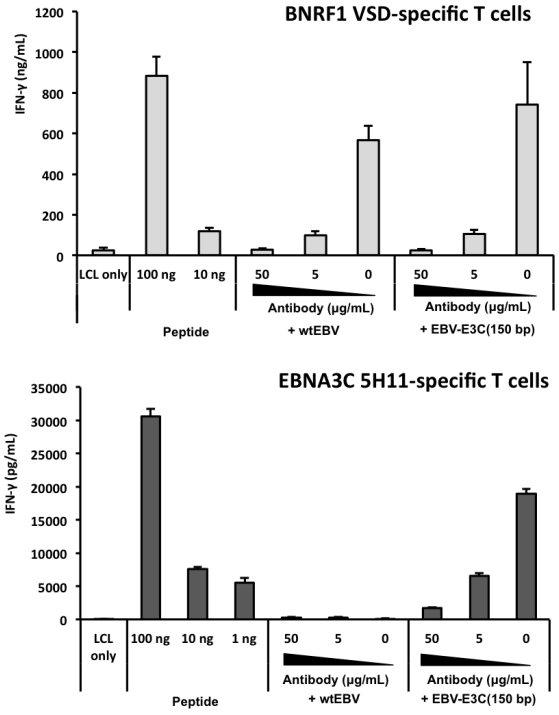

Figure 3.3: Neutralising antibody that recognises gp350 impairs the antigenicity of EBV containing BNRF1-EBNA3C fusion proteins. EBV-E3C (150 bp) and wtEBV supernatants containing 1 x 10^6 geq were pre-incubated with different concentrations of the 72A1 antibody (50, 5 and 0 μg/mL) and mixed with LCLs. Pulsed LCLs were cocultured with BNRF1 VSD- and EBNA3C 5H11-specific $CD4^+$ T and the release of IFN-γ was quantified by ELISA. Each data point shown in the presented graph is the average of triplicate values and error bars represent standard deviation. Furthermore, each graph is a representative experiment of at least three.

recognition assays as before (Fig. 3.3). This showed that the 72A1 neutralising antibody was able to diminish the antigenicity of EBV-E3C (150 bp) and wtEBV, with higher neutralising antibody concentrations having a greater impact. Furthermore, this was the case for BNRF1

and EBNA3C. This confirmed that EBV-E3C (150 bp) stimulates EBNA3C 5H11- and BNRF1 VSD-specific $CD4^+$ T cells with proteins contained within virions.

3.2. Confirming the antigenicity of BNRF1-latent protein fusions in $_{DF}$EBV

3.2.1. The construction of $_{DF}$EBV encoding a BNRF1-latent protein fusion

The next objective was to confirm whether BNRF1-latent protein fusions could also be used to enlarge the antigenic spectrum of $_{DF}$EBV. Since deletion of the glycoprotein gp110 prevents EBV from fusing with host cells [37] and eliminates the toxic potential of its structural proteins [141], only $_{DF}$EBV lacking gp110 was utilised in the present study.

The BNRF1 ORF of wtEBV and $_{DF}$EBV BAC DNA were concurrently modified to contain EBNA3C and EBNA1 coding-sequences. EBNA1 is the latent protein most frequently recognised by the population [144], and is expressed in all types of latency (except type 0) and in all EBV-positive malignancies [145]. This implies that EBNA1 is also a promising candidate for prophylactic vaccination in addition to EBNA3C. A 300 bp fragment encoding the EBNA3C 5H11 and EBNA1 3E10 epitopes was successfully introduced into wtEBV and $_{DF}$EBV BAC DNA (Fig. 3.4A and B). Next, recombinant BAC DNA mutants were introduced into 293 cells in order to generate producer cells. The BAC DNA contained within 293 producer cells were rescued in *E.coli* and were analysed alongside the BAC DNA originally generated in *E.coli* through galK recombination (Fig. 3.4C and D). Digestion of $_{DF}$EBV-E3C-E1 (300 bp) and $_{DF}$EBV-E3C-E1 (300 bp) BAC DNA with *Eco*RI gave rise to a 4.5 kb, while digestion with *Bam*HI gave rise to a 11 kb fragment. This showed that BAC DNA contained within producer cells was the same as the BAC DNA constructed in *E.coli*. Lastly, recombinant BAC DNA mutants were subjected to DNA sequencing to confirm that the BNRF1-EBNA3C-EBNA1 gene fusions were correctly constructed.

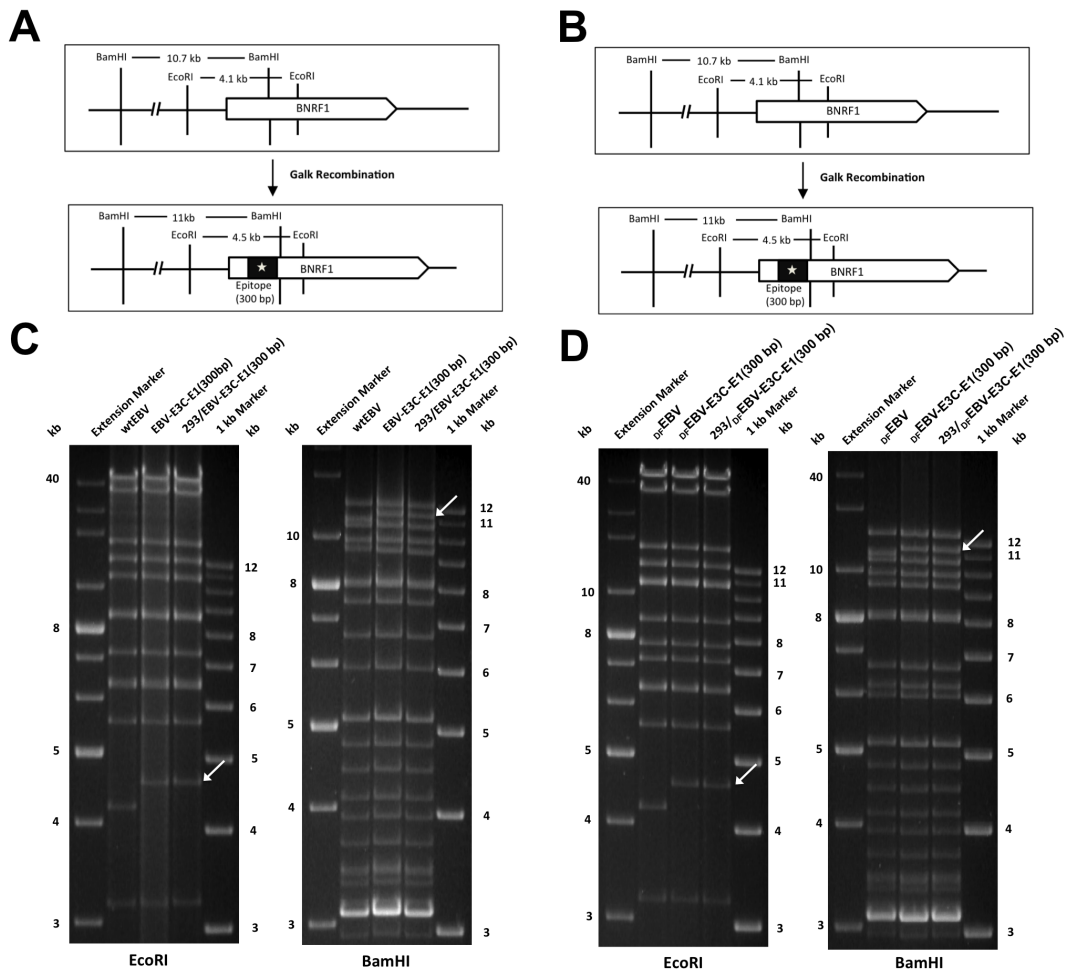

Figure: 3.4 Construction of wtEBV and $_{DF}$EBV BAC clones encoding BNRF1-EBNA3C-EBNA1 fusion proteins. The BNRF1 ORF from wtEBV (A) and $_{DF}$EBV (B) are shown before and after recombination with the 300 bp EBNA3C-EBNA1 fragment. The schematic indicates position of *Eco*RI and *Bam*HI restriction sites before and after recombination, as are the size of fragments generated by these enzymes. Digestion of EBV-E3C-E1 (300 bp) (C) and $_{DF}$EBV-E3C-E1 (300 bp) (D) BAC DNA from *E.coli* and 293 producer cells with *Eco*RI and *Bam*HI. White arrows emphasise DNA fragments that are different between unmodified and modified BAC DNA.

3.2.2. Quantification of $_{DF}$EBV with flow cytometry

The quantification of $_{DF}$EBV was a prerequisite to determine its antigenicity. However, since $_{DF}$EBV lacks DNA, one cannot use real-time qPCR for quantification purposes. Instead, the B-cell-binding ability of $_{DF}$EBV was exploited for quantification purposes (Fig. 3.5A). First, wtEBV was titrated and incubated with Elijah B cells and quantified with flow cytometry (Fig. 3.5B). This showed the amount of virus that bound to B cells correlated to virus titre. The median fluorescence intensity (MFI) was determined for each histogram and then plotted

against virus titre (geq) (Fig. 3.5C). This revealed that the relationship between the MFI and virus titre was linear. Since MFI values could be easily determined for $_{DF}$EBV, the linear relationship shown in Figure 3.5 C could be used to quantify the number of $_{DF}$EBV particles that were contained within cell culture supernatants.

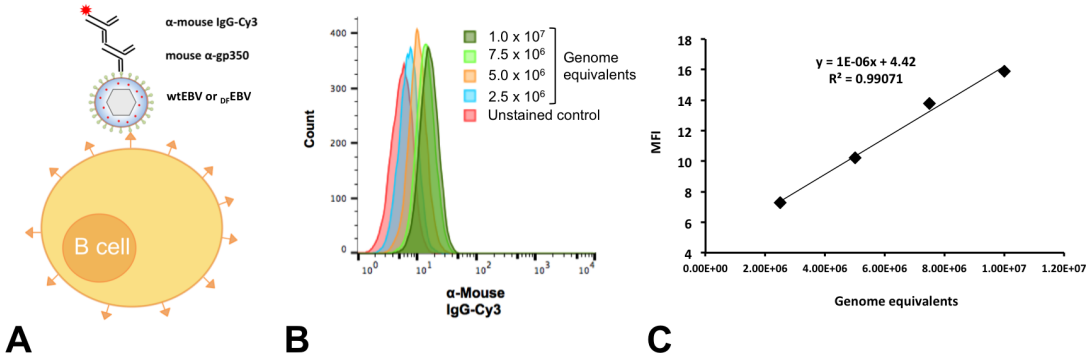

Figure 3.5: $_{DF}$EBV can be reliably quantified with flow cytometry. (A) Schematic representation of the experimental setup. B cells exposed to wtEBV or $_{DF}$EBV were stained with mouse α-gp350 (72A1 clone) and α-mouse IgG-Cy3 antibodies and analysed with flow cytometry. (B) wtEBV quantified with real-time qPCR was added in increasing amounts (2.5 x 10^6 - 1.0 x 10^7 geq) to B cells and analysed with flow cytometry. Histograms representing B cells bound by wtEBV are overlaid. (C) The median fluorescence intensity (MFI) values from the histograms shown in (B) were plotted against virus titre (qeq). This revealed a linear relationship between MFI and virus titre.

3.2.3. A comparison of EBV-E3C-E1 (300 bp) and $_{DF}$EBV-E3C-E1 (300 bp)

After normalisation with flow cytometry, the B-cell binding ability and antigenicity of EBV-E3C-E1 (300 bp) and $_{DF}$EBV-E3C-E1 (300 bp) were compared. Equal quantities of EBV-E3C-E1 (300 bp) and $_{DF}$EBV-E3C-E1 (300 bp) were incubated with EBV-negative Elijah B cells and then analysed with immunofluorescence (Fig. 3.6A). This indicated that EBV-E3C-E1 (300 bp) and $_{DF}$EBV-E3C-E1 (300 bp) bound to B cells to a similar degree, as is indicated by the number of particles bound to cells. Similarly, B cells were incubated with EBV-E3C-E1 (300 bp) and $_{DF}$EBV-E3C-E1 (300 bp) as before and analysed with flow cytometry (Fig. 3.6B). This showed that 82.6% of B cells incubated with EBV-E3C-E1 (300 bp) were gp350-postive, while 83.7% of B cells incubated with $_{DF}$EBV-E3C-E1 (300 bp) stained gp350-postive. This confirmed that

that both EBV-E3C-E1 (300 bp) and $_{DF}$EBV-E3C-E1 (300 bp) bound to B cells with a similar efficiency. Thus, confirming that $_{DF}$EBV can be reliably quantified with flow cytometry.

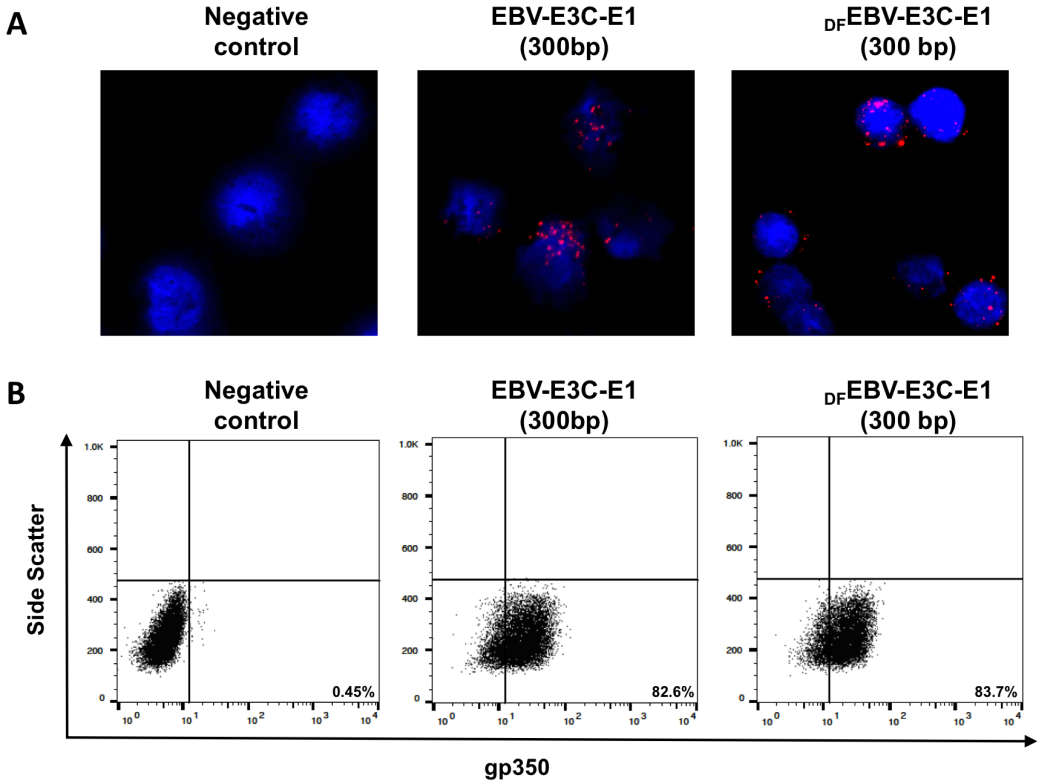

Figure 3.6: Normalised EBV-E3C-E1 (300 bp) and $_{DF}$EBV-E3C-E1 (300bp) bind to B cells to a similar degree. EBV-negative Elijah B cells were exposed to EBV-E3C-E1 (300 bp) (1 x 106 geq) and DFEBV-E3C-E1 (300bp) (1 x 106 particles) and analysed by immunofluorescence (A) and flow cytometry (B). Particles bound to B cells were stained with α-gp350 and α-mouseIgG-Cy3 antibodies prior to analysis. DAPI staining was carried out in order visualise individual cells with immunofluorescence. PBS was used as a negative control in all experiments.

Next, the antigenicity of normalised EBV-E3C-E1 (300 bp) and $_{DF}$EBV-E3C-E1 (300 bp) were compared in T-cell activation assays. T cells having four different specificities were analysed for their ability to recognise LCLs pulsed with EBV-E3C-E1 (300 bp) and $_{DF}$EBV-E3C-E1 (300 bp) (Fig. 3.7). This showed that BNRF1 VSD-, gp350 1D6-, EBNA3C 5H11-, EBNA1 3E10-specific $CD4^+$ T cells released similar amounts of IFN-γ when cocultured with EBV-E3C-E1 (300 bp)- or $_{DF}$EBV-E3C-E1 (300 bp)-pulsed LCLs. This confirmd that the antigenicity of modified $_{DF}$EBV, which lacked gp110, was the same as modified EBV that contained gp110.

Additionally, these results showed that $_{DF}$EBV could successfully be modified to contain different latent antigens.

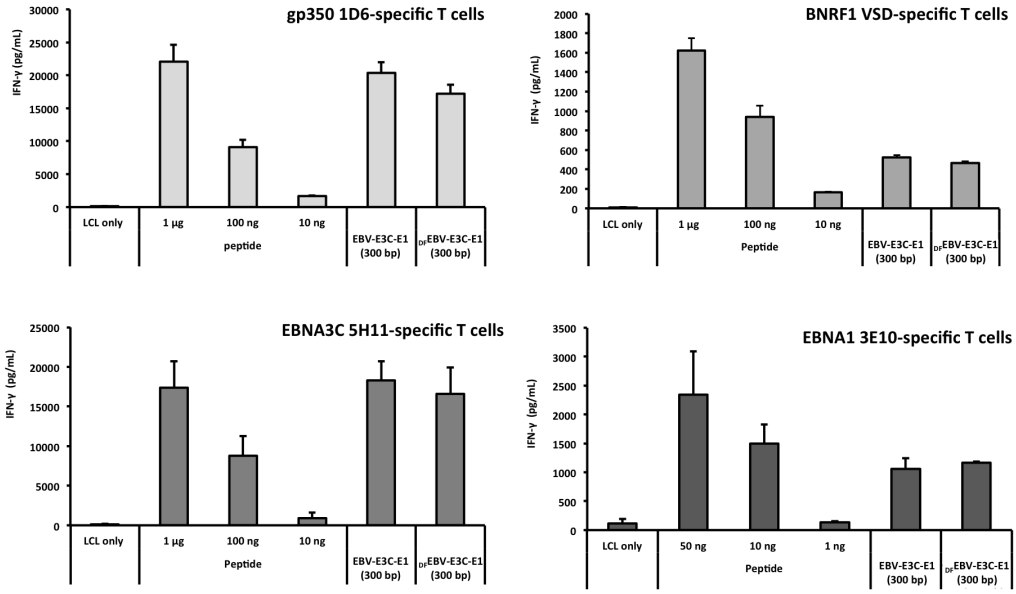

Figure 3.7: $_{DF}$EBV containing EBNA3C (E3C) and EBNA1 (E1) is antigenic despite lacking gp110. LCLs were concurrently pulsed with 1 x 10^6 particles of $_{DF}$EBV-E3C-E1 (300bp) and 1 x 10^6 geq of EBV-E3C-E1 (300 bp) and cocultured with BNRF1 VDS-, gp350 1D6-, EBNA3C 5H11- and EBNA1 3E10-specicific $CD4^+$ T cells. Additionally, LCLs were pulsed with the relevant control peptides prior to being cocultured with T cells. The recognition of LCLs by the relevant T cells was quantified with an IFN-γ ELISA. Each data point shown in the presented graph is the average of triplicate values and error bars represent standard deviation. Furthermore, each graph is a representative experiment of at least three.

3.3. BNRF1 mutants containing large latent protein fragments

3.3.1. The construction BNRF1 mutants containing large EBNA3C fragments

Thus far, $_{DF}$EBV was successfully engineered to contain well-defined epitopes from EBNA1 and EBNA3C. However, the ideal prophylactic candidate should contain enough latent protein epitopes to cover the majority of HLA haplotypes encoded by the human population. One way to maximise the number of epitopes within $_{DF}$EBV, is through the introduction of large latent protein fragments.

To explore this possibility, large EBNA3C coding-sequences were introduced into the BNRF1 of EBV. Specifically, 600 bp and 900 bp fragments from EBNA3C were introduced into the

BNRF1 ORF using galK recombination. Since, two EBV mutants have already been constructed that contain 150 bp or 300 bp within the BNRF1 ORF, it enabled the analysis of EBV mutants that encode BNRF1-latent protein fusions of different size. The construction of EBV-E3C (600 bp) and EBV-E3C (900 bp) BAC DNA mutants are shown in Figure 3.8 A and B. Producer cells were generated using the mutant EBV BAC DNA and BAC DNA from 293/EBV-E3C (600 bp) and 29/EBV-E3C (900 bp) producer cells digested with *Eco*RI and *Bam*HI to determine their integrity (Fig. 3.8 C and D). As expected, digestion with of EBV-E3C (600 bp)

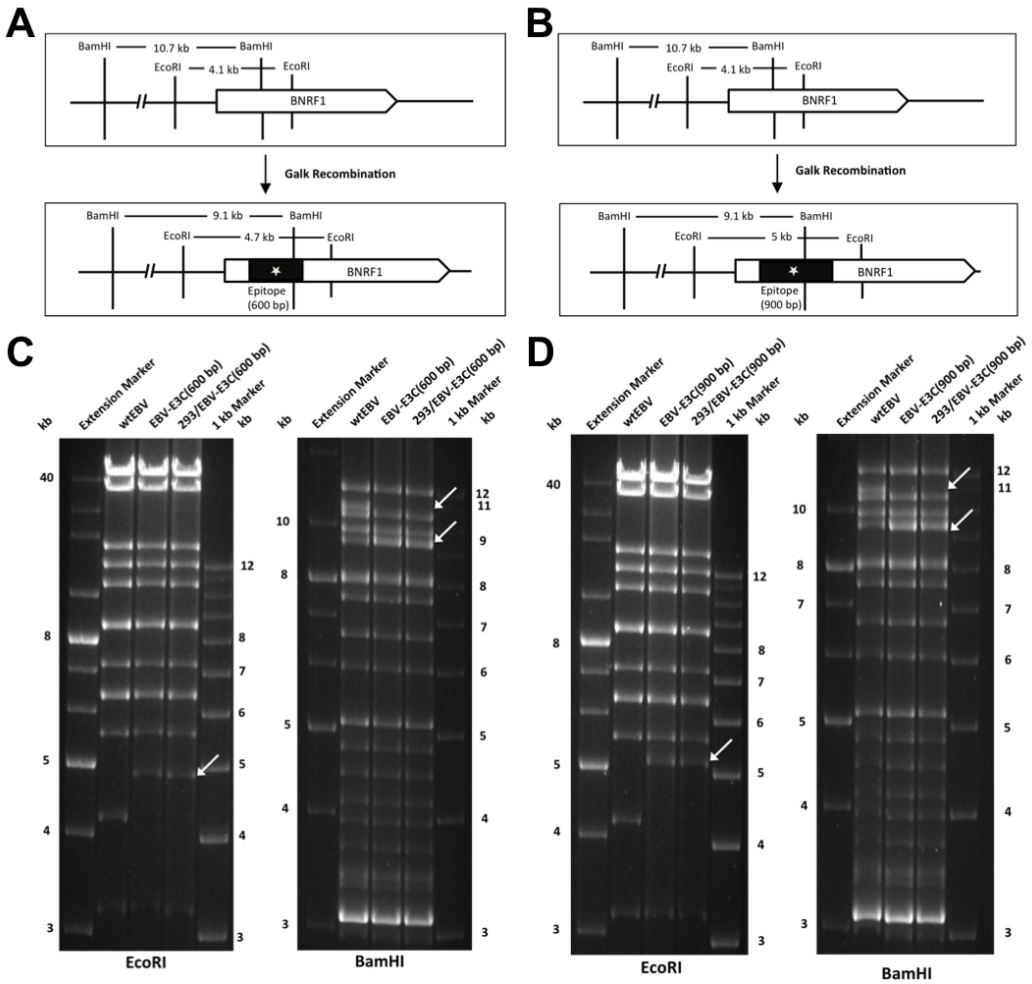

Figure 3.8: Construction of EBV BAC DNA encoding large BNRF1-EBNA3C fusions. Galk recombination was carried out with EBNA3C-coding sequences spanning 600 bp (A) and 900 bp (B). The schematic indicates position of *Eco*RI and *Bam*HI restriction sites before and after recombination, as well as the size of fragments generated by these enzymes. Recombinant BAC DNA from *E.coli* and 293 producer cells were analysed via restriction digestion. *Eco*RI and *Bam*HI were selected to interrogate the integrity of EBV-E3C (600 bp) (C) and EBV-E3C (900 bp) (D). White arrows emphasise DNA fragments that are different between wild-type EBV DNA (B95-8) and DNA modified with galK recombination.

and EBV-E3C (900 bp) BAC DNA with *Eco*RI respectively gave rise to 4.7 kb and 5 kb fragments, whilst digestion with *Bam*HI gave rise to a 9.1 kb band. Lastly, BAC DNA mutants were analysed by sequencing to confirm their integrity.

3.3.2. The expression and packaging of BNRF1-latent protein fusions of increasing size

The 293/EBV-E3C (150 bp), 293/EBV-E3-E1C (300 bp), 293/EBV-E3C (600 bp) and 293/EBV-E3C (900 bp) producer cells were analysed for their ability to express BNRF1-fusion proteins and package them into virions. The expression of BNRF1 within producer cell lines was tested after they had been induced to undergo lytic replication (Fig. 3.9A). This showed that almost all BNRF1-latent protein fusions, except for the one encoded by the 293/EBV-E3C (900 bp) producer cell line, were successfully expressed. In those producer cell lines that were positive for BNRF1-latent protein expression, the molecular weight of proteins were higher when they encoded larger latent protein-coding sequences. Additionally, the expression levels of different BNRF1-latent protein fusions were found to vary. It is unclear whether the slight variation in expression levels were due to differences in expression efficiency, protein stability or whether it was due to different degrees of lytic replication in the induced producer cells. However, none of these possibilities were followed-up.

Next, the ability of the different BNRF1-latent protein fusions to be packaged into virions was tested. The ability of virions to stimulate BNRF1 VSD-specific $CD4^+$ T cells (see section 3.1.2 and 3.2.3) implies that they contain BNRF1. Thus, the ability of virions to stimulate BNRF1-specific $CD4^+$ T cells was used as a read-out for successful packaging of BNRF1-latent protein fusions. This revealed that all modified viruses, except for EBV-E3C (900 bp), successfully stimulated BNRF1 VSD-specific $CD4^+$ T cells (Fig. 3.9B), indicating that the EBV-E3C (900 bp) virus was the only one that did not contain a BNRF1-latent protein fusion. This result is unsurprising, especially since the 293/EBV-E3C (900 bp) producer cell line was found

to lack BNRF1 protein upon western blot analysis. The the EBV-E3C (150 bp), EBV-E3C-E1 (300 bp) and EBV-E3C (600 bp) viruses were all shown to stimulate the BNRF1 VSD-specific $CD4^+$ T cells, indicating that they all successfully packaged their BNRF1-latent protein fusions. There was a slight reduction in recognition by the T cells as the size of the BNRF1-latent protein fusions increased, indicating that an increase in fusion protein size might have a slight negative impact on packaging into virions. Taken together, these results indicate that large BNRF1-latent epitope fusions, assuming they are expressed by producer cells, are successfully incorporated into virus particles. From the current set of experiments, it

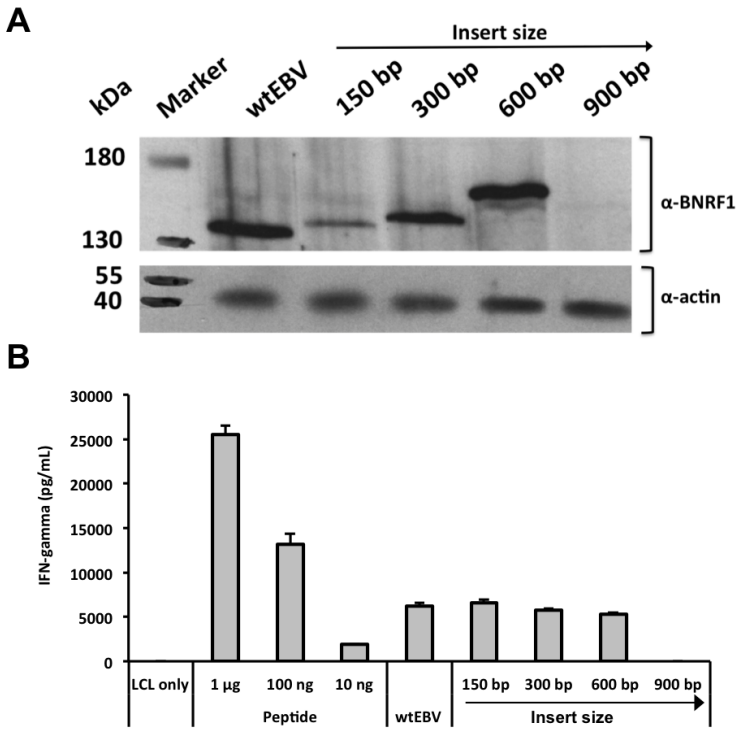

Figure 3.9: Testing the expression and antigenicity of BNRF1-EBNA3C fusions of increasing size. (A) Induced 293 producer cells containing various recombinant EBV mutants were analysed by western blot with α-BNRF1 and α-actin antibodies. (B) The antigenicity of BNRF1-EBNA3C fusions of increasing size. Autologous LCLs were pulsed with the same amount (1 x 10^6 genomes/mL) of modified EBV encoding BNRF1-latent protein fusions of increasing size. The pulsed LCLs were cocultured with BNRF1-specific $CD4^+$ T cells and the release of IFN-γ quantified with ELISA. Each data point shown in the presented graph is the average of triplicate values and error bars represent standard deviation. Furthermore, each graph is a representative experiment of at least three.

appears as though 600 bp is the largest latent protein coding-sequence that can successfully be accommodated by BNRF1. From this perspective it is unclear whether EBNA3C is optimal for fusion to BNRF1. EBNA3C has a very large ORF, 2982 bp to be exact, and only encodes a total of eleven CD4-restricted epitopes [115].

3.4. $_{DF}$EBV encoding BNRF1-EBNA1 fusion proteins

3.4.1. The construction of $_{DF}$EBV mutants encoding BNRF1-EBNA1 fusion proteins

A strategy for maximising the number of latent protein epitopes within $_{DF}$EBV is by exclusively utilising epitope-rich antigens. A previous study has mapped the epitopes of several latent proteins, and has shown that EBNA1 is particular abundant in CD4-restricted epitopes [115]. Furthermore, the majority of epitopes within EBNA1 are concentrated in a single region spanning roughly 200 amino acids (Fig. 3.10A).

The epitope-rich region of EBNA1 was used to construct three $_{DF}$EBV BAC DNA mutants (Fig. 3.10 B and C). One mutant, termed $_{DF}$EBV-EBNA1$^{RI:II}$, was constructed to encode the majority of $CD4^+$ epitopes from EBNA1. The EBNA1-coding sequence used to construct this mutant was around ~700 bp in length. Since 700 bp is very close to the upper limit identified in section 3.3, two additional mutants were constructed to contain smaller regions of EBNA1. These mutants, $_{DF}$EBV-EBNA1^{RI} and $_{DF}$EBV-EBNA1^{RII}, contained regions from the EBNA1 ORF that are ~350 bp in length. Recombinant BAC DNA mutants were introduced into 293 cells to generate producer cell lines. Restriction analysis of was performed with *Eco*RI (Fig. 3.10C) and *Bam*HI (not shown) to confirm the integrity of BAC DNA contained within producer cells. Digestion of $_{DF}$EBV-EBNA1^{RI}, $_{DF}$EBV-EBNA1^{RII} and $_{DF}$EBV-EBNA1$^{RI:II}$ with *Eco*RI and *Bam*HI gave rise to the expected restriction fragments. In particular, digestion of $_{DF}$EBV-EBNA1^{RI} and $_{DF}$EBV-EBNA1^{RII} with *Eco*RI rise to 4.5 kb fragment, while digestion of $_{DF}$EBV-EBNA1$^{RI:II}$ gave rise to a 4.8 kb fragment. Finally, BAC DNA was analysed with sequencing to validate the BNRF1-EBNA1 gene fusions.

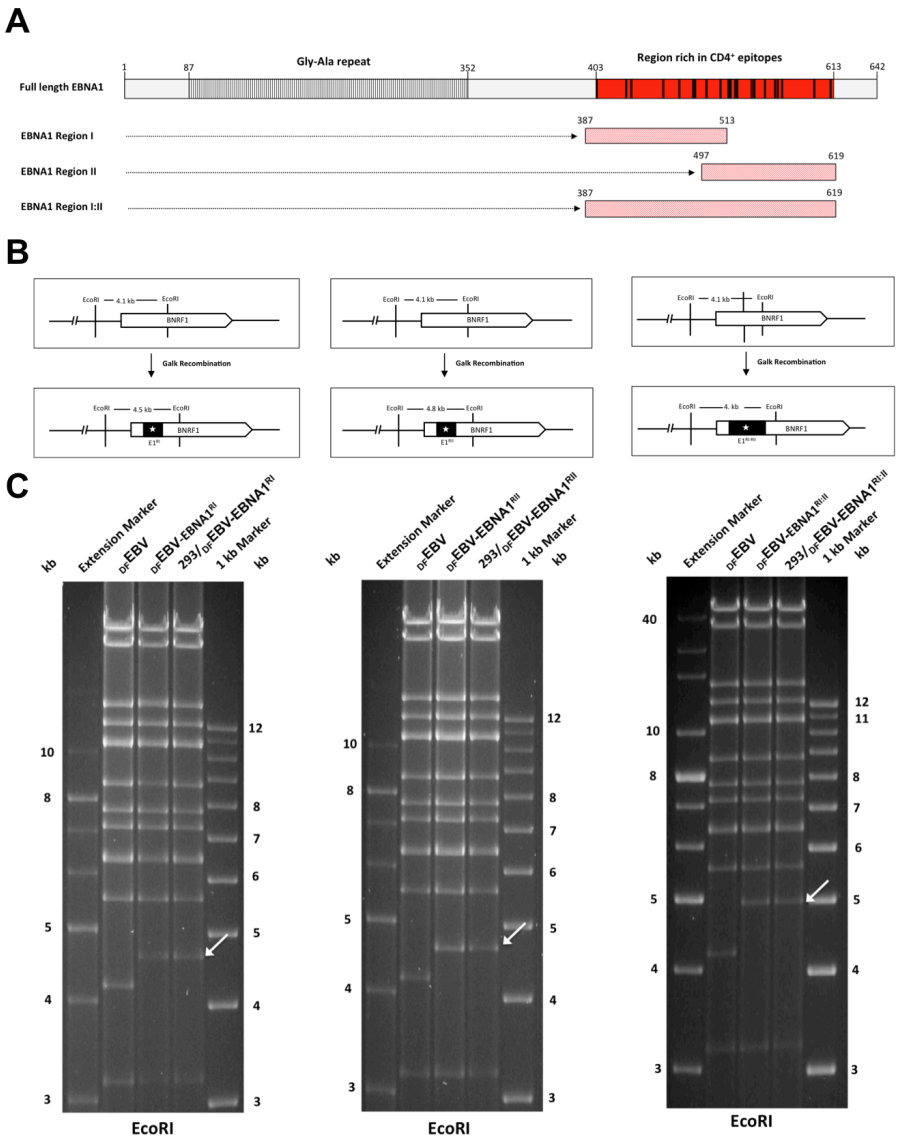

Figure 3.10: Construction of $_{DF}$EBV BAC DNA encoding BNRF1-EBNA1 fusions. (A) The EBNA1 protein contains numerous CD4^{+} T-cell epitopes. Many of the CD4^{+} T-cell epitopes contained within EBNA1 are found within a single stretch a little bit more than 200 aa in length. In total, the epitope rich region encompasses approximately 20 CD4-restricted epitopes, with each epitope being represented by a black bar. The EBNA1 gene also contains a stretch of gly-ala repeats that prevent presentation on HLA class I molecules. The coding sequences for region I, II and I:II, which were arbitrarily named, were introduced into the BNRF1 ORF to respectively give rise to $_{DF}$EBV-EBNA1^{RI,} $_{DF}$EBV-EBNA1^{RII} and $_{DF}$EBV-EBNA1$^{RI:II}$ BAC mutants. (B) Schematic representations of the BNRF1 ORF before and after recombination with EBNA1-coding sequences. The BNRF1 gene was modified to contain region I (left), region II (middle) and region I:II (right) of EBNA1. *Eco*RI restriction sites are indicated, as are restriction fragments generated by *Eco*RI digestion. (C) Recombinant $_{DF}$EBV BAC DNA constructed in *E.coli* is the same as BAC DNA contained within 293 producer cells. $_{DF}$EBV-EBNA1^{RI} (left), $_{DF}$EBV-EBNA1^{RII} (middle) and $_{DF}$EBV-EBNA1$^{RI:II}$ (right) BAC DNA from *E.coli* and 293 producer cells were analysed via restriction digestion with *Eco*RI. White arrows emphasise DNA fragments that are different between unmodified DFEBV BAC DNA and DNA modified with galK recombination.

3.4.2. The expression $_{DF}$EBV encoding BNRF1-EBNA1 fusions

The ability of 293/$_{DF}$EBV-EBNA1^{RI}, 293/$_{DF}$EBV-EBNA1^{RII} and 293/$_{DF}$EBV-EBNA1$^{RI:II}$ producer cells to express the BNRF1-EBNA1 fusion proteins was tested via western blot (Fig. 3.11). This showed that the 293/$_{DF}$EBV-EBNA1$^{RI:II}$ producer cell line failed to expressed its BNRF1-EBNA1 fusion protein, whilst the 293/$_{DF}$EBV-EBNA1^{RI} and 293/$_{DF}$EBV-EBNA1^{RII} producer cell lines successfully expressed their BNRF1-EBNA1 fusion proteins. This is the second instance in which the insertion of a latent protein-coding sequence larger than 600 bp precluded the expression of a BNRF1-latent protein fusion. Since the $_{DF}$EBV-EBNA1$^{RI:II}$ mutant failed to express the BNRF1-EBNA1 fusion protein, it was excluded from further analysis. Conversely, $_{DF}$EBV-EBNA1^{RI} and $_{DF}$EBV-EBNA1^{RII} successfully expressed their BNRF1-EBNA1 fusion proteins and were used in further experiments.

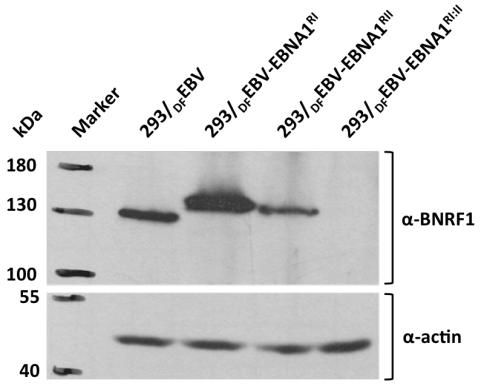

Figure 3.11: The expression of BNRF1-EBNA1 fusion proteins by the 293/$_{DF}$EBV-EBNA1^{RI}, 293/$_{DF}$EBV-EBNA1^{RII} and 293/$_{DF}$EBV-EBNA$^{RI:RII}$ producer cell lines. The lytic cycle transactivator BZLF1 was transfected into producer cells and they were analysed after 3 days with western blotting. Staining was pefromed with the α-BNRF1 and α-actin antibodies.

3.5. Investigating the antigenicity of $_{DF}$EBV containing EBNA1 *ex vivo*

Next, the antigenicity $_{DF}$EBV containing BNRF1-EBNA1 fusion proteins was tested in an *ex vivo* setting. To this end, $_{DF}$EBV-EBNA1^{RI} and $_{DF}$EBV-EBNA1^{RII} were combined in 1:1 ratio, hereafter referred to as $_{DF}$EBV-EBNA1^{RI+RII}, and used to stimulate memory CD4^{+} T cells from an unhaplotyped EBV-positive donor. However, since $_{DF}$EBV-EBNA1^{RI+II} is an assemblage of

several dozen EBV proteins [8], it would stimulate of a broad pool of EBV-specific memory T cells from EBV-positive donors. In order to assess the relevance of EBNA1 contained within $_{DF}$EBV *ex vivo*, it was necessary to develop a means of distinguishing EBNA1-specific T cells from structural protein-specific T cells. For this purpose, antigen-armed antibodies (AgAbs) were utilised [146]. AgAbs are antibody-antigen fusion proteins that enable the stimulation of $CD4^+$ T cells of interest. AgAbs deliver their antigenic attachments to antigen-presenting cells, which process and present the antigenic peptides on HLA class II molecules to $CD4^+$ T cells. Section 3.5.1 describe the construction of AgAbs that contain EBNA1 or gp350 antigenic attachments and their validation as tools for the *ex vivo* expansion of T cells, whilst section 3.5.2 describes the use of AgAbs to expand EBNA1- and gp350-specific $CD4^+$ T cells from polyclonal pools of T cells generated with $_{DF}$EBV-EBNA1^{RI+RII}.

3.5.1. Antigen-Armed antibodies as a means of expanding $CD4^+$ T cells *ex vivo*

3.5.1.1. Generation of Antigen-armed antibodies

In the present study, AgAbs were constructed by fusing antigenic moieties downstream of the CH3 domain of an α-CD20 antibody (see section 5.2.11 for details). Since the α-CD20 antibody specifically binds to CD20 on B cells, it enables α-CD20-based AgAbs to be delivered to LCLs. AgAbs that bind to LCLs are internalised, processed and their antigenic peptides are presented to the relevant T cells [146]. AgAbs containing EBNA1 and gp350 antigenic attachments are shown in Figure 3.12A. These AgAbs were engineered to contain large antigenic fragments from EBNA1 (232 aa) and gp350 (470 aa) to maximise their potential of expanding EBV-specific T cells from unhaplotyped EBV-positive individuals.

In the present study, the EBNA1-AgAb and gp350-AgAb were produced by transfecting 293 cells with AgAb heavy chains along with an α-CD20 light chain. Assembled AgAbs were secreted into the cell culture medium, quantified with ELISA and analysed with western blotting under non-reducing conditions (Fig. 3.12B). This showed that the EBNA1-AgAb and

gp350-AgAb were larger than the unmodified α-CD20 antibody. Next, the ability of the AgAbs to bind to LCLs was tested (Fig. 3.12C). LCLs were incubated with medium or equal quantities of EBNA1-AgAB, gp350-AgAb, α-CD20 or isotype control and analysed with flow cytometry. This showed that both AgAbs bound to LCLs to the same degree as unmodified α-CD20 antibody, whilst the isotope control antibody did not interact strongly with the LCLs. This indicated that the antigenic attachments of AgAbs do not interfere with their ability to bind to LCLs.

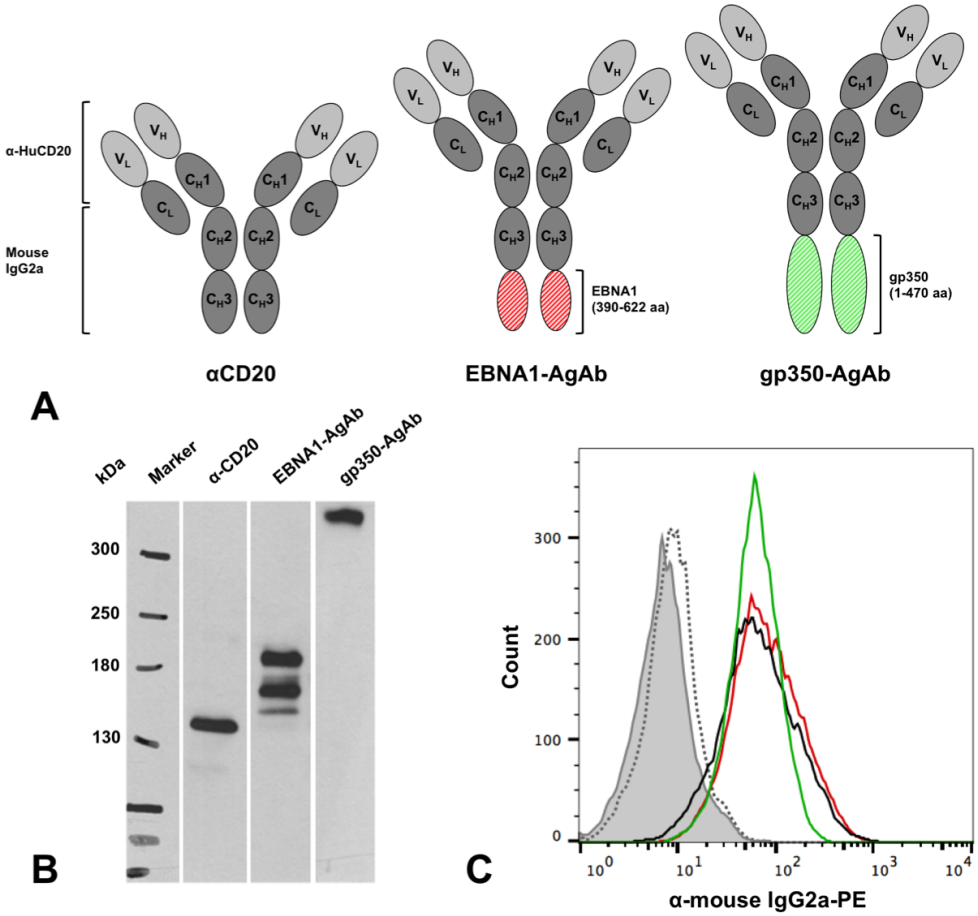

Figure 3.12: Production of EBNA1 and gp350 containing AgAbs. (A) The domain structure of assembled AgAb molecules compared to unmodified α-CD20. (B) Western blot analysis of AgAbs under non-reducing conditions. A total of 1 ng of each AgAb and α-CD20 antibody was loaded and staining was performed with α-mouse IgG-HRP. (C) AgAbs bind efficiently to B cells. LCLs were incubated with 125 pmole of α-CD20 (black line), EBNA1-AgAb (red line), gp350-AgAb (green line) or isotype control (dotted line), stained with α-mouse IgG2a-PE and analysed with flow cytometry. Unstained LCLs were analysed in parallel (solid grey).

3.5.1.2. Confirming the antigenicity of AgAbs

AgAbs were interrogated *in vitro* and *ex vivo* to confirm their antigenicity. For *in vitro* experiments, $CD4^+$ T cells were used that recognise the EBNA1 3G2 or gp350 1D6 epitopes. Autologous LCLs were pulsed with EBNA1-AgAb, gp350-AgAb, control peptides (3G2 and 1D6 epitopes) or medium (negative control) and then cocultured with the $CD4^+$ T cells. T-cell activity was determined by quantifying the release of IFN-γ with an ELISA (Fig. 3.13). This showed LCLs pulsed with EBNA1-AgAb, gp350-AgAb or control peptides were capable of stimulating the EBNA1- and gp350-specific $CD4^+$ T cells, whilst LCLs pulsed with medium only were not recognised by the T cells.

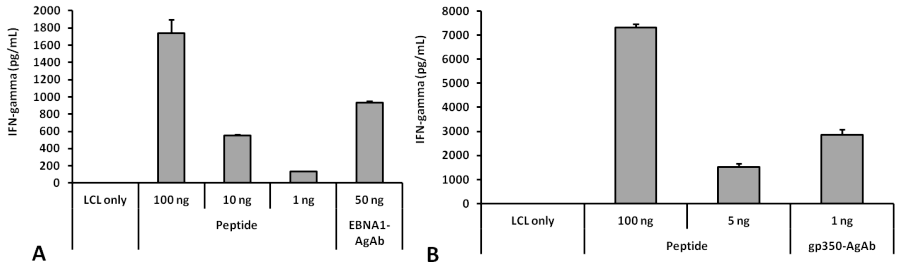

Figure 3.13: The EBNA1-AgAb and gp350-AgAb are antigenic. T cells specific for the EBNA1 3G2 epitope (A) and the gp350 1D6 epitope (B) were cocultured with LCLs pulsed with peptide controls, AgAbs or medium. The release of IFN-γ was measured with an ELISA. Each data point shown in the presented graph is the average of triplicate values and error bars represent standard deviation. Furthermore, each graph is a representative experiment of at least three.

Next, the ability of the gp350-AgAb and EBNA1-AgAb to expand EBV-specific memory T cells from EBV-positive donors was tested. Freshly isolated PBMCs from three donors were consecutively stimulated with AgAbs to expand gp350- and EBNA1-specific $CD4^+$ T cells (Fig. 3.14A). After a minimum of six round of stimulation, expanded cells were analysed with flow cytometry to confirm the presence of $CD4^+$ T cells (Fig. 3.14B). This showed that samples from all donors consisted primarily of $CD4^+$ T cells. Next, it was important to test whether the *ex vivo* expanded $CD4^+$ T cells were specific towards the EBNA1-AgAb or gp350-AgAb (Fig. 3.14C). T-cell activation assays showed that $CD4^+$ T cells specifically recognised LCLs pulsed with AgAbs containing EBNA1 or gp350 antigenic attachments, whilst LCLs pulsed

with α-CD20 or medium only were not recognised. These results confirm that AgAbs containing large antigenic attachments can be used to expand EBV-specific memory $CD4^+$ T cells *ex vivo*.

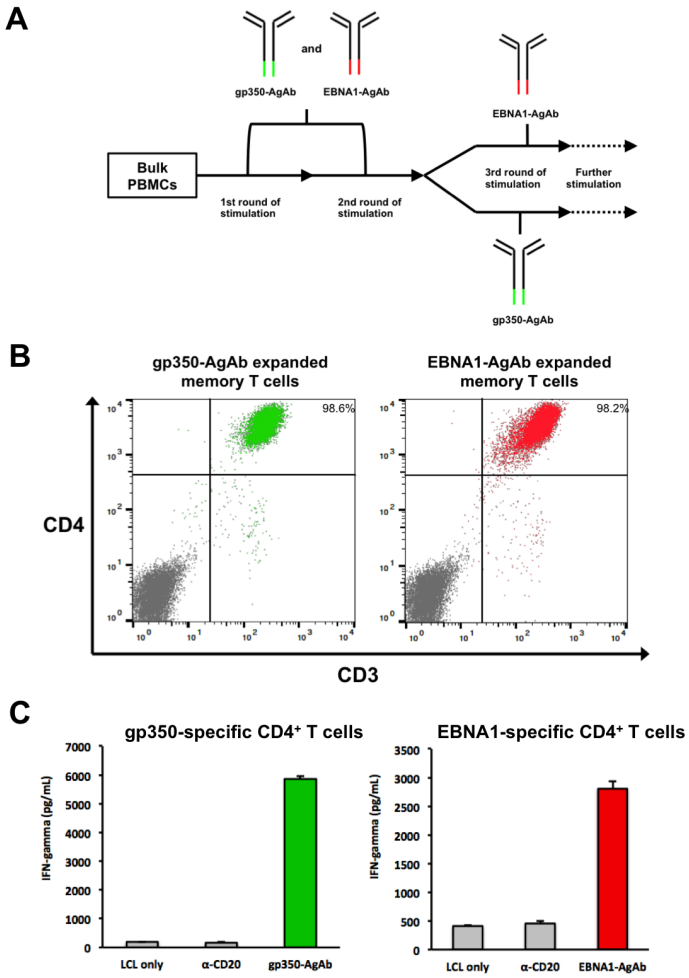

Figure 3.14: AgAbs specifically expand EBV-specific $CD4^+$ memory T cells from EBV-positive donors *ex vivo*. (A) Bulk PBMCs were stimulated with AgAbs for several rounds to enable the expansion of EBNA1- and gp350-specific cell lines. During the first two rounds of stimulation, cells were stimulated with both the EBNA1-AgAb and gp350-AgAb. However, after the second round the EBNA1-AgAb and gp350-AgAb were used separately to respectively enable the expansion of EBNA1- and gp350-specific T cells. (B) *Ex vivo* cultures consisted primarily of $CD4^+$ T cells. After a minimum of six rounds of stimulation, cells were stained with α-CD4-PE-Cy5 and α-CD3-FITC and analysed by flow cytometry. The percentage of CD3/CD4 double-positive cells are indicated. (C) *Ex vivo* expanded $CD4^+$ T cells are specific for AgAbs containing EBNA1 and gp350. Autologous LCLs were pulsed with EBNA1- or gp350-AgAbs, as well as α-C20 and medium. Pulsed LCLs were cocultured with T cells and IFN-gamma release was measured via an ELISA. Representative results from a single donor are given. Each data point shown in the presented graph is the average of duplicate values and error bars represent standard deviation. Furthermore, each graph is a representative experiment of at least two.

3.5.2. Expansion of EBV-specific memory CD4$^+$ T cells with $_{DF}$EBV-EBNA1 and AgAbs

Having validated AgAbs as tools for expanding EBV-specific memory CD4$^+$ T cells from EBV-positive donors, the EBNA1-AgAb and gp350-AgAb were respectively used to expand EBNA1- and gp350-specific CD4$^+$ T cells from PBMCs stimulated with unmodified $_{DF}$EBV or $_{DF}$EBV-EBNA1^{RI+RII} (Fig. 3.15).

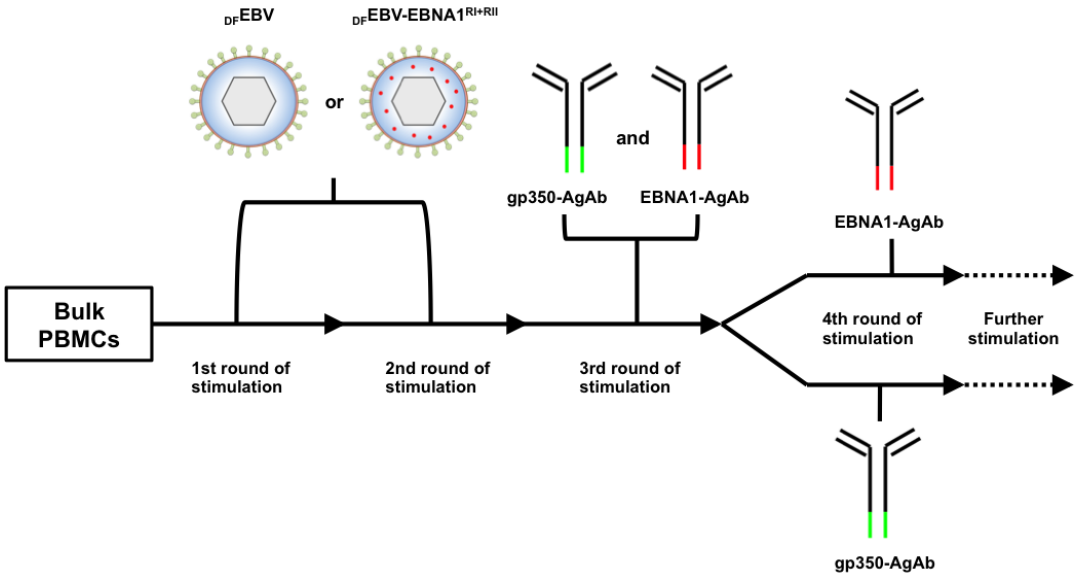

Figure 3.15: Stimulation scheme using $_{DF}$EBV or $_{DF}$EBV-EBNA1^{RI+RII} and AgAbs containing EBNA1 or gp350. Bulk PBMCs were exclusively stimulated with $_{DF}$EBV or $_{DF}$EBV-EBNA1^{RI+RII} for the first two stimulation rounds (~30 days). Thereafter, the EBNA1-AgAb or gp350-AgAb were used to enrich *ex vivo* cultures for the presence of gp350- or EBNA1-specific T cells.

Ex vivo cultures that resulted from at least six rounds of stimulation (see Fig. 3.15) were analysed by flow cytometry and interrogated with T-cell activation assays (Fig. 3.16). Flow cytomteric analysis confirmed that *ex vivo* cultures consisted primarily of CD4$^+$ T cells. T-cell recognition assays showed that gp350-specific CD4$^+$ T cells were expanded from PBMCs that were initially stimulated with $_{DF}$EBV or $_{DF}$EBV-EBNA1^{RI+RII}. However, EBNA1-specific T CD4$^+$ cells were only expanded from PBMCs that were stimulated with $_{DF}$EBV-EBNA1^{RI+RII}. This validated the antigenicity of the EBNA1 moieties contained within $_{DF}$EBV-EBNA1^{RI+RII}. The expanded CD4$^+$ T cells were also screened against several epitope peptides, and found that the EBNA1-specific T cells and gp350-specific T cells respectively responded to the EBNA1

3G2 and gp350 1D6 peptides. However, the gp350-specific T cells stimulated initially with $_{DF}$EBV-stimulated PBMCs were only weakly reactive to the gp350 1D6 epitope. Suggesting that the majority of gp350-specific T cells expanded in this instance are specific for another gp350 epitope.

Taken together, these results confirm that the EBNA1 contained within modified $_{DF}$EBV is antigenic in an *ex vivo* setting, enabling the stimulation of EBNA1-specific CD4$^+$ T cells from an unhaplotyped EBV-positive donor. Additionally, the antigenicity of gp350 contained within modified and unmodified $_{DF}$EBV was also confirmed.

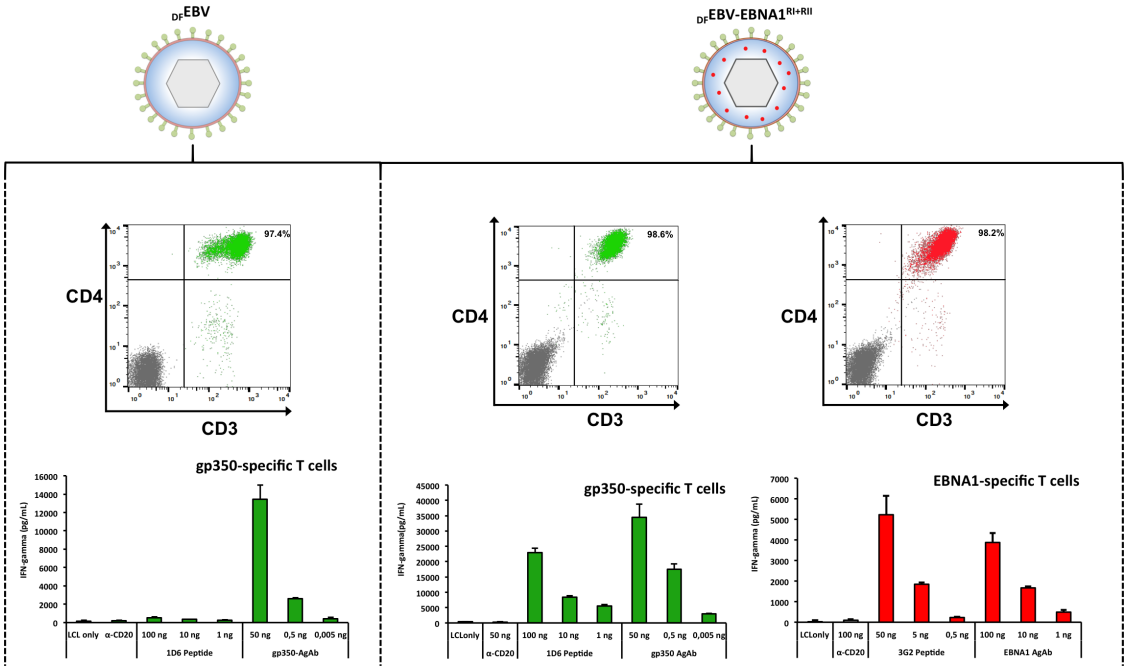

Figure 3.16: The expansion of antigen-specific CD4$^+$ T cells from PBMCs stimulated with $_{DF}$EBV and $_{DF}$EBV-EBNA1^{RI+RII}. PBMCs from a healthy EBV-positive donor were stimulated exclusively with unmodified $_{DF}$EBV or $_{DF}$EBV-EBNA1^{RI+RII} for two rounds. Subsequently, *ex vivo* cultures were stimulated with the gp350-AgAb and/or EBNA1-AgAb for a minimum of four rounds in order to enrich cultures for gp350- or EBNA1-specific T cells. (Top panel) After six rounds of stimulation *ex vivo* cultures contained primarily CD4$^+$ T cells. Cells were stained with α-CD4-PE-Cy5 and α-CD3-FITC prior to analysis. The percentage of CD3/CD4 double-positive cells in *ex vivo* cultures are shown. (Bottom panel) The expanded CD4$^+$ T cells are specific for EBV antigens. Autologous LCLs were pulsed with EBNA1-AgAb, gp350-AgAb, EBNA1 3G2 peptide or gp350 1D6 peptide. Pulsed LCLs were cocultured overnight with the expanded CD4 T-cell lines and IFN-γ release was quantified with an ELISA. Each data point shown in the presented graph is the average of triplicate values and error bars represent standard deviation. Furthermore, each graph is a representative experiment of at least three.

3.6. Determining the cytotoxic ability of ex vivo expanded memory $CD4^+$ T cells

Cytolytic $CD4^+$ T cells are important for controlling EBV infection and its malignant consequences [147-149]. Hence, the *ex vivo* stimulated EBNA1- and gp350-specific T cells (see section 3.5.2) were further characterised to determine whether they were cytolytic in character. First, the memory $CD4^+$ T cells were tested for the expression of CD107a, a surrogate marker for degranulation [150]. The EBNA1- and gp350-specific $CD4^+$ T cells were cocultured with LCLs that were pulsed with either α-CD20 or the relevant AgAb, and were stained for CD4 and CD107a and analysed via flow cytometry (Fig. 4.17). This showed that both EBNA1- and gp350-specific $CD4^+$ T-cells were capable of expressing CD107a when cocultured with the LCLs that were pulsed with the either EBNA1-AgAb or gp350-AgAb. Importantly, LCLs that were pulsed with α-CD20 were significantly less proficient at inducing CD107a expression in the $CD4^+$ memory T-cell lines. In the case of the EBNA1-specific $CD4^+$ T-cell line, CD107a expression was shown to range between 8 and 10%. While the gp350-specific $CD4^+$ T-cell line was shown to express CD107a considerably more, with expression ranging between 35 and 50%.

Once the memory T cells were shown to be positive for CD107 expression, it was necessary to determine whether they were capable of releasing molecules directly involved in cytolysis. Hence, memory $CD4^+$ T cells were analysed for their ability to release the serine protease granzyme B [151]. EBNA1- and gp350-specific $CD4^+$ T cells were cocultured with LCLs pulsed with the relevant AgAbs and epitope peptides and the secretion of granzyme B was detected with an ELISA (Fig. 3.18). This showed that EBNA1- and gp350-specific T cells released considerable amounts of granzyme B in the presence of LCLs pulsed with AgAb and epitope peptides derived from EBNA1 or gp350. Conversely, when the $CD4^+$ T cells were incubated with LCLs that were pulsed with medium or α-CD20, they did not release substantial amounts of granzyme B.

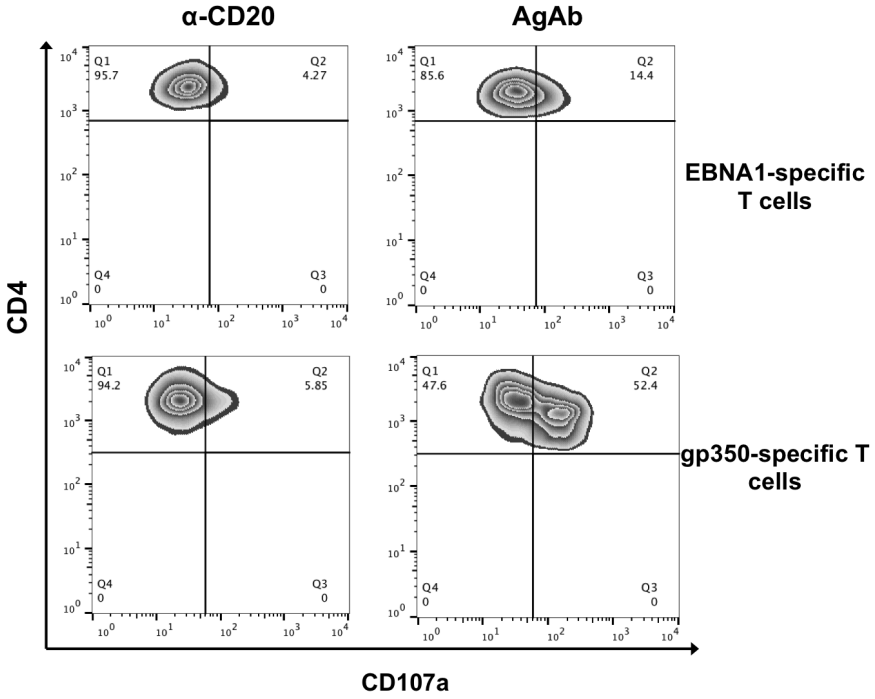

Figure 3.17: Memory $CD4^+$ T cells specific for EBNA1 and gp350 express CD107a. LCLs were pulsed with EBNA1-AgAb or gp350-AgAb and respectively cocultured with EBNA1- or gp350-specific $CD4^+$ T-cells. LCLs were pulsed with α-CD20 as a negative control prior to cocultured with the T cells. After a total of eight hours of coculture, cells were stained with α-CD4-PE-Cy5 and CD107a-FITC and analyzed with flow cytometry. The percentage of cells that were $CD4^+CD107a^+$ double-positive is shown. Representative results from at least three experiments are shown.

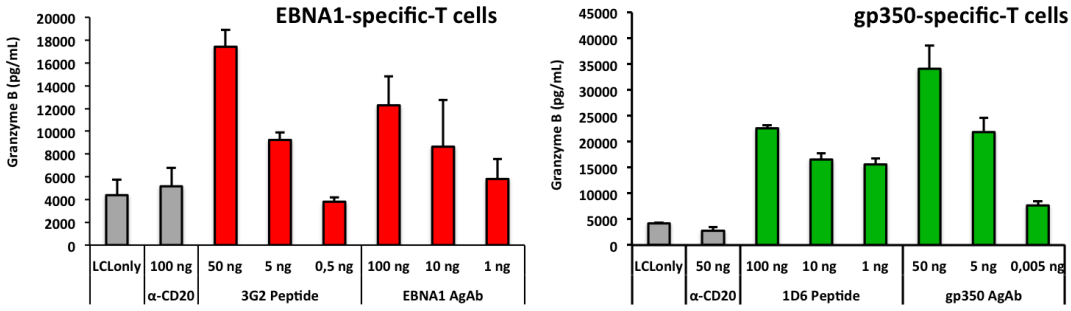

Figure 3.18: *Ex vivo* expanded memory $CD4^+$ T cells release granzyme B in response to EBNA1 or gp350. LCLs were pulsed with EBNA1-AgAb or gp350-AgAbs and were cocultured overnight with memory $CD4^+$ T cells. Similarly, LCLs were also pulsed with EBNA 3G2 or gp350 1D6 peptide and cocultured with the T cells. Cell culture supernatants were tested for granzyme B with an ELISA. Each data point shown in the presented graph is the average of triplicate values and error bars represent standard deviation. Furthermore, each graph is a representative experiment of at least three.

The expression of CD107a and the release of granzyme B suggested that both EBNA1- and gp350-specific $CD4^+$ memory T cells were cytolytic. However, for this to be confirmed it was important to determine whether they could directly kill target cells. To examine the cytolytic ability of the expanded $CD4^+$ memory T cells, a calcein release assay was performed [152]. Living cells convert non-fluorescent calcein AM to fluorescent calcein. The killing of target cells by cytolytic T cells releases calcein into the cell culture supernatant, which can be measured with a fluorimeter. LCLs were pulsed with EBNA1 3G2, gp350 1D6, EBNA3C 5H11 (unrelated peptide) peptides or $_{DF}$EBV-EBNA1^{RI+RII} and were used in calcein release assays with EBNA1- and gp350-specific $CD4^+$ T cells (Fig. 3.19). This showed that the gp350- and EBNA1-specific $CD4^+$ T cells were capable of specifically killing LCLs pulsed with $_{DF}$EBV-EBNA1^{RI+RII} and the appropriate peptide epitopes. Importantly, LCLs pulsed with the EBNA3C 5H11 peptide was incapable of inducing significant levels of killing. The expression of CD107a, the release of granzyme B and the specific killing of target cells confirm that both the EBNA1- and gp350-specific $CD4^+$ T-cell lines were cytotoxic.

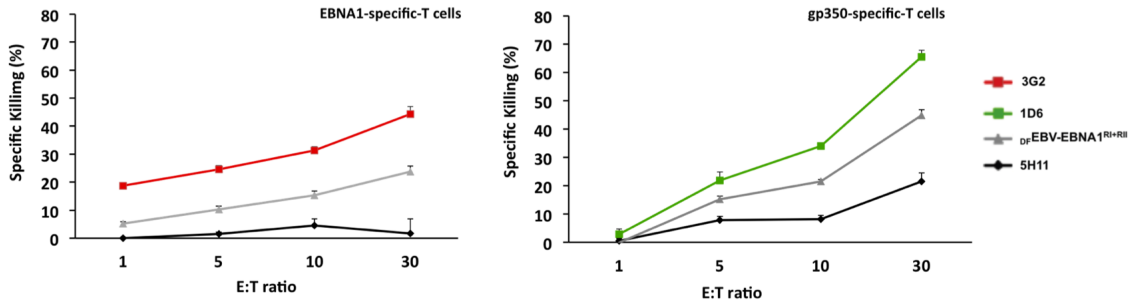

Figure 3.19: CD4+ memory T cells specific for EBNA1 and gp350 directly kill target cells. LCLs were pulsed with $_{DF}$EBV-EBNA1^{RI+RII} (grey line), EBNA1 3G2 (red line) or gp350 1D6 (green line) peptides, and were incubated with calcein AM. As a negative control, LCLs were pulsed with the EBNA3C 5H11 peptide (black line). The pulsed LCLs were incubated with calcein AM and then cocultured with $CD4^+$ T cells specific for EBNA1 or gp350. The release of calcein from targeted cells was measured at 535 nm after excitation with 485 nm light. Each data point shown in the presented graph is the average of triplicate values and error bars represent standard deviation. Furthermore, each graph is a representative experiment of at least two.

Next, the ability of EBNA1- and gp350-specific $CD4^+$ T cells to target recently infected B cells was tested. The infection of primary B cells results in their transformation, outgrowth and the expression of CD23. Thus, CD23 serves as a marker for EBV-mediated B-cell proliferation [153]. To this end, autologous primary B cells were infected with B95-8 EBV (moi = 10), cocultured with EBNA1- or gp350-specific $CD4^+$ T cells for 12 days and analysed with CD19- and CD23-specific antibodies by flow cytometry (Fig. 3.20). As a positive control for B-cell outgrowth, infected B cells were cultured in medium only. Conversely, freshly isolated PBMCs were analysed to identify untransformed B cells. Flow cytomteric analysis of *ex vivo* cultures revealed the presence of three B-cell populations, *viz*. $CD19^+CD23^-$, $CD19^+CD23^{low}$ and $CD19^+CD23^{high}$ populations. Infected B cells cultured in medium only were found to contain primarily (89.7 %) $CD19^+CD23^{high}$ B cells, whilst B cells from freshly isolated PBMCS contain almost no $CD19^+CD23^{high}$ B cells. Nearly all the B cells within freshly isolated PBMCs were $CD19^+CD23^-$. The coculture of EBNA1- or gp350-specific $CD4^+$ T cells with infected B cells was shown to reduce the percentage of $CD19^+CD23^{high}$ B cells. In the presence of gp350-specific $CD4^+$ T cells the $CD19^+CD23^{high}$ population only accounted for ~16 % of total B cells, whilst in the presence of EBNA1-specific $CD4^+$ T cells the $CD19^+CD23^{high}$ accounted for ~50 % of total B cells. These results suggest that both EBNA1- and gp350-specific $CD4^+$ T cells can target $CD19^+CD23^{high}$ infected B cells, but it is the gp350-specific T cells that are most capable of controlling infected B cells during the early stage of infection.

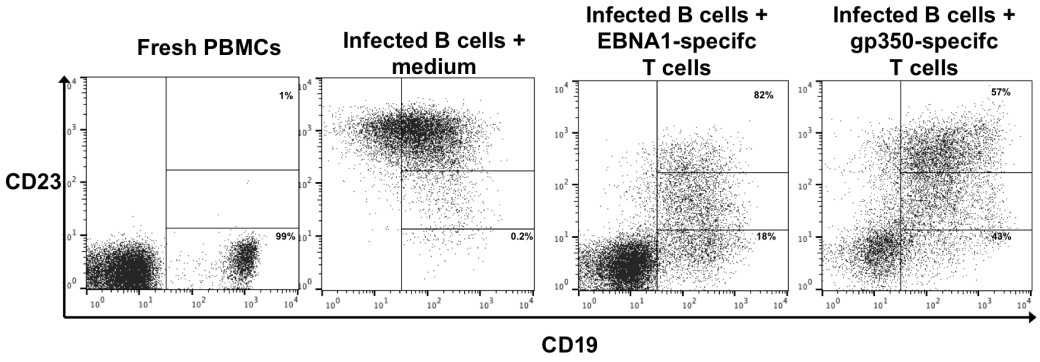

Figure 3.20: EBNA1- and gp350-specific $CD4^+$ T cells target EBV-infected B cells. Infected B cells were cocultured with $CD4^+$ T cells for 12 days, stained with α-CD19-APC and α-CD23-PE-Cy7 and analysed with flow cytometry. Additionally, infected B cells cultured in medium only served as a positive control for B-cell transformation, whilst the B cells from freshly isolated B cells served as a negative control for B-cell transformation. Total B cells were analysed for the relative percentages of $CD19^+CD23^-$, $CD19^+CD23^{low}$ and $CD19^+CD23^{high}$ populations.

3.7. Regression of EBV-infected B cells in the presence of $_{DF}$EBV-EBNA1^{RI+RII} -specific T cells

Since gp350- and EBNA1-specific $CD4^+$ T cells were shown target EBV-infected cells, polyclonal T cells specific for the whole spectrum of antigens contained within $_{DF}$EBV-EBNA1^{RI+RII} was tested for their ability to control EBV-infected B cells. Additionally, the ability of $_{DF}$EBV-EBNA1^{RI+RII}-specific T cells to target infected B cells was compared to gp350-specific T cells. In contrast to gp350, $_{DF}$EBV-EBNA1^{RI+RII} would enable the expansion of a broad range of EBV-specific T-cell clones, especially those that recognise structural proteins, from the PBMCs of EBV-positive individuals.

To generate $_{DF}$EBV-EBNA1^{RI+RII}- or gp350-specific T cells, PBMCs from four EBV-positive donors were stimulated in the presence of IL-2 for two rounds using $_{DF}$EBV-EBNA1^{RI+RII} or the gp350-AgAb. Thereafter, the T cells were cocultured with primary B cells that were infected with the B95.8 strain. In parallel, EBV-infected B cells were cocultured in medium only or in the presence of unstimulated CD19-depleted ($CD19^-$) PBMCs, respectively serving as negative and positive controls for T-cell mediated targeting of infected B cells. Five days post infection, *ex vivo* cultures were analysed with flow cytometry and immunofluorescence to observe EBV-infected B cells during the initial phase infection (Fig. 3.21 A and B). Infected B cells were detected by flow cytometry by identifying $CD19^+GFP^+$ double-positive cells. Since the B95-8 strain that was used for B-cell infection encodes GFP, infected B cells were positive for GFP expression. Flow cytomteric analysis revealed that infected B cells strongly expressed GFP when they were cultured in medium only, which indicates that EBV-infection occurred in these cells and that viral gene expression had ensued (Fig. 3.21A). Conversely, infected B cells that were cocultured with $CD19^-$ PBMCs were found to express GFP less intensely. $CD19^-$ PBMCs form EBV-positive donors would have contained the normal repertoire and frequency of EBV-specific memory T cells [45], enabling infected B cells to be

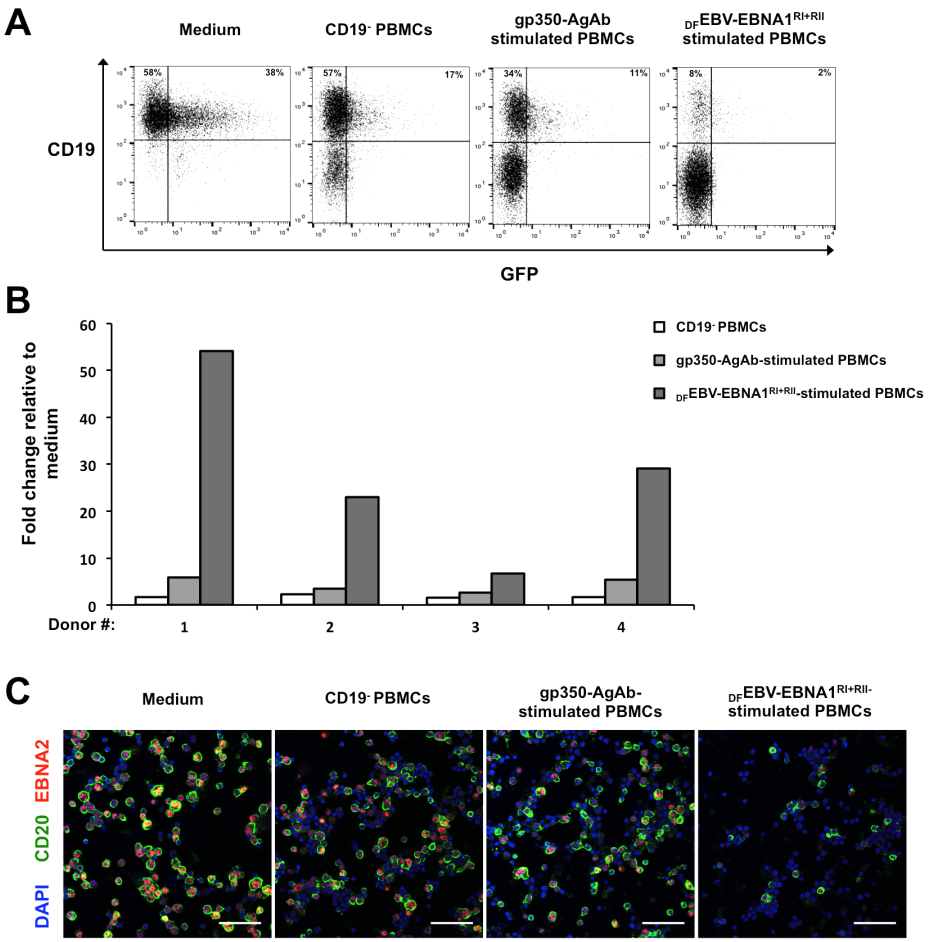

Figure 3.21: PBMCs stimulated with $_{DF}$EBV-EBNA1^{RI+RII} control EBV-infected B cells. Primary B cells infected with wtEBV (B95-8) were cocultured with PBMCs stimulated with either gp350-AgAb or $_{DF}$EBV-EBNA1^{RI+RII}. Infected B cells were also cultures with CD19$^-$ PBMCs or in medium only, respectively serving as positive and negative controls for T-cell-mediated targeting of infected B cells. (A) Analysis of *ex vivo* cultures for the presence of CD19$^+$GFP$^-$ and CD19$^+$GFP$^+$ B cells five days post infection. Since the B95-8 genome has been modified to encode GFP, it enabled the identification of cells in which viral gene transcription occurred based on GFP expression. Staining with anti-CD19-APC enables the identification of B cells. The result from a single donor is shown, with the percentage of cells that are CD19$^+$GFP$^-$ and CD19$^+$GFP$^+$ being highlighted. (B) Regression of EBV-infected B cells in *ex vivo* cultures of 4 donors. Results are expressed as fold change over the medium only control. (C) Immunofluorescence confirm that $_{DF}$EBV-EBNA1^{RI+RII} stimulated PBMCs can efficiently control EBV-infected B cells. Co-staining was performed with α-CD21 (green), α-EBNA2 (red) and DAPI (blue). Scale bars represent 50 µm.

targeted to some degree. Infected B cells that were cocultured with gp350-AgAb- and $_{DF}$EBV-EBNA1^{RI+RII}-stimulated PBMCs, showed a marked decrease in GFP-expressing cells. The results from four donors are summarised in Figure 3.21B. This confirms that memory T cells

specific for $_{DF}$EBV- EBNA1^{RI+RII} and gp350 can target EBV infected B cells during the early phase of infection. However, it is evident that $_{DF}$EBV- EBNA1^{RI+RII}-specific T cells are considerably more adept than the gp350-specific T cells. To confirm this result, *ex vivo* cultures were analysed by immunofluorescence (Figure 3.21C). *Ex vivo* cultures were stained for CD20 and EBNA2, respectively serving as a B-cell marker and an indicator of early gene expression in infected cells. This showed that there were very few EBNA2-expressing B cells in the presence of PBMCs stimulated with $_{DF}$EBV-EBNA1^{RI+RII}, indicating once more that these cells are most proficient at targeting EBV-infected B cells during the initial phase of infection. Collectively, these results show that $_{DF}$EBV-EBNA1^{RI+RII} can stimulate and expand T cells that can efficiently target recently infected B cells, even when compared to a well-known structural antigen like gp350.

3.8. PBMCs stimulated with $_{DF}$EBV-EBNA$^{RI+RII\ can}$ control the outgrowth of B cells infected with B95-8 and M81

Since polyclonal $_{DF}$EBV-EBNA1^{RI+RII}-specific T cells efficiently targeted EBV-infected B cells, their ability to prevent B-cell outgrowth was also tested. Additionally, the ability of $_{DF}$EBV-EBNA1^{RI+RII}-specific T cells to control B cells infected with the B95-8 and M81 strains was tested. The B95-8 strain is representative of strains found in Western countries, whilst the M81 strain was isolated from a Chinese nasopharyngeal carcinoma patient [87]. PBMCs from 8 donors were stimulated for two rounds as before (see section 3.7) with either $_{DF}$EBV-EBNA1^{RI+RII} or gp350-AgAb, and were incubated with B cells infected with B95-8 (moi = 5) or M81 (moi = 30). Since different EBV strains transform B cells at different rates, it was important to use the appropriate dose for each strain [153]. *Ex vivo* cultures were analysed after 15 days for the presence of CD19^{+}CD23^{+} double-positive cells (Fig. 3.22). This showed that PBMCs stimulated with $_{DF}$EBV-EBNA1^{RI+RII} and gp350-AgAbs were capable of controlling infected B cells over the 15 day period, with the former being superior at preventing B-cell outgrowth (Fig. 3.22A). Interestingly, the CD19^{-} PBMCs from some donors outperformed

gp350-specific T cells. This indicates that some donors contained EBV-specific T cells in addition to gp350 that have the ability to target EBV-infected B cells. Nonetheless, the $_{DF}$EBV-EBNA1^{RI+RII}-stimulated PBMCs were shown to be the most proficient at controlling the EBV-infected B cells. Indeed, cultures having $_{DF}$EBV-EBNA1^{RI+RII}-stimulated PBMCs were found

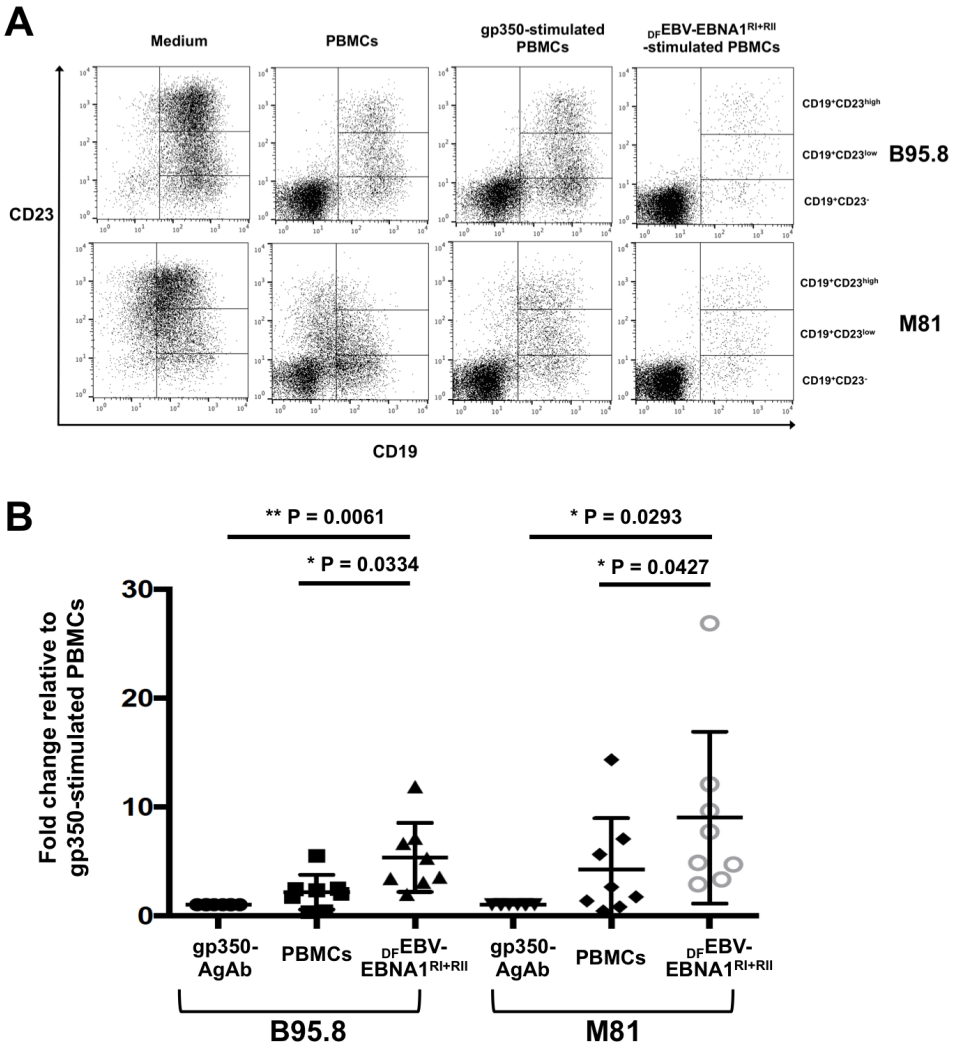

Figure 3.22: T cells specific for $_{DF}$EBV-EBNA1^{RI+RII} prevent the outgrowth of B95-8- and M81-infected B cells. PBMCs from 8 donors were expanded with either $_{DF}$EBV-EBNA1^{RI+RII} or gp350-AgAb and cocultured with primary B cells infected with B95-8 or M81 strains. CD19^{-} PBMCs and medium only, also cultured with infected B cells, respectively served as positive and negative controls for T-cell-mediated targeting of EBV-infected cells. (A) After 15 days, cells were strained with CD19-APC and CD23-PE-Cy7 antibodies and analysed by flow cytometry. Representative results are shown, indicating CD19^{+}CD23^{-}, CD19^{+}CD23^{low} and CD19^{+}CD23^{high} populations. (B) A result summary from 8 donors. The percentage of CD19^{+}CD23^{+} cells in *ex vivo* cultures were determined and are expressed as fold change relative to CD19^{+}CD23^{+} cells within cultures containing gp350-AgAb-stimulated PBMCs. Statistical analysis was performed using a two-tailed student T-test.

to contain very few total B cells after the 15-day culture period. Importantly, this was also found to be the case for B95-8- and M81- infected B cells. Considering the summarised result from eight donors (Fig. 3.22B), it is clear that the $_{DF}$EBV- EBNA1^{RI+RII}-specific T cells were extremely proficient at preventing B-cell outgrowth. This is the first instance where vaccine-specific T cells have been shown to efficiently target and control B cells infected with distantly related EBV-strains, albeit during short- term culture *ex vivo*.

3.9. Investigating the antigenicity of $_{DF}$EBV-EBNA1^{RI+RII} in humanised NSG-A2 mice

Humanised mouse models are powerful tools to investigate human viruses [154]. Mice reconstituted with human immune system components are susceptible to EBV infection and can exert EBV-specific immune control [155]. In the present study, humanised NSG-A2 (huNSG-A2) mice were used to assess the ability of $_{DF}$EBV-EBNA1^{RI+RII} to protect against wtEBV (B95-8 strain) infection. To this end, huNSG-A2 mice were injected intraperitoneally with PBS, unmodified $_{DF}$EBV and $_{DF}$EBV-EBNA1^{RI+RII}, using 50 µg of poly (I:C) as adjuvant (Fig. 3.23A). Subsequently, mice were boosted as before, challenged with 1 x 10^5 green Raji units (GRUs) of EBV and euthanised 8 weeks later. The spleens of challenged mice were analysed by histology (Fig. 3.23B). This revealed that mice contained B cells (CD19-positive) and T cells (CD3 positive) of human origin. Furthermore, the abundance of human B and T cells in spleens were not influenced by the different treatments. *In situ* hybridisation revealed that mice from the PBS and unmodified $_{DF}$EBV groups contained EBV-positive cells; i.e. splenocytes were shown to express Epstein-Barr virus (EBV)-encoded small RNAs (EBERs). Conversely, none of the mice from the $_{DF}$EBV-EBNA1^{RI+RII} group were found to contain EBERs in their spleens. In total, 60% of mice from the PBS group were found to contain EBER$^+$ cells, while 37.5% of mice in the from the unmodified $_{DF}$EBV group were shown to contain EBER$^+$ cells (Fig. 3.23C). Whilst mice vaccinated with unmodified $_{DF}$EBV had a lower incidence of EBV infection, statistical analysis (one-tailed Chi-square test) revealed this result was not

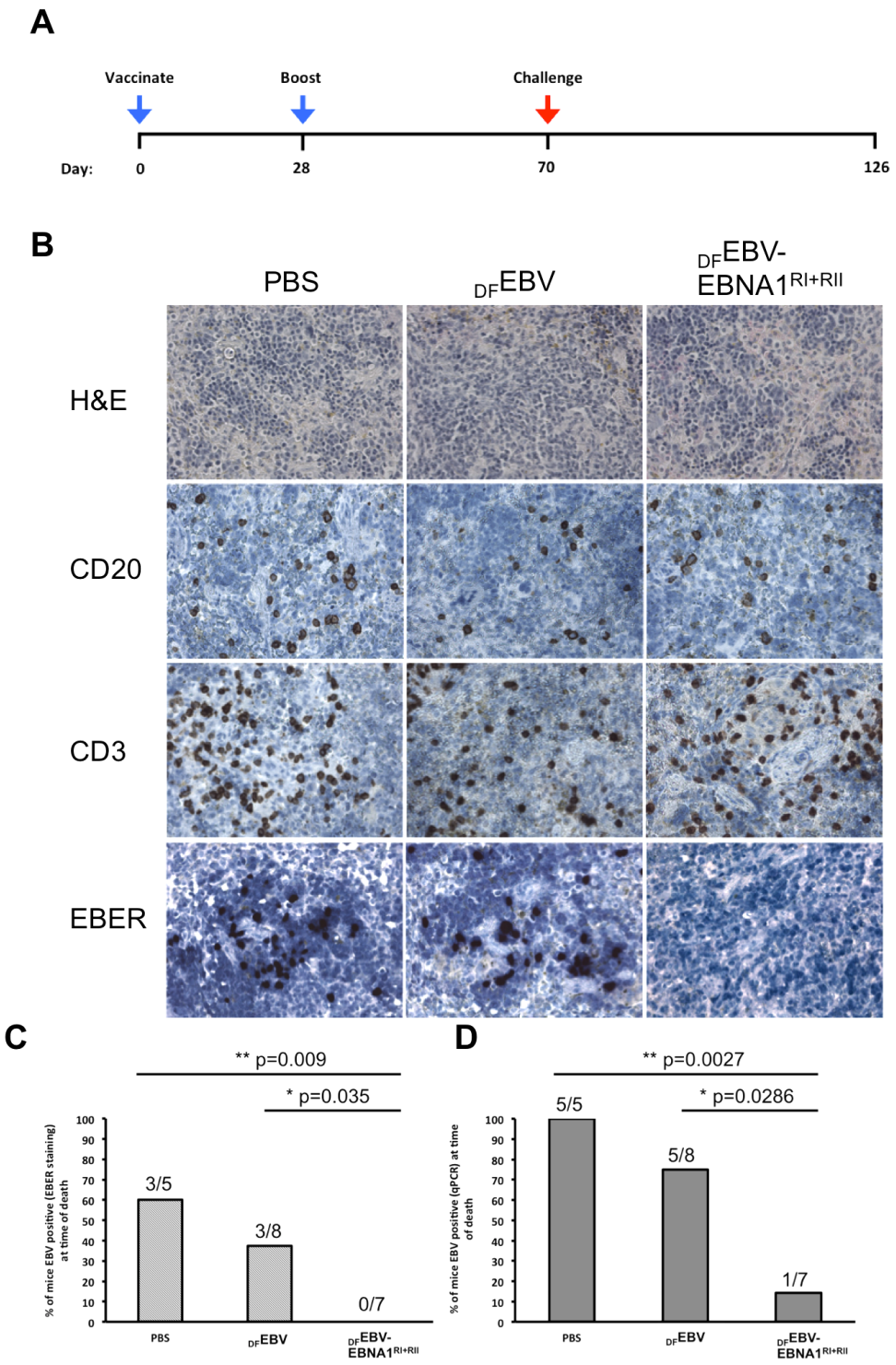

Figure 3.23: Vaccination of humanised mice with $_{DF}$EBV containing EBNA1 confers protective immunity. (A) Histological analysis of mice spleens 8 weeks after challenge with EBV. Spleen sections were stained with eosin and haematoxylin (H&E) and immunostained with antibodies specific for CD20 and CD3. The incidence of EBV infection amongst PBS, $_{DF}$EBV and $_{DF}$EBV-EBNA1^{RI+RII} vaccinated groups was determined from EBER staining (B) and RT-qPCR analysis (C). P values lower than 0.05 obtained after one-tailed Chi-square analysis are shown.

significant (P > 0.05). However, statistical analysis showed that $_{DF}$EBV-EBNA1^{RI+RII} afforded significantly more protection than the PBS (P = 0.009) and unmodified $_{DF}$EBV (P = 0.035). To detect EBV in peripheral blood of mice, real-time qPCR was used (Fig. 3.23D). EBV genomes were detected in 100% of mice from the PBS group and 75% of mice from the unmodified $_{DF}$EBV group. Real-time qPCR analysis of blood from $_{DF}$EBV-EBNA1^{RI+RII} vaccinated mice revealed that only one mouse, equivalent to 14%, was EBV-positive. Statistical analysis revealed that $_{DF}$EBV-EBNA1^{RI+RII} was significantly better than PBS (P = 0.0027) and $_{DF}$EBV (P = 0.0286). These results suggest that the presence of EBNA1 within $_{DF}$EBV significantly improved vaccine-induced immunity.

4. Discussion

$_{DF}$EBV is non-toxic, non-infectious, structurally complex and highly immunogenic [9, 141]. This infers that $_{DF}$EBV retains the antigenicity of wtEBV virions, without the potential to recapitulate the adverse consequences of EBV infection. However, vaccination with $_{DF}$EBV would not be able to sensitise the immune system against proteins that are expressed during viral latency. Latency is an essential aspect of the EBV life cycle, and the establishment of latency enables life-long carriage of EBV within memory B cells [156]. Furthermore, it is latency transcription programs that take place in EBV-associated diseases and malignancies. To facilitate sensitisation against latent proteins, the antigenic spectrum of $_{DF}$EBV was enlarged to include latent antigens. The fusion of latent antigen moieties to the major tegument protein BNRF1 successfully enabled the incorporation of latent antigens into $_{DF}$EBV. The incorporated latent antigens were successfully processed by APCs, which in turn presented the antigenic epitopes to the relevant T cells. The antigenic potential of modified $_{DF}$EBV was confirmed *in vitro*, *ex vivo* and *in vivo*. $_{DF}$EBV equipped with latent epitopes is the first prophylactic vaccine candidate with the potential to sensitise the immune system against many of the proteins expressed throughout the EBV life cycle.

4.1. BNRF1 as a carrier of latent antigens

BNRF1 was selected in the present study as a carrier of latent antigens due to its abundance within particles and its well-documented antigenicity [8, 9, 22]. BNRF1-fusion proteins containing latent antigen moieties of moderate size, up to 200 aa in size, were well expressed and successfully incorporated into $_{DF}$EBV particles. Fusing latent antigens to BNRF1 was not found to influence the production of $_{DF}$EBV particles, nor the antigenicity of envelope (e.g. gp350) and tegument (e.g. BNRF1) proteins. Importantly, the incorporation of latent antigens into $_{DF}$EBV successfully enlarged their antigenic spectrum. This indicates that BNRF1-latent antigen fusion proteins are antigenic and do not impact on the antigenicity of

structural proteins, validating their use to enlarge the antigenic spectrum of $_{DF}$EBV. However, the insertion of latent antigens into the BNRF1 larger than 200 aa was found to preclude BNRF1 expression. Whilst the exact reason for this observation was not followed up, it is possible that the insertion of large foreign fragments into BNRF1 prevented proper folding, leading to its degradation within producer cells. It is known that misfolded proteins are degraded by the mammalian cells, preventing their build-up within cells and mitigating their toxicity [157].

Since *ex vivo* and *in vivo* experiments were performed with unhaplotyped donors, it was necessary to incorporate as many latent epitopes as possible into $_{DF}$EBV. However, since BNRF1 could only accommodate antigenic fragments of a relatively small size, epitope-rich fragments from EBNA1 were selected to fuse to BNRF1. Using EBNA1, $_{DF}$EBV could successfully be modified to contain as much as 10 epitopes through the introduction of EBNA1 fragments of approximately 110 amino acids. In comparison, a protein like EBNA3C is very large, and whilst being highly immunogenic, it only has 11 epitopes distributed throughout its 992 amino acids [115, 158]. This suggests that EBNA3C is not the as suitable for fusion to BNRF1 as EBNA1. Furthermore, EBNA3C is only expressed during type III latency, whilst EBNA1 is expressed in all forms of latency (except for type 0) and in all EBV-positive malignancies [145]. Taken together, this implies that EBNA1 is more suitable for fusion to BNRF1 from a technical, immunological and virological perspective. However, since latent antigens from the EBNA3 and LMP families are expressed in latently infected cells and are immunogenic [45], $_{DF}$EBV would surely benefit from their inclusion. However, it is likely that additional tegument proteins would have to be explored to accommodate these latent antigens.

4.2. The antigenicity of $_{DF}$EBV equipped with proteins.

The antigenicity of $_{DF}$EBV containing latent proteins was extensively examined in the present work. *In vitro* interrogation of modified particles was performed with LCLs and HLA-matched T-cell clones that were established previously [111, 146]. These experiments confirmed that that modified $_{DF}$EBV could successfully stimulate gp350-, BNRF1-, EBNA3C- and EBNA1-specific $CD4^+$ T cells. *Ex vivo* stimulation of bulk PBMCs from an unhaplotyped EBV-positive individual with $_{DF}$EBV containing EBNA1 enabled the expansion of gp350- and EBNA1-specific $CD4^+$ T cells. Conversely, the stimulation of the same PBMCs with unmodified $_{DF}$EBV only enabled the expansion of gp350-specific $CD4^+$ T cells. This confirmed that the EBNA1 contained within modified $_{DF}$EBV was antigenic in an *ex vivo* setting. In addition to confirming the antigenicity of modified $_{DF}$EBV, it also showed that memory $CD4^+$ T cells from an EBV-positive individual recognises modified $_{DF}$EBV.

The T cells from EBV-positive individuals have been found to recognise an impressive variety of EBV proteins [45] and there is considerable evidence that implicates EBV-specific T cells in the control of EBV-associated malignancies. Immunocompromised individuals have an increased risk of developing life-threatening EBV-associated lymphoproliferative disease [158] and the adoptive transfer of cytolytic EBV-specific T cells have been shown to can combat EBV-associated malignancies [159, 160]. Along these lines, the EBV-specific memory $CD4^+$ T cells expanded in the present study were shown to express CD107a, release granzyme B and specifically lysed target cells exposed to modified $_{DF}$EBV. This in accordance with previous studies that have identified EBNA1- [145, 161, 162] and gp350- [108] specific cytolytic $CD4^+$ T cells. The cytolytic ability of $_{DF}$EBV-specific T cells suggests that vaccination with modified $_{DF}$EBV has the potential to prime T cells that play a role in controlling EBV infection. Testing the EBNA1- and gp350-specific $CD4^+$ T cells in an *ex vivo* model of EBV infection confirmed that they were capable of targeting proliferating ($CD19^+CD23^{high}$) B cells

during short-term culture. However, it was the gp350-specifc T cells that were shown to be more adept at targeting the proliferating B cells. The observed difference between the gp350- and EBNA1-specific T cells can be accounted for when the antigenic load of structural and latent proteins during EBV infection is considered. Structural proteins are directly delivered to B cells during infection and are presented to $CD4^+$ T cells via the canonical MHC class II pathway [50]. Conversely, latent proteins are only expressed once viral DNA reaches the nucleus and requires autophagy before being presented on MHC class II molecules [116]. Hence, structural proteins are efficiently presented to $CD4^+$ T cells soon after infection (<24 hours), while latent proteins are only efficiently recognised by $CD4^+$ T cells ~1 week after infection [50].

The efficient presentation of structural proteins during the initial phase of EBV infection is also likely to explain why T cells specific for modified $_{DF}$EBV were so efficient at targeting infected B cells during the early phase of infection. Modified $_{DF}$EBV contains several dozen structural proteins [8], and it would have enabled the expansion of a polyclonal pool of T cells that recognise glycoproteins, tegument proteins and capsid proteins. Analysis of *ex vivo* cultures shortly after infection (5 days) and at a later time point (15 days) showed that $_{DF}$EBV-EBNA1^{RI+RII}-specific T cells were considerably more efficient than gp350-specific T cells at controlling EBV-infected cells. $_{DF}$EBV-EBNA1^{RI+RII}-specific T cells not only reduced the presence of infected cells 5 days post infection, but also prevented B cell outgrowth over a 15 day culture period. The superior ability of $_{DF}$EBV-EBNA1^{RI+RII}-specific T cells to control infected B cells compared to gp350-specific T cells likely stems from their polyclonal nature. Numerous T-cell clones that simultaneously recognise epitopes from different antigens are likely to have a protective benefit over T cells that only recognise one or two epitopes from a single antigen. This suggests that $_{DF}$EBV contain multiple T-cell epitopes that contribute to immune responses during the early phase of infection. However, since structural antigens

are also expressed during virus reactivation [163], it suggests that the same polyclonal T cells could potentially target infected B cells undergoing reactivation.

To assess the immunogenicity of $_{DF}$EBV containing EBNA1 *in vivo*, a humanised mouse model was employed. Mice reconstituted with human immune system components were vaccinated and boosted with PBS, unmodified $_{DF}$EBV or $_{DF}$EBV-EBNA1^{RI+RII} prior to being challenged with the B95-8 EBV strain. This showed that $_{DF}$EBV containing EBNA1 afforded protection to 86% of mice, whilst unmodified $_{DF}$EBV only afforded protection to 38% of mice. This suggests that EBNA1-specific T cells play an important role in controlling EBV infection, likely by directly targeting infected cells displaying EBNA1 peptides [145, 161, 162]. Since the *in vivo* challenge experiment extended for 8 weeks, it would have enabled the antigenic load of latent proteins to be higher than in the *ex vivo* experiments. This is especially true for the B95-8 strain used for challenge, since it does not readily reactivate once it establishes latency [153].

Taken together, these results confirm that the antigenic spectrum of $_{DF}$EBV was successfully enhanced using BNRF1-lanent antigen fusion proteins. It is also evident that T cells are more efficient at targeting EBV-infected B cells during the early phase of infection when they recognise a broad spectrum of EBV antigens. This suggests that vaccine candidates that contain only a few EBV structural antigens are likely to induce suboptimal EBV-specific T cell responses. Furthermore, the inclusion of a latent antigen, in this case EBNA1, significantly improved vaccine-induced immunity. This suggests that prophylactic EBV candidates benefit from the inclusion of both latent and lytic proteins.

4.3. Modified $_{DF}$EBV compared to other prophylactic EBV vaccines

Prophylactic EBV vaccines that consist of the latent protein EBNA3A [164] or the late lytic protein gp350 [71, 165-167] have previously been tested in humans. Of these, gp350 is the only one that was tested in a phase II clinical trial, which confirmed that the gp350 subunit

vaccine was unable to prevent EBV infection. Despite the underperformance this vaccine, gp350 has subsequently continued to receive attention as a vaccine candidate. This is understandable considering the important role gp350 plays in attaching virions to B cells during the infection process [168], and when one considers that gp350 is a frequent target of neutralising antibodies [107, 169]. However, instead of being used as a subunit vaccine, emerging prophylactic vaccines have introduced gp350 into nanoparticles [170] or Newcastle disease virus (NDV) VLPs [171]. It is well established that subunit vaccines are relatively weak immunogens, and that their incorporation into nanoparticles or VLPs improve their immunogenicity [172-174]. Indeed, gp350 contained within nanoparticles and NDV-VLPs was shown to dramatically improve neutralising antibody responses, with both vaccines clearly outperforming soluble gp350 [170, 171]. Interestingly, one of these studies analysed NDV-VLPs containing gp350 and UV-inactivated EBV in parallel, and found UV-inactivated EBV to be even more potent at inducing neutralising antibodies [171]. Since UV-inactivated EBV contains several EBV glycoproteins, it would have enabled the generation of antibody responses that target several glycoproteins in addition to gp350. This bodes well for $_{DF}$EBV as a prophylactic vaccine, as suggests that $_{DF}$EBV might be able to generate neutralising antibody responses in addition to protective T-cell immunity. However, since humanised mice have low antibody responses, which stems from their inability to execute affinity maturation and class switch recombination [154], modified $_{DF}$EBV was not tested in the present work for its ability to generate neutralising antibodies responses. The inability of humanised mice to generate normal antibody reponses might also partly explain why vaccination with unmodified $_{DF}$EBV did not afford significant protection upon challenge with infectious viruses. $_{DF}$EBV certainly contains several glycoproteins that are targeted by antibody responses [107, 175]. In particular, $_{DF}$EBV contains gp350 and gH/gL, which respectively enable the attachment EBV to B cells and epithelial cells [33, 34]. This implies that $_{DF}$EBV has an advantage over vaccines that consist exclusively of gp350, since it could

potentially elicit antibody responses that target glycoproteins responsible for B-cell and epithelial cell infection. A mouse challenge model has been developed to test the ability of EBV vaccine candidates to elicit protective antibody responses [170]. However, in this model, vaccine success or failure is solely based on weight loss and does not allow sterile immunity to be assessed. Nonetheless, testing $_{DF}$EBV in such a model will certainly be a good starting point to assess the quality of $_{DF}$EBV elicited neutralising antibodies *in vivo*.

Whilst neutralising antibodies are likely to provide a protective benefit against EBV infection [176, 177], it is uncertain whether neutralising antibodies alone are sufficient to prevent EBV infection. EBV has a complex lifecycle that comprises several latency programs and healthy individuals keep EBV-infected cells under control through an assortment of EBV-specific T cells, many of which recognise latently proteins [110]. It was for this reason $_{DF}$EBV was modified in the present study to contain latent antigens. In principle, a vaccine that solely contains lytic antigens (e.g. gp350 or gH/gL) would not provide protection against latently infected cells. Hence, vaccines that are comprised of structural proteins would have to elicit neutralisation antibodies and T-cell responses that are 100% effective at targeting incoming virus or recently infected B cells. If latency is established in just a handful of cells, it would enable the viral genome to amplify through simple cell division. The inability to protect against latently infected cells is especially important to consider, since it is the establishment of latency that enables EBV to be carried lifelong [47] and it is latency transcription programs that are carried-out in EBV-associated malignancies [178].

Using VZV as example, the only herpesvirus for which there is a vaccine available, vaccination generates immune responses that mirror those observed during wild-type infections, with vaccinated individuals having humoral and cell-mediated immune responses that recognise a broad range of lytic and latent proteins [179-182]. This implies that the ideal EBV vaccine should prime humoral and cell-mediated immunity against a broad set of

latent and lytic antigens [45]. However, prophylactic EBV vaccines have traditionally aimed at either targeting lytic or latent antigens, suggesting that they are inherently incapable of targeting EBV during all the stages of its life cycle. However, $_{DF}$EBV equipped with latent antigens would enable the induction of immune responses that target antigens that predominate throughout the EBV life cycle.

4.4. EBV strain heterogeneity

EBV strains that are found around the world have been classified as either type 1 or 2 based on the sequence of their EBNA2 gene [183]. Recently, the advent of next generation sequencing has produced complete genomes from 23 EBV stains, enabling detailed analysis of genome-wide polymorphism [184]. This has revealed that some proteins are more polymorphic than others, with latent proteins having the tendency of being more polymorphic than lytic proteins.

Thus far, EBV vaccine candidates have not addressed the intimidating task of affording protection against the plethora of EBV strains found around the world. A recently study has analysed polymorphisms within T-cell epitopes [158], as well as their flanking regions, between three distantly related EBV strains (*viz.* B95-8, M81 and AG876). This revealed that there is considerable variation between the three strains in terms of their $CD4^+$ and $CD8^+$ epitopes. The B95-8 and M81 strains were found to respectively differ by almost 30% and 50% in their CD8 and CD4 epitopes. Several of these polymorphisms were shown to present a hurdle to T cells by influencing the recognition of pulsed target cells. However, despite these polymorphisms, M81- and B95-8-infected B cells were efficiently controlled during short-term *ex vivo* culture by T cells specific for modified $_{DF}$EBV.

Epitope variations between different EBV strains could be addressed by generating a prophylactic vaccine that only focuses only highly conserved proteins. However, the most conserved proteins are not always the most immunologically relevant [184]. This suggests

that vaccines might be fair better if they contain multiple EBV proteins [158]. Since $_{DF}$EBV already contains multiple structural antigens, it would not only be beneficial for generating polyclonal T-cell pools that simultaneously target recently infected B cells, but it would be beneficial from the standpoint of EBV strain heterogeneity. However, since latent antigens tend to be more polymorphic than structural proteins, it is likely that $_{DF}$EBV would need to contain several latent antigens to be optimal for prophylactic vaccination around the globe.

4.5. The therapeutic potential of modified $_{DF}$EBV

Whilst modified $_{DF}$EBV was investigated in the present study as a prophylactic vaccine, it is also possible for modified $_{DF}$EBV to have therapeutic applications. The adoptive transfer of EBV-specific T cells has successfully been used to treat EBV-associated lymphoproliferative diseases [159]. Since EBV-associated lymphoproliferative diseases arise due to impaired T-cell responses, the adoptive transfer of EBV-specific T cells combats proliferating EBV-infected cells. Such EBV-specific T-cell lines were originally generated by simply stimulating PBMCs with autologous LCLs [113]. However, using this method, the expanded T cells recognised primarily EBV structural antigens. More recent methods have been developed to expand latent protein-specific T cells using peptide mixes [185-187].

Since $_{DF}$EBV can be engineered to contain latent antigens of relevance to EBV-associated lymphoproliferative diseases, i.e. antigens like EBNA1 and EBNA3C that are expressed during type III latency, it could be used to expand a broad range of EBV-specific T cells that recognise structural and latent antigens. The engineering of $_{DF}$EBV to contain large antigenic segments from various latent antigens would be especially useful, since it might negate the haplotyping of patients, enabling modified $_{DF}$EBV to serve as an off-the-shelf product.

4.6. Future studies

In the present study, $_{DF}$EBV containing EBNA1 was shown to significantly improve vaccine-induced immunity. EBNA1 is a good option for prophylactic vaccination due to its immunogenicity [144] and presence in latently infected cells and EBV-associated malignancies [145]. However, this does not imply EBNA1 is the only latent protein that can be beneficial for prophylactic vaccination. Indeed, healthy individuals frequently develop T-cell responses against EBNA-2, -3A, -3B, -3C and to some degree LMP-1 and-2 [45]. Whilst many of these are interesting candidates, EBNA2 is a particularly attractive option. EBNA2 is relatively small (~ 450 aa) and is one of the first proteins expressed in infected cells. Hence it would enable the recognition of B cells at a very early time point after infection [50]. In addition to latent proteins, several immediate early and early lytic proteins are also expressed early after infection (e.g. BZLF1 and BHRF1), marking them as potential candidates [50, 188].

Since BNRF1 was found in the present work to only accommodate antigens with a maximum of size of 200 amino acids, it is likely that it would not enable the incorporation of several antigens. An alternate candidate for accommodating latent antigens within $_{DF}$EBV is the large tegument protein BPLF1. Since it is BPLF1 is 350 kDa in size and BNRF1 is 140 kDa in size, it might be more suitable for the introduction of latent antigens into $_{DF}$EBV.

The incorporation of the most conserved and immunologically relevant antigens into $_{DF}$EBV, expressed in infected B cells and EBV-malignancies, is likely to induce highly potent T-cell responses upon vaccination, whilst enabling the generation of neutralising antibodies in their natural context. Such a multipronged approach is likely to increase the protective ability of $_{DF}$EBV, and maximise its potential to be used around the globe.

5. Materials and Methods

5.1. Materials

5.1.1. Cells

5.1.1.1. Bacteria

Strain	Primary Use	Genotype
***E.coli* DH5α**	Molecular cloning	F- Φ80lacZΔM15 Δ(lacZYA-argF) U169 recA1 endA1 hsdR17 (rk-, mk+) phoA supE44 λ-thi-1 gyrA96 relA1
***E.coli* DH10B**	Plasmid rescue	mcrA Δ (mrr-hsdRMS-mcrBC) Φ 80dlacZ Δ M15 Δ lacX74 recA1 endA1 araD139 Δ (ara, leu)7697 galU pglΔ8 rpsL nupG [189]
***E.coli* SW102**	Recombineering with galK counter selection	mcrA Δ (mrr-hsdRMS-mcrBC) Φ 80dlacZ Δ M15 Δ lacX74 recA1 endA1 araD139 Δ (ara, leu)7697 galU pglΔ8 rpsL nupG λ(cI857ind1) Δ{(cro-bioA)<>tetRA} (TetR) gal490 ΔgalK [190]

5.1.1.2. Eukaryotic cells

Name	Description
HEK293	Human embryonic kindey cell line transformed with sheared Adenovirus 5 DNA [191]
$CD4^+$ and $CD8^+$ clones/lines	T-cell clones/lines were generated through *ex vivo* stimulation of PBMCs from healthy donors with peptide. They were kindly provided by Prof. Josef Mautner (Helmholz-Zentrum, München, Germany).
LCL JM, GB and HM	B cells from healthy donors were transformed through infection with EBV. They were kindly provided by Prof. Josef Mautner (Helmholz-Zentrum, München, Germany).
Elijah negative	An EBV-negative B cell lymphoma cell line. It was kindly provided by Prof. Alan Rickinson (University of Birmingham).
Raji Cells	An EBV-positive Burkitt's lymphoma cell line [192].
Producer cells	Several EBV and $_{DF}$EBV producer cell lines were used in this study. Producer cell lines were generated by transfecting HEK293 cells with BAC DNA and selecting with hygromycin (100 µg/mL).

5.1.2. Mice

Strain	Supplier
NSG-A2 mice (NOD.Cg-Prkdc^{scid}Il2rg^{tm1Wjl}Tg (HLA-A2.1) [155]	The Jackson Laboratory

5.1.3. Cell culture media

Name	**Supplier**
RPMI 1640	GIBCO by Life Technologies
FreeStyle™ 293	GIBCO by Life Technologies
AIM V® Medium	GIBCO by Life Technologies
Opti-MEM®	GIBCO by Life Technologies

Composed media

Name	**Composition**
LCL Medium	RPMI supplemented with 10% fetal calf serum, 1 mM sodium pyruvate, 2 mM L-glutamine, 1% nonessential amino acids and 50 µg/ml gentamicin
T-cell medium	AIM V® Medium supplemented with 10% pooled human serum (heat-inactivated), 10 mM HEPES, 2 mM L-glutamine, 50 µg/mL gentamicin and 0.4 mg/ mL ciprofloxacin

5.1.4. Plasmids

Internal lab. Label	Description
p509	encodes BZLF1
2670_(pRA)	pRK5-B95-8.BALF4(=gp110=gB)
B1261	pRK5-aHuCD20.HC-NotI
B1342	gp350 ligand binding domain (1 to 1410 bp) HuCD20 AgAb
B1394	BNRF1 (EBNA1 1168bp-1548bp)
B1395	BNRF1 (EBNA1 1498bp-1866bp)
B1396	BNRF1 (EBNA1 1168bp-1866bp)
B1450	EBNA1 huCD20 AgAb (EBNA1 fragment = 1158 to 1856 bp)
B581	pRK5-aCD20-Light chain
B673	pCDNA3.1(+)-CD2
B560	anti-CD20 Heavy chain in pRK5
pGal	Galk casette

5.1.5. EBV-BACs

Internal lab. Label	Description
2089	Prototypic EBV strain
M81	EBV strain from Hong Kong
B1009	EBV-E3C (150 bp)
B1118	EBV + galK
B1151	EBV-E3C-E1(300 bp)
B1191	EBV-E3C(600 bp)
B1192	EBV-E3C(600 bp)
B1287	$_{DF}$EBV-E3C-E1(300 bp)
B1229	$_{DF}$EBV + galK
B1400	$_{DF}$EBV-EBNA1^{RI}
B1401	$_{DF}$EBV-EBNA1^{RII}
B1402	$_{DF}$EBV-EBNA1$^{RI:RII}$

5.1.6. Oligonucleotides

Aim	Name	Sequence
α-CD20 HC	fwd	TCGATTGAATTCATGGCTGTCC
	rev	TTTCATAAGCTTTATTAGATCTAATTGCGGCCGCTTTACCCGGAGTCCGGGAG
EBNA1-AgAb	fwd	CGTAGCGGCCGCACAGTCATCATCATCCGGGTCTCC
	rev	TTTCATAGATCTTAATGGTGATGGTGATGATGCGCGGCAGCCCCTTCC
gp350-AgAb	fwd	CGTAGCGGCCGCAATGGAGGCAGCCTTGCTTG
	rev	TTTCATAGATCTTAATGGTGATGGTGATGATGGGTGGATACAGTGGGGCCTG
EBV-galK	fwd	GAGCAGGGTGAACACTTGGGCACGGAGAGTGCCCTGGAGGCCTCAGGCAACCTGTTGACA ATTAATCATCGGCA
	rev	ATGTGGAAGGCCTTGCCATCCAGTCTGGTCCGTAGGCATACACATAGTTGTCAGCACTGTCC TGCTCCTT
VLPs/LPs-galK	fwd	GAGCAGGGTGAACACTTGGGCACGGAGAGTGCCCTGGAGGCCTCAGGCAACCTGTTGACA ATTAATCATCGGCA
	rev	ATGTGGAAGGCCTTGCCATCCAGTCTGGTCCGTAGGCATACACATAGTTGTCAGCACTGTCC TGCTCCTT
EBV-E3C (150 bp)	fwd	GAGCAGGGTGAACACTTGGGCACGGAGAGTGCCCTGGAGGCCTCAGGCAATGCACCACCT AATGAAAATCCATATCAC
	rev	ATGTGGAAGGCCTTGCCATCCAGTCTGGTCCGTAGGCATACACATAGTTGCCTGACGCAGGT TTACGGC
EBV-E3C-E1 (300 bp)	fwd	AGCAGGGTGAACACTTGGGCACGGAGAGTGCCCTGGAGGCCTCAGGCAACAATGCACCAC CTAATGAAAATCC
	rev	CATGTGGAAGGCCTTGCCATCCAGTCTGGTCCGTAGGCATACACATAGTTTCCAGGGGCCAT TCCAAAG

EBV-E3C (600 bp)	fwd	GTGCCCTGGAGGCCTCAGGCAACATAATGGCGCCTCCCGTC
	rev	CATCCAGTCTGGTCCGTAGGCATACACATAGTTCTGGGTGTGCCCATGCAC
EBV-E3C (900 bp)	fwd	GTGCCCTGGAGGCCTCAGGCAACATAATGGCGCCTCCCGTC
	rev	CATCCAGTCTGGTCCGTAGGCATACACATAGTTACTGGCAAAGGGCATGCTTG
$_{DF}$EBV-E3C-E1 (300 bp)	fwd	AGCAGGGTGAACACTTGGGCACGGAGAGTGCCCTGGAGGCCTCAGGCAACAATGCACCAC CTAATGAAAATCC
	rev	CATGTGGAAGGCCTTGCCATCCAGTCTGGTCCGTAGGCATACACATAGTTTCCAGGGGCCAT TCCAAAG
$_{DF}$EBV-EBNA1^{RI}	fwd	TAATCCCTCAGGCCAGTCATCATCATCCGGGTCTCCAC
	rev	TTAGATCCTGAGGCACTACCTCCATATACGAACACACCGGC
$_{DF}$EBV-EBNA1^{RII}	fwd	GGCACTACCGACGAAGGAACTTGGGTCG
	rev	GGCCGCGGCAGCCCCTTCCAC
$_{DF}$EBV-EBNA1$^{RI:RII}$	fwd	GGCACTACCGACGAAGGAACTTGGGTCG
	rev	GGCCGCGGCAGCCCCTTCCAC

5.1.7. Antibodies

Name	Supplier (catalog no.)
α-gp350	supernatant from hybridoma clone 72A1
α-mouse IgG	Promega (W402b)
α-mouseIgG Cy3	Dianova (115-165-146)
α-BNRF1	Antiserum collected from rabbit ([22])
α-CD3-FITC	Miltenyi Biotech(130-080-401)
α-CD4-PE-Cy5	eBioscience (15-0042-82)
α-CD19-APC	eBioscience (17-0199-41)
α-CD23-PE-Cy7	eBioscience (25-0238-42)
α-EBNA2	kind gift from E.Kremmer
α-C20	Dako (M0755)
CD107a-FITC	eBioscience (11-1079-42)

5.1.8. Enzymes

Name	Supplier
Bgl II	ThermoFisher Scientific
Xba I	ThermoFisher Scientific
Eco RI	ThermoFisher Scientific
Bam HI	ThermoFisher Scientific

Dra I	ThermoFisher Scientific
Hind III	ThermoFisher Scientific
Not I	ThermoFisher Scientific
Dpn I	ThermoFisher Scientific
Phusion high-fidelity polymerase	ThermoFisher Scientific
Proteinase K	Roche
DNase I	ThermoFisher Scientific
T4 DNA ligase	ThermoFisher Scientific
RNase A	ThermoFisher Scientific
Calf intestinal alkaline phosphatase	Roche

5.1.9. Chemicals, reagents, Kits and peptides

Name	Suplpier
Absolute Ethanol	Sigma
1-butanol	AppliChem
10 bp DNA ladder	Invitrogen
1kb DNA ladder	Invitrogen
SDS solution (20%)	MP Biomedics
Acetic Acid	Sigma-Aldrich
Agarose	Sigma-Aldrich
Bromphenol blue	Serva
CaCl2	Invitrogen
Chloroform	Carl Roth
Complete Mini Protease Inhibitor	Roche
Biotin	Sigma-Aldrich
Galactose	Sigma-Aldrich
2-deoxy-galactose	Sigma-Aldrich
DMSO	Sigma-Aldrich
dNTP mix	Roche
Ethanol	Sigma-Aldrich
Ethidiumbromide	Carl Roth
Fetal Bovine Serum	Biochrom
Ficoll Plus	Amersham Biosciences
Glycerol	VWR International
Glycine	GERBU
GlycoBlue	Invitrogen
Hygromycin B	Invitrogen
Isopropanol	Sigma-Aldrich
Agar	Sigma-Aldrich
Yeast extract	Sigma-Aldrich

Tryptone	Sigma-Aldrich
Metafectene	Biontex
MNCl2	Sigma-Aldrich
NP-40	Biochemika
4% Paraformaldehyde (PFA)	AppliChem
PBS tablets for cell culture	Gibco
Phenol	Carl Roth
Potassium acetate (KAc)	Carl Roth
NucleoBond® BAC 100	Macherey-Nagel
Plasmid Midi Kit	QIAGEN
Human Granzyme B ELISA develpment kit (HRP)	MABTECH
Human IFN-gamma ELISA develpment kit (HRP)	MABTECH
Dynabeads CD19 Pan B	ThermoFischer
DETACHaBEAD CD19	ThermoFischer
EBNA3C 5H11 peptide	
EBNA1 3E10 peptide	
EBNA1 3G2 peptide	Kindly donated by Prof. J. Mautner
gp350 1D6 peptide	
BNRF1 VSD peptide	

5.1.10. Buffers and solutions

Name	Composition
PBS	137mM NaCl, 2.7 mM KCl, 10 mM Na2HPO4 and 1.8 mM KH2PO4 (pH 7.4)
PBS-T	PBS containing 0.05% Tween-20
5x RIPA buffer	100 mM Tris-HCl (pH 7.5), 750 mM NaCl, 25 mM EDTA, 2,5 % NP-40 and 5% Sodium deoxycholate
4x Protein loading buffer	200 mM Tris.Cl (pH 6.8), 8 % SDS, 1% bromophenol blue, 40% glycerol and 10% 2-mercaptoethanol
10x DNA loading buffer	200 µL 0.5 M EDTA, 10 % SDS, 0.5% bromophenol blue, and 40% glycerol
10x SDS-PAGE running buffer	30 g Tris base, 144 g glycine, and 10 g SDS in 1 L of dH20
PFA	4% paraformaldehyde in PBS (pH 7.4)
ACK buffer	0.15 M NH4CL, 1 mM KHCO3 and 0,1 mM EDTA (autoclaved)
Potassium Acetate buffer	3 M Potassium acetate, add glacial acetic acetate to pH 5.5
Blocking buffer	5% Skim milk powder in PBST
TE buffer	10 mM Tris-HCL and 1 mM EDTA (pH 8.0)
Blotting buffer	25 mM Tris base, 150 mM Glycine and 20% Methanol
50 x TAE	2.0 M Tris base 0,05 M EDTA and 1.0 M glacial acetic acid
Polyacrylamide separating gel (10 %)	335 mM Tris (pH 8.9), 25 % (v/v) acrylamide stock, 3.3 mM EDT
Polyacrylamide	335 mM Tris (pH 8.9), 42 % (v/v) acrylamide stock, 3.3 mM EDT

separating gel (7,5 %)	
Polyacrylamide stacking gel (4.5 %)	125 mM Tris (pH 6.8), 15 % (v/v) acrylamide stock, 4.4 mM EDT
Lysis buffer for circle prep	SDS 1%, EDTA 2 mM, NaCl 50 mM and 40 mM NaOH
M9 medium	6 g Na2HPO4, 3 g KH2PO4, 1 g NH4Cl and 0.5 g NaCl and fill to 1 L with water
M63 minimal medium	10 g (NH4)2SO4, 68 g KH2PO4 and 2.5 mg FeSO4·7H2O, adjust to pH 7 with KOH and fill to 1 L with water

5.1.11. Consumables, software and equipment

Name	Supplier
Software:	
CellQuest Prosoftware	BD Biosciences
FlowJo Software	FlowJo, LLC
Prism	GraphPad
MacVector Software 15.1.1	MacVector Inc.
Consumables:	
Amersham membrane Hybond ECL	GE Healthcare
Cell culure plates	Techno Plastic Products
Cell strainer 70 µm	Falcon
Cryo vials	Greiner Bio-one
Disposable Scalpel	Feather
Falcon Tubes (15/50 mL)	Techno Plastic Products
Safe-Lock tubes (0.5/1.5/2.0 mL)	Eppendorf AG
Vivaspin 20 centrifugal conectrators (10 000 MWCO)	Satorus
Ultrafree-CL centrifugal device (0.22 µm)	Merck Millipore
Electroporation civettes (1 mm)	Carl Roth
1 x 8 Stripwell 96 well plates	Corning
Cell strainer (70 µm)	Corning
Equipment:	
BD FACSCalibur flow cytometer	BD Biosciences
HydroFlex™ microplate washer	Tecan

OLS200 Shaking waterbath	Grant Scientific
Incubator Hood TH 30	Edmund Bühler GmbH
Incubator for bacteria (B 5060)	Heraeus
Hera Cell 150 incubator	Thermo Scientific
Light inverted microscope, DMIL-Led	Leica
Fluorescent microscope DM5000B	Leica
Heraues Pico17	Thermo Scientific
GSA rotor (RC-5C)	Thermo Scientific
SS34 rotor (RC-5C)	Thermo Scientific
RC-5C centrifuge	Thermo Scientific
Multidoc-It Digital Imaging System	UVP
MultiscanEx microplate reader	Thermo Elctron Corporation
Nanodrop 2000	Thermo Scientific
pH-meter 766	Knick
Power PAC 300	BioRad
Sonicator UW2070	Bandelin Electronics
Vortex-Genie 2	Sceintific Industies
Step One Plus™ qPCR machine system	Applied Biosystems
TProfessional Thermocycle	Biometra
Large Gel Horizontal Electrophoresis System (OWL A5)	ThermoFisher Scientific
Gene Pulser II Electroporation system	BioRad

5.2. Methods

5.2.1. Culture of bacteria

In all cases, unless specified otherwise, low-salt Luria-Bertani (LB) medium was used for liquid or agar culture. Liquid cultures were maintained at 170 rpm.

5.2.2. Transformation of Bacteria

5.2.2.1. Heat shock of E.coli DH5α

Chemically competent *E.coli* DH5α was transformed via a heat shock protocol. Competent cells were thawed on ice and mixed with 10 µL of ligation mixture or 1 µL of covalently closed circular DNA. The cell-DNA mixture was incubated on ice for 20 minutes, after which cells were incubated at 42°C for 90 seconds. Next, the cells were returned to ice for another 90 seconds. The transformed cells were mixed with 700 µL of LB medium and incubated at 37°C with shaking (180 rpm) for 30 – 60 minutes. The cells were centrifuged at 13000 x g for 1 min and the culture supernatant was removed. The pelleted bacterial cells were resuspended in 100 µL of fresh LB medium and plated on LB agar containing the appropriate antibiotic. The plates were incubated for 16-20 hours and stored at 4°C for no more than 2 week.

5.2.2.2. Electroporation of E.coli with BAC DNA

To introduce BAC DNA into *E.coli,* cells were transformed through electroporation. A small aliquot of BAC DNA (5-10 µL) was added to the side of a pre-chilled electroporation cuvette (0.1 cm gap). Next, electrocompetent cells were removed from -80°C, thawed on ice, added to the chilled electroporation cuvette and incubated on ice for 5 minutes. Cells were electroporated with 100 Ω, 25 µFd and 1200 V with the Gene Pulser II Electroporation system. Electroporated cells were immediately resuspended, mixed with 3 mL of LB medium and recovered at 37°C (180 rpm) for 2 hours. The cells were centrifuged at 3000 x g for 10

minutes, resuspended in 100 µL of fresh LB medium and plated on LB agar containing the appropriate antibiotic. Cells were incubated overnight at 37°C and the plate stored at 4°C for no longer than 2 weeks.

5.2.3. Sequencing of plasmid DNA

Plasmid DNA sequencing was performed by Eurofins MWG Operon (Ebersberg, Gemrany). Samples to be sent for sequencing were prepared by mixing 13,5 µL of template DNA (100 ng/µL) and 1,5 µL of the appropriate oligonucleotide (10 mM). Sequencing results were analysed with MacVector software 15.1.1.

5.2.4. Sequencing of BAC DNA

BAC DNA sequencing was performed by SequiServe GmbH (Vaterstetten, Germany). BAC DNA samples to be sequenced were resuspended in dH_2O at 100 ng/mL. Oligonucleotides to be used for sequencing were resuspended at 10 mM in dH_2O. BAC DNA (15 µL) and oligonucleotides (15 µL) were sent separately. Sequencing results were analysed by MacVector software 15.1.1.

5.2.5. Agarose gel electrophoresis

Agarose DNA electrophoresis (AGE) was used for analytical and preparative purposes. In all cases, agarose gels were made with 1 x TAE and 0.8% agarose. Prior to separation, DNA samples were mixed with 10 x DNA loading buffer.

To separate plasmid DNA and PCR products, the Owl B2 mini gel system (ThermoFischer Scientific) was used at 120 V and 400 mA for 45 minutes. Mini gels were made with 0.1 µg/mL of ethidium bromide. To separate digested BAC DNA, the Owl A5 large gel system (ThermoFischer Scientific) was used at 65 V and 400 mA for 16 hours or more. After separation, large gels were stained for 30 minutes with dH_2O containing 1 µg/mL ethidium

bromide. Subsequently, large gels were washed twice with 400 mL dH_2O for 30 minutes. For size determination of DNA, the 1 kb Plus DNA ladder and/or the 1 kb Extension ladder was used. Transilluminated UV light was used for visualisation of DNA and images were recorded using the Multidoc-It Digital Imaging System.

5.2.6. SDS-PAGE and Immunoblotting

Proteins from 293 cells and cell culture supernatants were separated by SDS-PAGE according to Laemmli (1970). Proteins contained within gels were transferred to nitrocellulose membranes (Hybond C, Amersham) using electroblotting. Membranes were blocked overnight at 4°C with blocking buffer. Primary and secondary antibodies were diluted in blocking buffer and were added sequentially. In both cases, antibodies were incubated for 1 hour at room temperature. Washes were performed 3 times with PBST to remove unbound antibodies. Bound antibodies were detected with Western Lightning Plus-ECL substrate (PerkinElmer) and Hyperfilm ECL (Amersham).

5.2.7. Isolation of plasmid DNA from *E.coli*

5.2.7.1. Alkaline lysis minipreparation of plasmid and BAC DNA

Alkaline lysis minipreparation of plasmid and BAC DNA was carried out to obtain small quantities of DNA. Bacteria were cultured overnight at 37°C in 5 mL of LB medium (supplemented with the appropriate antibiotic) and were harvested with centrifugation at 13 000 x g for 2 minutes. The medium was removed and the bacterial pellet was resuspended in 250 µL of TE buffer containing 50 µg/mL of RNase. The bacterial suspension was transferred to a clean 1.5 mL eppendorf tube and one volume of freshly prepared lysis buffer (1% SDS and 0.2 M NaOH in water) was added to the resuspended cells. Immediately after adding the lysis solution, the tube was gently inverted two times and incubated at room temperature for 2 minutes. A 250 µL aliquot of 3 M Potassium Acetate was added to lysed cells and the tube inverted two times. The mixture was incubated on ice for 10

minutes and centrifuged at 13 000 x g for 5 minutes. The supernatant was transferred to a clean tube and centrifuged as before. The supernatant was transferred to a clean tube and mixed with 635 µL of isopropanol. The DNA was precipitated on ice for 5 minutes and pelleted at 13 000 x g for 15 minutes. The supernatant was removed and the pellet washed in 1 mL of 70% ethanol. The pellet was air-dried for 5 minutes and the pellet was resuspended in 50 µL TE buffer and stored long term at -20°C.

5.2.7.2. Isolation of plasmid DNA using the PureLink HiPure Plasmid Maxiprep kit

To isolate large quantities of pure plasmid DNA, the PureLink HiPure Plasmid Maxiprep kit (ThermoFischer Scientific) was used. Plasmid DNA isolation was always carried out according to the manufacturers instruction.

5.2.7.3. Isolation of BAC DNA using the NucleoBond BAC 100 kit

To isolate large quantities of pure BAC DNA, the NucleoBond BAC 100 kit (Macherey-Nagel) was used. BAC DNA isolation was always carried out according to the manufacturers instruction.

5.2.8. Restriction digestion

All restriction enzymes were obtained from ThermoFishcer Scientific and all digestions were carried out according to manufacturer's instructions. Restriction enzymes never comprised more than 1/10 of the total reaction mixture, minimising the occurrence of star activity due to excessive levels of glycerol.

5.2.9. Determination of virus titre by quantitative PCR (qPCR)

Virus supernatants were analysed by qPCR to determine their titre [9]. Prior to qPCR analysis, the supernatants were first subjected to DNaseI and Proteinase K treatment.

DNaseI removed free-floating viral DNA, while Proteinase K released virus-associated DNA from capsids.

For DNaseI digestion, 45 µL of virus supernatant was mixed with 5 µL of 10 X reaction buffer (with $MgCl_2$) and 1 unit of RNase-free DNaseI. The mixture was incubated at 37°C for 1 hour and at 70°C for 10 minutes. For Proteinase K treatment, 5 µL of DNaseI-treated supernatant was mixed with 5 µL of Proteinase K (100 µg/mL). The mixture was incubated at 50°C for 1 hour and then at 75°C for 20 minutes. After Proteinase K treatment, 90 µL of dH_2O water was added to each sample.

To quantify the amount of virus genomes, qPCR was carried out with primers that target the EBV DNA polymerase gene (BALF5) was used. The following reaction mixture was set up per sample:

12,5 µL	TaqMan Fast PCR Master mix (2x)
2.5 µL	Forward primer
2.5 µL	Reverse primer
1.0 µL	Probe
1.5 µL	H_2O
5 µL	DNaseI and Proteinase K treated sample
25 µL Total	

With all the samples set up the following thermocyling conditions were used:

Step 1- 50°C 2 minutes
Step 2- 95°C 10 minutes
Step 3- 95°C 15 seconds
Step 4- 60°C 1 minute] 40 cycles

Threshold cycle (C_t) values were used to calculate the genomes per millilitre of virus supernatant. This was achieved through the use of a standard curve in which the linear relationship between C_t values and genome/mL have been established.

5.2.10. Recombineering

Latent protein-coding sequences were introduced into the BNRF1 gene of BAC DNA through galK recombination. GalK recombination is an elegant technique that enables positive and negative selection to be carried out using a single selection marker; i.e. the galK gene [190]. This recombination strategy relies on the use of the SW102 *E.coli* strain, which lacks the galK gene. This is in contrast to wild-type *E.coli*, which contains an intact galactose operon. The galactose operon is comprised of the galE, galT, galK and galM genes, with galK encoding a galactokinase that carries out the first step in the pathway. Figure 5.1 illustrates the use of galk recombination construct BNRF1-latent protein gene fusions.

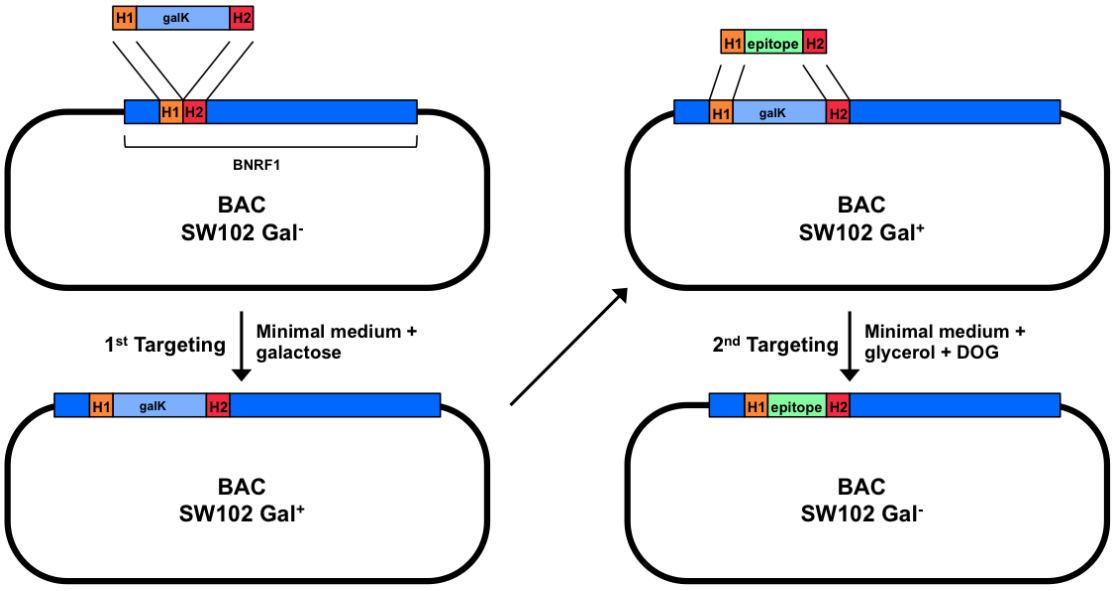

Figure 5.1: GalK recombination enabled the introduction of latent protein-coding sequences into the BNRF1 ORF. SW102 cells that contained wtEBV or $_{DF}$EBV BAC DNA were unable to grow in minimal medium containing galactose. However, once the BNRF1 ORF was targeted with the galK expression cassette, containing the H1 and H2 homology arms, cells were able to grow in minimal medium containing galactose as the sole carbon source. This targeting event constituted positive selection and converted Gal^- cells to Gal^+. The cells containing the galK expression cassette were then used to initiate a second targeting event. Latent protein-coding sequences, flanked by the H1 and H2 homology arms, replaced the galK cassette in BAC DNA. This caused the Gal^+ cells to be converted to Gal^-. Cells that lacked the galK cassette were selected for on medium containing glycerol and the galactose analogue known as 2-deoxy-galactose (DOG). Phosphorylation of DOG by galaktokinase generated a toxic product that could not be further metabolised by the cells, resulting in their death. Hence, only cells lacking the galK cassette survived.

5.2.10.1. Introducing the galK cassette into BAC DNA

To initiate galK recombination, the BAC DNA of interest was first introduced into SW102 cells via electroporation (see section 5.2.2.2). Next, the integrity of BAC DNA within SW102 cells was assessed through restriction analysis of miniprep DNA. The SW102 cells were then prepared for the first targeting event. SW102 cells containing the appropriate BAC were inoculated into 5 mL LB broth (containing 12.5 μg/mL chloramphenicol) and incubated overnight at 32°C with shaking. The following day, 2 mL of the overnight culture was diluted into 100 mL LB broth (containing 12.5 μg/mL chloramphenicol) and incubated at 32°C (180 rpm) until an OD600 of 0.5 was reached. The cells were then transferred to a shaking-waterbath at 42°C and incubated for exactly 15 min. This induced the expression of Exo, Beta and Gam; i.e. the proteins carry out recombination [190]. Exo generates 3' overhangs from dsDNA, Beta binds the 3' overhangs and mediates homologous recombination and Gam protects linear DNA from degradation by inhibiting the RecBCD exonuclease of *E.coli*. After induction at 42°C, the cells were rapidly cooled in an ice-water bath. The cooled cells were centrifuged at 3000 x g for 10 minutes at 3°C. The culture medium was removed and the cells resuspended in 50 mL ice-cold ddH_2O. The cells were centrifuged and resuspended as before. The cells were centrifuged one last time, the supernatant removed and the pellet resuspended in 150 μL ddH_2O. The cells were now ready to be used for electroporation. The cells were electroporated with 60 ng of the galK cassette. The galK cassette was amplified from the pGALK vector via PCR (see section 5.1.6 for the primers used). The electroporated cells were recovered in 3 mL LB broth for 4 hours at 32°C. After the recovery period, the bacteria were centrifuged, the medium removed and the cells washed in 10 mL 1x M9 salts. Washing in 1x M9 salts serves to remove residual medium from cells before plating on minimal medium. Washed cells were pelleted and resuspended in 1 mL of 1x M9 salts. Cells were diluted 1:100 in 100 μL of 1 x M9 salts and plated onto M63 minimal medium (containing 20% galactose and 12.5 μg/mL chloramphenicol). Cells were incubated at 32°C

for 4 days. Single colonies were streaked out on LB agar (containing 12.5 µg/mL chloramphenicol and 10 µg/mL tetracycline) and their BAC DNA analysed by restriction digestion to determine if the insertion of galK was successful. Colonies that were positively identified by restriction digestion were analysed by DNA sequencing.

5.2.10.2. Introducing latent protein coding sequences into BAC DNA

A Gal^+ SW102 clone containing the appropriate BAC DNA was used to carry out counter selection. Cells were made competent, heat induced, electroporated and recovered as outlined in section 5.2.10.1. However, in this case latent protein-coding fragments were generated through PCR or digested from a shuttle vector (see section 5.1.6 for the primers used). Recovered cells were pelleted at 3000 x g for 10 minutes at 3°C, the supernatant removed and the cells washed in 10 mL 1 x M9 salts. Washed cells were centrifuged as before and were resuspended in 1 mL in 1 mL of 1 x M9 salts. Cells were diluted 1:100 in 100 µL of 1x M9 salts and plated onto M63 minimal medium (containing 20% DOG and 12.5 µg/mL chloramphenicol). Cells were incubated at 32°C for 4 days. Single colonies were streaked out on LB agar (containing 12.5 µg/mL chloramphenicol and 10 µg/mL tetracycline) and their BAC DNA analysed by restriction digestion to determine if the latent protein-coding sequences were successfully inserted. Colonies that were positively identified by restriction digestion were analysed by DNA sequencing.

5.2.11. Cloning of Antigen-Armed Antibodies

Antigen-armed antibodies (AgAbs) are antibodies that are fused to antigen. Previously, B cells have been targeted with AgAbs generated from α-CD19, α-CD20, α-CD21 and α-CD22 antibodies [146]. Targeting of B cells with AgAbs enable their internalisation and the concomitant presentation of antigenic peptides to $CD4^+$ T cells.

In this study, AgAbs were used to deliver antigens to antigen-presenting cells (APCs) to enable the expansion of memory $CD4^+$ T cells from EBV-positive individuals. AgAb heavy chains were constructed by fusing antigen-coding sequences from EBNA1 and gp350 to an α-CD20 heavy chain (HC) gene (Figure 5.2). The α-CD20 HC used in this study consisted of domains of human and mouse origin and was previously cloned [146]. The constant regions

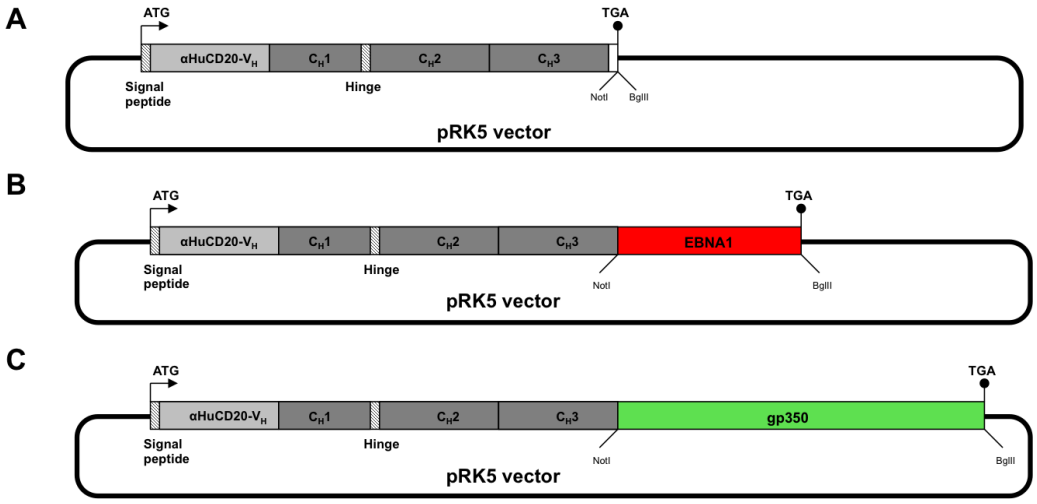

Figure 5.2: AgAb heavy chains were cloned into the mammalian expression vector pRK5. (A) An α-CD20 HC expression vector was cloned to contain NotI and BglII restriction sites. Expression vectors encoding the EBNA1-AgAb HC (B) and gp350-AgAb HC (C) are shown.

originated from mouse IgG2a, while the variable regions originated from human α-CD20.The first step in generating AgAb expression vectors was the construction of an α-CD20 heavy chain-expression vector with *Not*I and *Bgl*II restriction sites downstream of the CH3 domain. This enabled the cloning of antigen-coding sequences downstream of the α-CD20 HC. To this end, EBNA1 or gp350 coding-sequences were PCR amplified (see section 5.1.6 for the primers), digested with *Not*I and *Bgl*II and introduced to the α-CD20 HC encoding vector using.

5.2.12. Eukaryotic cell culture

5.2.12.1. Generation of wtEBV and $_{DF}$EBV producer cells lines

Producer cell lines were generated by transfecting 293 cells with BAC DNA. BAC DNA was prepared as described in section 5.2.7.3. 293 cells were plated in 6 well plates at 3 x 10^5 cells per well and allowed to attach overnight at 37°C. For each well, a transfection mixture was prepared by mixing 800 µL of RPMI 1640 (containing 5 µL BAC DNA) and 200 µL of RPMI 1640 (containing 7 µL Metafectne). The mixture was incubated at room temperature for 20 minutes and added dropwise to the cells. The cells were incubated overnight at 37°C and inspected for GFP expression using a fluorescent microscope. Generally, a transfection efficiency of 20% was satisfactory. Once the appropriate level of GFP expression was confirmed, the cells were collected by gentle pipetting and added to a 15 cm plate in 30 mL RPMI medium (supplemented with 10 % FBS**,** 300 µL of 1 x sodium pyruvate**,** 30 µL of aTG/BCA mix and 100 µg/mL of hygromycin). The cells were incubated at 37°C for 2-3 weeks until single colonies grew out. The medium was aspirated and the single colonies were covered with a small volume of 0.05% trypsin (30 µL) and collected with a micropipette. Each colony was added to a six well plate in containing 2 mL RPMI 1640 medium (10 % FBS and 100 µg/mL hygromycin) per well. Cells were expanded to 10 cm plates and clones were tested for their ability to express the late lytic gene product gp350 upon induction with BZLF1 (p509) (see section 5.2.12.2). Clones that had between 5 and 20% gp350 positive cells were further analysed. Cells that were contained EBV BAC were further screened by qPCR. However, this was not possible for $_{DF}$EBV producer cell lines since their particles lacked DNA. Hence, their supernatants were analysed in a B cell binding assay (see section 5.2.12.6). As a control wtEBV with a titre of 1 x 10^7 was analysed alongside $_{DF}$EBV supernatants. The BAC DNA from clones giving high titres were analysed by restriction digestion after plasmid rescue (see section 5.2.12.4).

5.2.12.2. Production of EBV and $_{DF}$EBV

Cell lines stably transfected with BAC DNA were used to produce virus or $_{DF}$EBV. Viable cells were plated at 3.5 x 10^5 in a 6 well plate and incubated overnight at 37°C. The cells were then transfected with a total of 1 µg of DNA. EBV producer cell lines were transfected with 0.5 µg of the BZLF1-encoding vector (p509) to induce lytic replication and 0.5 µg of a gp110-encoding vector (pRA). Increased amounts of gp110 within the viral envelope increase virus infection 100 times [193]. $_{DF}$EBV producer cell lines were always infected with 0.5 µg of p509 and 0.5 µg of empty pCDNA. Transfection mixes were set-up mixing 100 µL of RPMI 1640 containing DNA and 100 µL of RPMI 1640 containing metafectene. Transfection mixes were incubated at room temperature for 20 minutes and added to cells in a drop-wise fashion. Cells were incubated for 8 to 12 hours and the metafectene-containing medium was replaced with fresh RPMI 1640 supplemented with 10% FBS. The cells were incubated at 37°C for three days and supernatants were collected. The supernatants were centrifuged at 400 x g for 10 minutes and filtered through a 0.44 µm filter. EBV and $_{DF}$EBV used for the *ex vivo* expansion of T cells or *in vivo* experiments were produced in serum-free FreeStyle 293 medium instead of RPMI 1640 containing 10% FBS. Additionally, EBV and $_{DF}$EBV used for *in vivo* experiments were concentrated at 18 000 x g for 3 hours and resuspended in PBS.

5.2.12.3. Transient expression of AgAbs in HEK 293 cells

293 cells (3 x 10^6 cells) were seeded in 10 cm plates and incubated overnight at 37°C to allow them to attach. Next, the AgAb expression vectors described in section 5.2.11, along with an expressing vector encoding an α-CD20 light chain, were transfected into 293 cells using polyethylenimine (PEI). To prepare the transfection mixture for each plate, 20 µg of heavy chain and 20 µg of light chain encoding plasmid were added to 750 µL of Opti-MEM. Then, 50 µg of PEI was added to the DNA mixture and incubated at room temperature for 30 minutes. The transfection mix was carefully added to a plate containing the 293 cells and

incubated overnight. The medium was aspirated the following day and replaced with FreeStyle 293 expression medium and incubated for 3 more days. The AgAb containing supernatant was centrifuged at 500 x g for 15 minutes to remove cell debris. The supernatant was then filtered through a 0.22 µm Acetate filter and concentrated with ultrafiltration through the use of Vivaspin 20 centrifugal concentrators (10 000 MWCO). The concentrated AgAbs were supplemented with 2 x HEPES buffer and quantified with an IgG-specific ELISA. The quantified AgAbs were aliquoted and stored at -20°C.

5.2.12.4. Plasmid rescue protocol

Producer cells from a 15 cm plate were transferred to 50 mL falcon tube and collected by centrifugation at 400 x g. The pelleted cells were washed twice with 10 mL PBS, the supernatant gently poured off and the cells resuspended in the remaining liquid. Circle prep lysis buffer (10 mL) was added to the cells and the mixture incubated for 5 minutes, after which 500 µL of Tris-HCL (pH 7.1) was added in a dropwise fashion. During the dropwise addition of Tris-HCL, gentle mixing was performed in a circular motion. Subsequently, 2 mL of 3 M NaCl was added to the lysed cells and the mixture was inverted three times. Proteinase K (0.7 mg) was added and digestion was carried out overnight at 37°C. The following day, one volume of Phenol/NaCl was added and the solution was mixed in an end-over-end fashion for 10 minutes. Centrifugation was performed at 3400 x g for 15 minutes and the upper aqueous phase was immediately transferred to a clean 50 mL falcon tube. One volume of n-Butanol was then added and end-over-end mixing carried out as before. Centrifugation was carried out at 2000 x g for 10 minutes and the upper phase was carefully removed and discarded. The bottom phase was collected and transferred to a 50 mL falcon tube containing 2.5 volumes containing ice-cold ethanol (100%). The DNA was precipitated at -20°C for 1 hour and pelleted by centrifugation at 4000 x g for 1 hour at room temperature. The supernatant was removed, the pellet washed in 1 mL ethanol (70%) and

resuspended in 50 µL dH_2O. The DNA was allowed to dissolve overnight at 4°C and was used to electroporate DH10B cells. The DNA contained within single colonies was, isolated and analysed by restriction digestion to confirm the BAC integrity.

5.2.12.5. Determination of green fluorescent units (GRU)

The green fluorescent units (GFU) of viral supernatants were used to determine infectivity. Virus supernatant with a concentration of 1 x 107 genomes/mL, as determined by qPCR, was serially diluted in 96 well plate with RPMI 1640 (supplemented with 10% FBS and Penstrep (1%). Viable Raji cells (1 x 10^4 cells) were added to each well and the plate incubated at 37°C for 2 days. Subsequently, 1M n-butyrate and 30 µL (20 ng/mL) 12-O-tetradecanoylphorbol-13-acetate (TPA) was added to each well and the plate incubated overnight at 37°C. The following day the cells were examined under a fluorescent microscope (Leica DM IRB) and the percentage GFP-positive cells were determined.

5.2.12.6. B cell binding assay

Binding assays were performed with Elijah negative B cells to obtain an estimation of virus or $_{DF}$EBV titre. Viable Elijah negative cells (1 x 10^5 cells) were incubated with 1 mL of virus or $_{DF}$EBV supernatant at 4°C on a neutator for 2 hours. Cells were collected at 300 x g (4°C) and washed 3 times with ice-cold PBS. Washed cells were dropped on slides and air-dried. Cells were fixed with acetone for exactly 20 minutes and stained in a humidity chamber with α-gp350 (clone 72A1) antibody at 37°C for 30 minutes. Cells were washed three times in PBS and stained with α-mouse Cy3 in a humidity chamber at 37°C for 30 minutes. Cells were washed as before, mounted with glycerol and analysed with a fluorescent microscope (Leica DM 500B).

5.2.12.7. Maintenance of T-cell clones/ lines.

5.2.12.7.1. Preparation of Human serum

For T-cell maintenance, fresh serum was used to formulate T-cell medium. In general, fresh serum was prepared every 10 days. Blood from two healthy donors (~ 75 mL each) were drawn and added to 50 mL falcon tubes. The blood was then left at room temperature for 2 hours to allow clotting take place. During this incubation period the blood was mixed three times through inversion. The blood was centrifuged at 600 x g for 15 minutes without brake and the upper phase transferred to a sterile 50 mL falcon tube. The collected serum from two donors was then pooled and centrifuged at 600 x g one last time to remove any contaminating red blood cells. The clear serum then heat inactivated at 56°C for 30 minutes. The resulting serum was allowed to cool to room temperature and used immediately to supplement T-cell medium. For short term storage, serum was kept at 4°C for no more than two weeks.

5.2.12.7.2. Isolation of Peripheral Mononuclear Cells (PBMCs)

PBMCs were isolated from buffy coats that were obtained from the '*Institut für Klinische Transfusionsmedizin und Zelltherapie'* (IKTZ) Heidelberg. Blood (~ 50 mL) from a single donor was added to a sterile 250 mL conical centrifuge tube containing 50 mL pre-chilled PBS (supplemented with 500 µL 0.5 M EDTA (pH 8.0)). Ficoll-Paque™ (50 mL) was then carefully layered underneath the diluted blood and centrifuged without brake at 500 x g for 30 minutes. The layer containing the PBMCs was carefully transferred to sterile 50 mL falcon tubed, diluted 1:2 with ice-cold RPMI 1640 medium and centrifuged at 500 x g for 15 minutes. The supernatant was removed and the pellet resuspended in 50 mL ice-cold RPMI 1640. The PBMCs were then centrifuged twice at 80 x g for 15 minutes to remove contaminating platelets. The resulting PBMCs were resuspended in 50 mL PRMI 1640 and counted in a Neubauer counting chamber. The PBMCs were then added to T-cell medium at a concentration of 1 x 10^6 cells/mL and irradiated with 40 Gray.

5.2.12.7.13. Pulsing of LCLs with antigen

In order to stimulate T cells, LCLs were pulsed with the appropriate peptides. LCLs at a concentration of 1 x 10^6 cells/mL were mixed with at total of 1 µg peptide and then incubated at 37°C for 3 hours. The pulsed LCLs were centrifuged at 500 x g for 10 minutes and the peptide containing supernatant removed. Pelleted LCLs were washed twice with room temperature RPMI 1640 to remove unbound peptide. LCLs were resuspended at a concentration of 1 x 10^6 cells/mL in T-cell medium and irradiated with 80 Gray.

5.2.12.7.14. Mix T cells with pulsed LCLs and feeder cells

The final step in the stimulation protocol entails mixing the T cells with PBMCs (see section 5.2.12.7.12) and pulsed LCLs (see section 5.2.12.7.13). Viable T cells were quantified in a Neubauer counting chamber and resuspended in T-cell medium (supplemented with IL-2 10U/mL and 250 ng/mL of PHA) at 1 x 10^6 cells/mL. To each millilitre of T cells another millilitre of T-cell medium (supplemented with 10U/mL of IL-2 and 250 ng/mL of PHA) containing 2 x 10^5 LCLs and 1 x 10^6 PMBCs were added. The T-cell-LCL-PBMC mixture was then incubated at 37°C. After two days, the PHA containing medium was removed and replaced with T-cell medium containing 10U/mL of IL-2.

5.2.12.8. The ex vivo of $CD4^+$ T cells

AgAbs were utilised in the present study to expand $CD4^+$ T cells from EBV-positive donors. The use of EBNA1-AgAb and gp350-AgAb respectively enabled the expansion of EBNA1- and gp350-specific $CD4^+$ T cells from bulk PBMCs or modified $_{DF}$EBV-stimulated PBMCs. Once expanded, these cells were maintained in a similar fashion as described in section 3.2.12.7.

To expand the relevant T cells, they were stimulated biweekly, using PBMCs or LCLs as APCs . A total of 50 ng of each AbAb was used to pulse enough APCs for 1 million T cells. Prior to cocultured with T cells, PBMCs and LCLs were respectively irradiated with 40 and 80 Gray.

5.2.12.9. T-cell activation assays

T-cell activation was determined by quantifying the amount of IFN-γ released from T cells that were cocultured with pulsed LCLs. T cells were cocultured with pulsed LCLs at a ratio of 1:1 for 16-20 hours and cell culture supernatants were then analysed for the presence of IFN-γ with an ELISA (see section 5.2.15.4.1).

5.2.12.10. Isolation of B cells from PBMCs

In the present study B cells were prepared from freshly isolated PBMCs (see section 3.2.12.7) using the Dynabeads CD19 Pan (Invitrogen) and DETACHaBEADs CD19 kit (Invitrogen).

Isolated PBMCs from a single donor were resuspended in 5 mL RPMI 1640 (supplemented with 2% FBS), to which a total of 1.4 x 10^8 Dynabeads CD19 Pan were added. The mixture was neutated at room temperature for 45 minutes and B cell-Dynabead complexes were collected with a magnet. The supernatant was removed and the pellet was washed in three times 10 mL of RPMI 1640 (supplemented with 2% FBS). The pellet was resuspended in 1mL of RPMI 1640 (supplemented with 2% FBS) and a small volume (100 µL) of DETACHaBEADs was added. The mixture was neutated at room temperature for 45 minutes and the Dynabeads CD19 Pan was collected with a magnet. The supernatant, containing purified B cells was collected and transferred to sterile 15 mL falcon tube. The Dynabeads CD19 Pan fraction was washed twice with 5 mL RPMI 1640 (supplemented with 10% FBS) to remove residual B cells. The B cell containing fractions were pooled and washed one last time in 5 mL RPMI 1640 (supplemented with 10% FBS).

5.2.13. Depletion of $CD8^+$ T cells from T-cell cultures

On a few occasion, $CD8^+$ T cells managed to grow and expand after the stimulation of PBMCs with AgAbs or $_{DF}$EBV (see section 5.2.12.8). Whilst the proportion of $CD8^+$ T cells in these

cultures were always less than $CD4^+$ T cells, *ex vivo* cultures were depleted of $CD8^+$ T cells to enable the exclusive analysis of $CD4^+$ T cells.

$CD8^+$ T cells were depleted from T-cell cultures using anti-PE MicroBeads (cat no: 130-097-054). A total of 1 x 10^7 cells were incubated with 10 µL anti-human CD8a PE antibody (cat no: 12-0087-41) at 4°C for 1 hour and pelleted at 300 x g for 5 minutes. The supernatant was removed and the cell pellet was resuspended in 1 mL cold MACS buffer (PBS supplemented with 0.5% BSA and 2nM EDTA). The cells were washed as before and resuspended in 100 µL of cold MACS buffer and 20 µL of anti-PE MicroBeads was added. The mixture was incubated at 4°C for 1 hour, washed as described above and resuspended in 500 µL of cold MACS buffer. An LS MACS column (cat no:130-041-306) was placed in magnetic MACS separator, washed with 3 mL MACS buffer and loaded with the cell suspension. The flow through containing $CD4^+$ T cells was collected. The column was washed with 2 x 5 mL to collect any unbound cells $CD4^+$ T cells.

5.2.14. LCL generation

LCLs were generated by from B cells that were freshly isolated from the PBMCs (see section 5.2.12.10). B cells were infected with B95-8ΔBZLF1/BRLF1 at an MOI of 10 at room temperature for 2 hours. Thereafter, cells were washed with RPMI 1640, mixed with RPMI 1640 (supplemented with 10% FBS) and incubated for 1 to 2 weeks at 37°C until LCLs grew out. LCLs were maintained as suspension cultures in LCL medium (RPMI 1640 with 10% fetal calf serum, 1 mM sodium pyruvate, 2 mM L-glutamine, 1% nonessential amino acids and 50 µg/ml gentamicin)

5.2.15. Flow cytomteric analyses

5.2.15.1. Quantification of $_{DF}$EBV

Flow cytometry was used as the principal method for quantifying $_{DF}$EBV. Elijah negative cells were harvested at 400 x g for 10 minutes and washed once with PBS (3% BSA). The cells were resuspended in ice-cold PBS (3% BSA) and 5 x 10^5 cells were aliquoted into sterile 1.5 mL eppendorf tubes for every $_{DF}$EBV supernatant to be analysed. $_{DF}$EBV containing supernatant (1 mL), pre-chilled on ice, was mixed with Elijah negative cells and neutated at 4°C for 2 hours. Cells were centrifuged at 400 x g for 5 minutes, the supernatant containing unbound $_{DF}$EBV removed and the cells resuspended in 1 mL ice-cold PBS (3% BSA). The cells were centrifuged as before and resuspended in 100 µL of ice-cold PBS (3% BSA). A gp350-specific mouse antibody (clone 72A1) was added to the cells at 6 µg/mL and incubated on ice for 1 hour. Subsequently, the cells were washed as before and an α-mouse IgG-Cy3 antibody (115-165-146) was then added (1:100 dilution). The mixture was incubated on ice for 1 hour, the cells washed and resuspended in 400 µL of ice-cold PBS (3% BSA). The cells were then passed through a cells strainer and measured with a BD FACSCalibur™.

5.2.15.2. Quantification of $CD4^+$ T cells

FACS was used to identify $CD4^+$ T cells in *ex vivo*-expanded cultures. Expanded cells were collected by centrifugation at 400 x g for 10 minutes, washed with 5 mL of PBS (containing 1% BSA) resuspended in 100 µL of PBS (containing 1% BSA) at a concentration of 5 x 10^5 cells/100 µL. For each sample to be analysed, single stains (α-huCD4 PE-Cy5 or α-huCD3-PE) and double stains (α-huCD4 PE-Cy5 and α-huCD3-PE) were performed, with unstained cells serving as a negative control. Antibodies were used at the dilution suggested by the manufacturer. Cells were incubated for 1 hour on ice, washed thrice with 1 mL ice-cold PBS (containing 1% BSA) and resuspended in ice-cold PBS (containing 1% BSA). Cells were passed through a cells strainer and analysed with a FACSCalibur device.

5.2.15.3. Quantification of CD107a expression by $CD4^+$ T cells

LCLs were pulsed overnight with AgAbs (200 ng), α-CD20 or medium (negative control). The next day, LCLs were washed with PBS and mixed with T cells at an E:T ratio of 3:1. A total of 8 µL of α-CD107a-FITC (eBioH4A3) was immediately added to the T-cell-LCL mixture and incubated for 8 hours. Cells were collected at 400 x g, washed and 3 µL of α-CD4-PE-Cy5 (RPA-T4) and 3 µL α-CD107a-FITC (eBioH4A3) was added to cells and further incubated for 30 minutes. Cells were washed three times with PBS, resuspended in 500 µL of PBS (1% BSA) and analysed by flow cytometry with a FACSCalibur device.

5.2.15.4. Infection of primary B cells in the presence of EBNA1- and gp350-specific T cells

Primary B cells were infected overnight using B95-8 (MOI = 10), washed with RPMI 1640 without additions and cocultured with EBNA1- or gp350-specific T cells at a E:T ratio of 1:2 in T-cell medium supplemented with IL-2 (10U/mL). B cells cultured in medium alone served as a positive control of B cell outgrowth. Cells were incubated for 12 days and analysed by flow cytometry for the presence of $CD19^+CD23^+$ double-positive cells by staining with α-CD19-APC (HIB19 clone) and α-CD23-PE-Cy7 (EBVCS2 clone).

5.2.15.5. Infection of primary B cells in the presence of $_{DF}$EBV-EBNA^{RI+RII}-stimulated PBMCs

Freshly isolated PBMCs were stimulated for two rounds with either gp350-AgAb or $_{DF}$EBV-EBNA1^{RI+RII}. Thereafter, primary B cells were infected with either B95-8 (MOI = 3) or M81 (MOI = 30) overnight. Different amounts of each strain were used for infection due to their different transforming abilities. Infected B cells were cocultured with gp350-AgAb or $_{DF}$EBV-EBNA1^{RI+RII}-stimulated PBMCs or $CD19^-$PBMCs at an E:T ratio of 1:1 in T-cell medium supplemented with IL-2 (10U/mL) for a total of 15 days. At day 5, *ex vivo* cultures were analysed by immunofluorescence. Cells were stained with α-CD20 (L26 clone), α-EBNA2 (PE2

clone) and DAPI prior to immunofluorescence. Cells were also analysed after 15 days, but with flow cytometry instead of immunofluorescence. Cells were stained with α-CD19-APC (HIB19 clone) and α-CD23-PE-Cy7 (EBVCS2 clone) prior to flow cytomteric analysis.

5.2.15.4. Enzyme-linked immunosorbent assays

5.2.15.4.1. Interferon-γ ELISA

The human IFN-γ ELISA kit (HRP) from Mabtech was used for all interferon-γ based T-cell assays. Stripwell 96 well plates (Sigma) were coated overnight with 100 µL of mAB 1-D1k (2 µg/ml) in PBS per well at room temperature. The following day, the 96 well plates were washed three times with 300 µL of PBS (0,05% Tween-20) per well using a HydroFlex microplate washer (Tecan). Throughout the duration of this protocol, all washes were carried out in the same manner. The washed plates were blocked for two hours at room temperature with 300 µL of PBS (1% BSA) per well. Plates were washed and 100 µL of cell culture supernatants (see section 5.2.12.9) and IFN-γ standard (2-0.03 ng) was added per well. Plates were incubated at room temperature for 2 hours, washed and 100 µL of mAb 7-B6-1-biotin (1 µg/ml) in PBS (1% BSA) was added to each well. Incubation was carried out at room temperature for 2 hours. The plates were washed, 100 µL Streptavidin-HRP (1:1000 dilution) in PBS (1% BSA) was added to each well and plates incubated at room temperature, in the dark, for 30 minutes. The plates were washed and 100 µL of TMB substrate (BD Biosciences) was added to each well and incubated for a maximum of 5 minutes. The reaction was stopped by adding 50 µL of 2M H_2SO_4 to each well. The absorbance of each well was measured at 450 nm and 540 nm in a MultiscanEx microplate reader (Thermo Fischer Scientific). Absorbance values measured at 540 nm were subtracted from those obtained for 450 nm.

5.2.15.4.2. Granzyme B ELISA

Granzyme B release from T cells was measured using the Granzyme B ELISA kit (HRP) from Mabtech. Stripwell 96 well plates (Sigma) were coated overnight with 100 µL mAb GB10 (2 µg/ml) in PBS at room temperature. Plates were washed three times with 300 µL of PBS (0.05% Tween 20) using a HydroFlex microplate washer (Tecan). All washes within this protocol were carried out in this manner. Thereafter, plates were blocked at room temperature with 300 µL of PBS (1% BSA) for two hours. Plates were washed as before and 100 µL of cell culture supernatant or Granzyme standard (10-0.3 ng) in PBS (containing 1% BSA) was added. Plates were incubated at room temperature for 2 hours, washed and incubated at room temperature with 100 µL of mAb GB11-biotin (1 µg/ml) in PBS (1% BSA) for an additional 2 hours. Washing was performed and plates were incubated at room temperature, in the dark, for 30 minutes with 100 µL of Steptavadin-HRP (1:1000 dilution) in PBS (1 % BSA). The plates were washed one last time and developed as detailed in section 5.2.13.4.1.

5.2.15.4.3. IgG2a ELISA

An IgG2a ELISA was used to quantify α-CD20 and AgAbs. Stripwell 96 well plates (Sigma) were coated overnight at room temperature with 100 µL (5 µg/mL) of α-mouse IgG (Dianova) in PBS. Plates were washed three times with 300 µL of PBS (0.05% Tween 20) using a HydroFlex microplate washer (Tecan). All washes in this protocol were conducted in this manner. Blocking was performed by incubating plates with 300 µL PBS (1% BSA) for two hours at room temperature. Plates were washed and incubated with 100 µL of sample and standard (4-0.0625 ng/mL) for 1 hour at room temperature. Washing was performed and plates were incubated with 100 µL of α-mouse IgG-HRP (0.5 µg/mL) (Promega) in PBS (1% BSA) for 30 minutes. Plates were washed one last time and developed as detailed in section 5.2.13.4.1.

5.2.16. Experiments with humanised NSG-A2 mice

5.2.16.1. Humanisation of NSG-A2 mice

Mice with reconstituted human immune system components serve as a powerful tool to study human-tropic pathogens such as EBV [154]. In this study, NSG-A2 mice (NOD.Cg-Prkdc^{scid}Il2rg^{tm1Wjl}Tg (HLA-A2.1) 1Enge/SzJ) were humanised to provide a model for studying the antigenicity of $_{DF}$EBV *in vivo*. Newborn NSG-2A mice were irradiated with 1 Gy and injected intrahepatically with 2 x 10^5 CD34$^+$ hematopoietic progenitor cells (HPCs). The CD34$^+$ HPCs were isolated from human fetal liver tissue (Advanced Bioscience Resources, USA) using a human CD34 MicroBead kit (Miltenyi Biotec). Humanisation was determined 12 weeks after engraftment by assessing the presence of huCD45$^+$ cells in the peripheral blood of mice via flow cytometry.

5.2.16.2. Vaccination and challenge of humanised NSG-A2 mice

In total 20 Humanised NSG-A2 (huNSG-A2) mice were randomly sorted into three groups so that each group contained similar humanisation percentages. Thereafter, mice were injected in a single blind fashion with PBS, 1 x 10^6 particles of $_{DF}$EBV, or 1 x 10^6 particles of $_{DF}$EBV-EBNA1^{RI+RII}. In all cases, 50 µg of poly (I:C) was used as adjuvant. Animals were boosted one month after vaccination using the same treatments and adjuvant. One and a half months after the boost, mice were infected intraperitoneally with B95-8 (1 x 10^5 GRU). Mice were euthanised after 8 weeks and their spleen and blood analysed for evidence of EBV infection as previously described [194].

5.2.17. Statistical analysis

A two-tailed student T-test was performed to compare the ability of CD19$^-$ PBMCs, gp350- or $_{DF}$EBV-EBNA1^{RI+RII}-specific T cells to control B cells infected with B95-8 or M81. A One-tailed

Chi-square test was used to analyse the incidence of EBV infection in humanised mice. All statistical analyses were performed using GraphPad Prism 6 software.

8. References

1. McGeoch, D.J., A. Dolan, and A.C. Ralph, *Toward a comprehensive phylogeny for mammalian and avian herpesviruses.* J Virol, 2000. **74**(22): p. 10401-6.
2. Davison, A.J., et al., *The order Herpesvirales.* Arch Virol, 2009. **154**(1): p. 171-7.
3. Davison, A.J., *Herpesvirus systematics.* Vet Microbiol, 2010. **143**(1): p. 52-69.
4. McGeoch, D.J., *Molecular evolution of the gamma-Herpesvirinae.* Philos Trans R Soc Lond B Biol Sci, 2001. **356**(1408): p. 421-35.
5. Ehlers, B., et al., *Lymphocryptovirus phylogeny and the origins of Epstein-Barr virus.* J Gen Virol, 2010. **91**(Pt 3): p. 630-42.
6. Rickinson, A.B. and P.J. Lane, *Epstein-Barr virus: Co-opting B-cell memory and migration.* Curr Biol, 2000. **10**(3): p. R120-3.
7. Kieff, E., et al., *The biology and chemistry of Epstein-Barr virus.* J Infect Dis, 1982. **146**(4): p. 506-17.
8. Johannsen, E., et al., *Proteins of purified Epstein-Barr virus.* Proc Natl Acad Sci U S A, 2004. **101**(46): p. 16286-91.
9. Pavlova, S., et al., *An Epstein-Barr virus mutant produces immunogenic defective particles devoid of viral DNA.* J Virol, 2013. **87**(4): p. 2011-22.
10. Germi, R., et al., *Three-dimensional structure of the Epstein-Barr virus capsid.* J Gen Virol, 2012. **93**(Pt 8): p. 1769-73.
11. Henson, B.W., et al., *Self-assembly of Epstein-Barr virus capsids.* J Virol, 2009. **83**(8): p. 3877-90.
12. Dai, X., et al., *CryoEM and mutagenesis reveal that the smallest capsid protein cements and stabilizes Kaposi's sarcoma-associated herpesvirus capsid.* Proc Natl Acad Sci U S A, 2015. **112**(7): p. E649-56.
13. Scrima, N., et al., *Insights into herpesvirus tegument organization from structural analyses of the 970 central residues of HSV-1 UL36 protein.* J Biol Chem, 2015. **290**(14): p. 8820-33.
14. Vittone, V., et al., *Determination of interactions between tegument proteins of herpes simplex virus type 1.* J Virol, 2005. **79**(15): p. 9566-71.
15. Dai, W., et al., *Unique structures in a tumor herpesvirus revealed by cryo-electron tomography and microscopy.* J Struct Biol, 2008. **161**(3): p. 428-38.
16. Rozen, R., et al., *Virion-wide protein interactions of Kaposi's sarcoma-associated herpesvirus.* J Virol, 2008. **82**(10): p. 4742-50.
17. Phillips, S.L. and W.A. Bresnahan, *Identification of binary interactions between human cytomegalovirus virion proteins.* J Virol, 2011. **85**(1): p. 440-7.
18. Dai, X., et al., *Organization of capsid-associated tegument components in Kaposi's sarcoma-associated herpesvirus.* J Virol, 2014. **88**(21): p. 12694-702.
19. Duarte, M., et al., *An RS motif within the Epstein-Barr virus BLRF2 tegument protein is phosphorylated by SRPK2 and is important for viral replication.* PLoS One, 2013. **8**(1): p. e53512.
20. Sathish, N., X. Wang, and Y. Yuan, *Tegument Proteins of Kaposi's Sarcoma-Associated Herpesvirus and Related Gamma-Herpesviruses.* Front Microbiol, 2012. **3**: p. 98.
21. Calderwood, M.A., et al., *Epstein-Barr virus and virus human protein interaction maps.* Proc Natl Acad Sci U S A, 2007. **104**(18): p. 7606-11.
22. Feederle, R., et al., *Epstein-Barr virus BNRF1 protein allows efficient transfer from the endosomal compartment to the nucleus of primary B lymphocytes.* J Virol, 2006. **80**(19): p. 9435-43.

23. Wang, L., et al., *Distinct domains in ORF52 tegument protein mediate essential functions in murine gammaherpesvirus 68 virion tegumentation and secondary envelopment.* J Virol, 2012. **86**(3): p. 1348-57.
24. Bortz, E., et al., *Murine gammaherpesvirus 68 ORF52 encodes a tegument protein required for virion morphogenesis in the cytoplasm.* J Virol, 2007. **81**(18): p. 10137-50.
25. Sathish, N., F.X. Zhu, and Y. Yuan, *Kaposi's sarcoma-associated herpesvirus ORF45 interacts with kinesin-2 transporting viral capsid-tegument complexes along microtubules.* PLoS Pathog, 2009. **5**(3): p. e1000332.
26. Cantin, R., S. Methot, and M.J. Tremblay, *Plunder and stowaways: incorporation of cellular proteins by enveloped viruses.* J Virol, 2005. **79**(11): p. 6577-87.
27. Hutt-Fletcher, L.M., *EBV glycoproteins: where are we now?* Future Virol, 2015. **10**(10): p. 1155-1162.
28. Young, K.A., et al., *Molecular basis of the interaction between complement receptor type 2 (CR2/CD21) and Epstein-Barr virus glycoprotein gp350.* J Virol, 2008. **82**(22): p. 11217-27.
29. Szakonyi, G., et al., *Structure of the Epstein-Barr virus major envelope glycoprotein.* Nat Struct Mol Biol, 2006. **13**(11): p. 996-1001.
30. Janz, A., et al., *Infectious Epstein-Barr virus lacking major glycoprotein BLLF1 (gp350/220) demonstrates the existence of additional viral ligands.* J Virol, 2000. **74**(21): p. 10142-52.
31. Busse, C., et al., *Epstein-Barr viruses that express a CD21 antibody provide evidence that gp350's functions extend beyond B-cell surface binding.* J Virol, 2010. **84**(2): p. 1139-47.
32. Ogembo, J.G., et al., *Human complement receptor type 1/CD35 is an Epstein-Barr Virus receptor.* Cell Rep, 2013. **3**(2): p. 371-85.
33. Chen, J. and K. Sathiyamoorthy, *Ephrin receptor A2 is a functional entry receptor for Epstein-Barr virus.* 2018. **3**(2): p. 172-180.
34. Zhang, H., et al., *Ephrin receptor A2 is an epithelial cell receptor for Epstein-Barr virus entry.* 2018. **3**(2): p. 164-171.
35. Tugizov, S.M., J.W. Berline, and J.M. Palefsky, *Epstein-Barr virus infection of polarized tongue and nasopharyngeal epithelial cells.* Nat Med, 2003. **9**(3): p. 307-14.
36. Xiao, J., et al., *The Epstein-Barr virus BMRF-2 protein facilitates virus attachment to oral epithelial cells.* Virology, 2008. **370**(2): p. 430-42.
37. Neuhierl, B., et al., *Primary B-cell infection with a deltaBALF4 Epstein-Barr virus comes to a halt in the endosomal compartment yet still elicits a potent CD4-positive cytotoxic T-cell response.* J Virol, 2009. **83**(9): p. 4616-23.
38. Sathiyamoorthy, K., et al., *Assembly and architecture of the EBV B cell entry triggering complex.* PLoS Pathog, 2014. **10**(8): p. e1004309.
39. Longnecker, L.K., E.; Cohen, J.I., *Epstein-Barr Virus*. Fields Virology, ed. D.M.H. Knipe, P.M.; Cohen, J.I.; Griffith, D.E.; Lamb, R.A.; Martin, M.A.; Racaniello, V.; Roizman, B. Vol. 6th. 2013, Phiadelphia, PA, USA Lippincott Williams and Wilkins.
40. Lake, C.M. and L.M. Hutt-Fletcher, *Epstein-Barr virus that lacks glycoprotein gN is impaired in assembly and infection.* J Virol, 2000. **74**(23): p. 11162-72.
41. Baer, R., et al., *DNA sequence and expression of the B95-8 Epstein-Barr virus genome.* Nature, 1984. **310**(5974): p. 207-11.
42. Kwok, H., et al., *Genomic sequencing and comparative analysis of Epstein-Barr virus genome isolated from primary nasopharyngeal carcinoma biopsy.* PLoS One, 2012. **7**(5): p. e36939.

43. Langerak, A.W., et al., *Detection of clonal EBV episomes in lymphoproliferations as a diagnostic tool.* Leukemia, 2002. **16**(8): p. 1572-3.
44. Hammerschmidt, W. and B. Sugden, *Identification and characterization of oriLyt, a lytic origin of DNA replication of Epstein-Barr virus.* Cell, 1988. **55**(3): p. 427-33.
45. Taylor, G.S., et al., *The immunology of Epstein-Barr virus-induced disease.* Annu Rev Immunol, 2015. **33**: p. 787-821.
46. Young, L.S. and P.G. Murray, *Epstein-Barr virus and oncogenesis: from latent genes to tumours.* Oncogene, 2003. **22**(33): p. 5108-21.
47. Heslop, H.E., *How I treat EBV lymphoproliferation.* Blood, 2009. **114**(19): p. 4002-8.
48. Young, L.S., L.F. Yap, and P.G. Murray, *Epstein-Barr virus: more than 50 years old and still providing surprises.* Nat Rev Cancer, 2016. **16**(12): p. 789-802.
49. Hodin, T.L., T. Najrana, and J.L. Yates, *Efficient replication of Epstein-Barr virus-derived plasmids requires tethering by EBNA1 to host chromosomes.* J Virol, 2013. **87**(23): p. 13020-8.
50. Brooks, J.M., et al., *Early T Cell Recognition of B Cells following Epstein-Barr Virus Infection: Identifying Potential Targets for Prophylactic Vaccination.* PLoS Pathog, 2016. **12**(4): p. e1005549.
51. Radkov, S.A., et al., *Epstein-Barr virus nuclear antigen 3C interacts with histone deacetylase to repress transcription.* J Virol, 1999. **73**(7): p. 5688-97.
52. Young, L.S., C.W. Dawson, and A.G. Eliopoulos, *The expression and function of Epstein-Barr virus encoded latent genes.* Mol Pathol, 2000. **53**(5): p. 238-47.
53. Kang, M.S. and E. Kieff, *Epstein-Barr virus latent genes.* Exp Mol Med, 2015. **47**: p. e131.
54. Cai, Q., K. Chen, and K.H. Young, *Epstein-Barr virus-positive T/NK-cell lymphoproliferative disorders.* Exp Mol Med, 2015. **47**: p. e133.
55. Siegler, G., et al., *Epstein-Barr virus encoded latent membrane protein 1 (LMP1) and TNF receptor associated factors (TRAF): colocalisation of LMP1 and TRAF1 in primary EBV infection and in EBV associated Hodgkin lymphoma.* Mol Pathol, 2003. **56**(3): p. 156-61.
56. Xiao, H.J., et al., *Epstein-Barr Virus-Positive T/NK-Cell Lymphoproliferative Disorders Manifested as Gastrointestinal Perforations and Skin Lesions: A Case Report.* Medicine (Baltimore), 2016. **95**(5): p. e2676.
57. Kenney, S.C., *Reactivation and lytic replication of EBV*, in *Human Herpesviruses: Biology, Therapy, and Immunoprophylaxis*, A. Arvin, et al., Editors. 2007, Cambridge University Press

Copyright (c) Cambridge University Press 2007.: Cambridge.

58. Bailey, S.G., et al., *Functional interaction between Epstein-Barr virus replication protein Zta and host DNA damage response protein 53BP1.* J Virol, 2009. **83**(21): p. 11116-22.
59. Inman, G.J., et al., *Activators of the Epstein-Barr virus lytic program concomitantly induce apoptosis, but lytic gene expression protects from cell death.* J Virol, 2001. **75**(5): p. 2400-10.
60. Kudoh, A., et al., *Reactivation of lytic replication from B cells latently infected with Epstein-Barr virus occurs with high S-phase cyclin-dependent kinase activity while inhibiting cellular DNA replication.* J Virol, 2003. **77**(2): p. 851-61.
61. Mauser, A., et al., *The Epstein-Barr virus immediate-early protein BZLF1 regulates p53 function through multiple mechanisms.* J Virol, 2002. **76**(24): p. 12503-12.
62. Hong, G.K., et al., *Epstein-Barr virus lytic infection contributes to lymphoproliferative disease in a SCID mouse model.* J Virol, 2005. **79**(22): p. 13993-4003.

63. Kalla, M., C. Gobel, and W. Hammerschmidt, *The lytic phase of epstein-barr virus requires a viral genome with 5-methylcytosine residues in CpG sites.* J Virol, 2012. **86**(1): p. 447-58.
64. Feederle, R. and H.J. Delecluse, *Low level of lytic replication in a recombinant Epstein-Barr virus carrying an origin of replication devoid of BZLF1-binding sites.* J Virol, 2004. **78**(21): p. 12082-4.
65. Makhov, A.M., et al., *The Epstein-Barr virus polymerase accessory factor BMRF1 adopts a ring-shaped structure as visualized by electron microscopy.* J Biol Chem, 2004. **279**(39): p. 40358-61.
66. Neuhierl, B. and H.J. Delecluse, *The Epstein-Barr virus BMRF1 gene is essential for lytic virus replication.* J Virol, 2006. **80**(10): p. 5078-81.
67. Zimmermann, J. and W. Hammerschmidt, *Structure and role of the terminal repeats of Epstein-Barr virus in processing and packaging of virion DNA.* J Virol, 1995. **69**(5): p. 3147-55.
68. Chiu, S.H., et al., *Epstein-Barr virus BALF3 has nuclease activity and mediates mature virion production during the lytic cycle.* J Virol, 2014. **88**(9): p. 4962-75.
69. Cohen, J.I., *Optimal treatment for chronic active Epstein-Barr virus disease.* Pediatr Transplant, 2009. **13**(4): p. 393-6.
70. Tangye, S.G. and U. Palendira, *Human immunity against EBV-lessons from the clinic.* 2017. **214**(2): p. 269-283.
71. Sokal, E.M., et al., *Recombinant gp350 vaccine for infectious mononucleosis: a phase 2, randomized, double-blind, placebo-controlled trial to evaluate the safety, immunogenicity, and efficacy of an Epstein-Barr virus vaccine in healthy young adults.* J Infect Dis, 2007. **196**(12): p. 1749-53.
72. Balfour, H.H., Jr., S.K. Dunmire, and K.A. Hogquist, *Infectious mononucleosis.* Clin Transl Immunology, 2015. **4**(2): p. e33.
73. Cohen, J.I., et al., *Epstein-Barr virus: an important vaccine target for cancer prevention.* Sci Transl Med, 2011. **3**(107): p. 107fs7.
74. Kutok, J.L. and F. Wang, *Spectrum of Epstein-Barr virus-associated diseases.* Annu Rev Pathol, 2006. **1**: p. 375-404.
75. Odumade, O.A., K.A. Hogquist, and H.H. Balfour, Jr., *Progress and problems in understanding and managing primary Epstein-Barr virus infections.* Clin Microbiol Rev, 2011. **24**(1): p. 193-209.
76. Loren, A.W., et al., *Post-transplant lymphoproliferative disorder: a review.* Bone Marrow Transplant, 2003. **31**(3): p. 145-55.
77. Geng, L. and X. Wang, *Epstein-Barr Virus-associated lymphoproliferative disorders: experimental and clinical developments.* Int J Clin Exp Med, 2015. **8**(9): p. 14656-71.
78. Green, M. and M.G. Michaels, *Epstein-Barr virus infection and posttransplant lymphoproliferative disorder.* Am J Transplant, 2013. **13 Suppl 3**: p. 41-54; quiz 54.
79. Burkitt, D., *A sarcoma involving the jaws in African children.* Br J Surg, 1958. **46**(197): p. 218-23.
80. Epstein, M.A., B.G. Achong, and Y.M. Barr, *VIRUS PARTICLES IN CULTURED LYMPHOBLASTS FROM BURKITT'S LYMPHOMA.* Lancet, 1964. **1**(7335): p. 702-3.
81. Neparidze, N. and J. Lacy, *Malignancies associated with epstein-barr virus: pathobiology, clinical features, and evolving treatments.* Clin Adv Hematol Oncol, 2014. **12**(6): p. 358-71.
82. Bornkamm, G.W., *Epstein-Barr virus and the pathogenesis of Burkitt's lymphoma: more questions than answers.* Int J Cancer, 2009. **124**(8): p. 1745-55.
83. Kelly, G.L., et al., *Different patterns of Epstein-Barr virus latency in endemic Burkitt lymphoma (BL) lead to distinct variants within the BL-associated gene expression signature.* J Virol, 2013. **87**(5): p. 2882-94.

84. Rowe, M., L. Fitzsimmons, and A.I. Bell, *Epstein-Barr virus and Burkitt lymphoma.* Chin J Cancer, 2014. **33**(12): p. 609-19.
85. Massini, G., D. Siemer, and S. Hohaus, *EBV in Hodgkin Lymphoma.* Mediterr J Hematol Infect Dis, 2009. **1**(2): p. e2009013.
86. Vockerodt, M., et al., *Epstein-Barr virus and the origin of Hodgkin lymphoma.* Chin J Cancer, 2014. **33**(12): p. 591-7.
87. Tsai, M.H., et al., *Spontaneous lytic replication and epitheliotropism define an Epstein-Barr virus strain found in carcinomas.* Cell Rep, 2013. **5**(2): p. 458-70.
88. Taylor, G.S., et al., *A recombinant modified vaccinia ankara vaccine encoding Epstein-Barr Virus (EBV) target antigens: a phase I trial in UK patients with EBV-positive cancer.* Clin Cancer Res, 2014. **20**(19): p. 5009-22.
89. Straathof, K.C., et al., *Treatment of nasopharyngeal carcinoma with Epstein-Barr virus--specific T lymphocytes.* Blood, 2005. **105**(5): p. 1898-904.
90. Young, L.S. and C.W. Dawson, *Epstein-Barr virus and nasopharyngeal carcinoma.* Chin J Cancer, 2014. **33**(12): p. 581-90.
91. Frappier, L., *Role of EBNA1 in NPC tumourigenesis.* Semin Cancer Biol, 2012. **22**(2): p. 154-61.
92. Wang, L., et al., *Epstein-Barr virus nuclear antigen 1 (EBNA1) protein induction of epithelial-mesenchymal transition in nasopharyngeal carcinoma cells.* Cancer, 2014. **120**(3): p. 363-72.
93. Lamouille, S., J. Xu, and R. Derynck, *Molecular mechanisms of epithelial-mesenchymal transition.* Nat Rev Mol Cell Biol, 2014. **15**(3): p. 178-96.
94. Wei, W.I. and D.L. Kwong, *Current management strategy of nasopharyngeal carcinoma.* Clin Exp Otorhinolaryngol, 2010. **3**(1): p. 1-12.
95. Zhang, L., et al., *Emerging treatment options for nasopharyngeal carcinoma.* Drug Des Devel Ther, 2013. **7**: p. 37-52.
96. Razak, A.R., et al., *Nasopharyngeal carcinoma: the next challenges.* Eur J Cancer, 2010. **46**(11): p. 1967-78.
97. Murphy, K.T.P., Walport, M., Janeway, C., *Janeway's Immunobiology*. Vol. 8th edn. 2012, New York: Garland Science.
98. Lunemann, A., M. Rowe, and D. Nadal, *Innate Immune Recognition of EBV.* Curr Top Microbiol Immunol, 2015. **391**: p. 265-87.
99. O'Leary, J.G., et al., *T cell- and B cell-independent adaptive immunity mediated by natural killer cells.* Nat Immunol, 2006. **7**(5): p. 507-16.
100. Chijioke, O., et al., *Innate immune responses against Epstein Barr virus infection.* J Leukoc Biol, 2013. **94**(6): p. 1185-90.
101. Chijioke, O., et al., *Human natural killer cells prevent infectious mononucleosis features by targeting lytic Epstein-Barr virus infection.* Cell Rep, 2013. **5**(6): p. 1489-98.
102. Munz, C., *Dendritic cells during Epstein Barr virus infection.* Front Microbiol, 2014. **5**: p. 308.
103. Gaudreault, E., et al., *Epstein-Barr virus induces MCP-1 secretion by human monocytes via TLR2.* J Virol, 2007. **81**(15): p. 8016-24.
104. Strowig, T., et al., *Human NK cells of mice with reconstituted human immune system components require preactivation to acquire functional competence.* Blood, 2010. **116**(20): p. 4158-67.
105. Rickinson, A.B., et al., *Cellular immune controls over Epstein-Barr virus infection: new lessons from the clinic and the laboratory.* Trends Immunol, 2014. **35**(4): p. 159-69.
106. De Paschale, M. and P. Clerici, *Serological diagnosis of Epstein-Barr virus infection: Problems and solutions.* World J Virol, 2012. **1**(1): p. 31-43.

107. Bu, W., et al., *Kinetics of Epstein-Barr Virus (EBV) Neutralizing and Virus-Specific Antibodies after Primary Infection with EBV.* Clin Vaccine Immunol, 2016. **23**(4): p. 363-9.
108. Adhikary, D., et al., *Control of Epstein-Barr virus infection in vitro by T helper cells specific for virion glycoproteins.* J Exp Med, 2006. **203**(4): p. 995-1006.
109. Hislop, A.D., et al., *A CD8+ T cell immune evasion protein specific to Epstein-Barr virus and its close relatives in Old World primates.* J Exp Med, 2007. **204**(8): p. 1863-73.
110. Hislop, A.D., et al., *Cellular responses to viral infection in humans: lessons from Epstein-Barr virus.* Annu Rev Immunol, 2007. **25**: p. 587-617.
111. Adhikary, D., et al., *Immunodominance of lytic cycle antigens in Epstein-Barr virus-specific CD4+ T cell preparations for therapy.* PLoS One, 2007. **2**(7): p. e583.
112. Linnerbauer, S., et al., *Virus and autoantigen-specific CD4+ T cells are key effectors in a SCID mouse model of EBV-associated post-transplant lymphoproliferative disorders.* PLoS Pathog, 2014. **10**(5): p. e1004068.
113. Mautner, J. and G.W. Bornkamm, *The role of virus-specific CD4+ T cells in the control of Epstein-Barr virus infection.* Eur J Cell Biol, 2012. **91**(1): p. 31-5.
114. Takeuchi, A. and T. Saito, *CD4 CTL, a Cytotoxic Subset of CD4+ T Cells, Their Differentiation and Function.* Front Immunol, 2017. **8**: p. 194.
115. Long, H.M., et al., *CD4+ T-cell responses to Epstein-Barr virus (EBV) latent-cycle antigens and the recognition of EBV-transformed lymphoblastoid cell lines.* J Virol, 2005. **79**(8): p. 4896-907.
116. Paludan, C., et al., *Endogenous MHC class II processing of a viral nuclear antigen after autophagy.* Science, 2005. **307**(5709): p. 593-6.
117. Ressing, M.E., et al., *Immune Evasion by Epstein-Barr Virus.* Curr Top Microbiol Immunol, 2015. **391**: p. 355-81.
118. Rowe, M., et al., *Host shutoff during productive Epstein-Barr virus infection is mediated by BGLF5 and may contribute to immune evasion.* Proc Natl Acad Sci U S A, 2007. **104**(9): p. 3366-71.
119. Horst, D., et al., *The "Bridge" in the Epstein-Barr virus alkaline exonuclease protein BGLF5 contributes to shutoff activity during productive infection.* J Virol, 2012. **86**(17): p. 9175-87.
120. Jochum, S., et al., *The EBV immunoevasins vIL-10 and BNLF2a protect newly infected B cells from immune recognition and elimination.* PLoS Pathog, 2012. **8**(5): p. e1002704.
121. Tsai, K., et al., *EBV tegument protein BNRF1 disrupts DAXX-ATRX to activate viral early gene transcription.* PLoS Pathog, 2011. **7**(11): p. e1002376.
122. van Gent, M., et al., *Epstein-Barr virus large tegument protein BPLF1 contributes to innate immune evasion through interference with toll-like receptor signaling.* PLoS Pathog, 2014. **10**(2): p. e1003960.
123. Tsai, K., et al., *Viral reprogramming of the Daxx histone H3.3 chaperone during early Epstein-Barr virus infection.* J Virol, 2014. **88**(24): p. 14350-63.
124. Huang, H., et al., *Structural basis underlying viral hijacking of a histone chaperone complex.* Nat Commun, 2016. **7**: p. 12707.
125. Epstein, M.A. and B.G. Achong, *The EB virus.* Annu Rev Microbiol, 1973. **27**: p. 413-36.
126. Papaloukas, O., G. Giannouli, and V. Papaevangelou, *Successes and challenges in varicella vaccine.* Ther Adv Vaccines, 2014. **2**(2): p. 39-55.
127. Wang, L., L. Zhu, and H. Zhu, *Efficacy of varicella (VZV) vaccination: an update for the clinician.* Ther Adv Vaccines, 2016. **4**(1-2): p. 20-31.

128. Schmidt, S.A.J., et al., *Prevaccination epidemiology of herpes zoster in Denmark: Quantification of occurrence and risk factors.* Vaccine, 2017.
129. Gonzalez-Motos, V., et al., *Varicella zoster virus glycoprotein C increases chemokine-mediated leukocyte migration.* 2017. **13**(5): p. e1006346.
130. Li, S., et al., *Metabolic Phenotypes of Response to Vaccination in Humans.* Cell, 2017. **169**(5): p. 862-877.e17.
131. Cohen, J.I., *Epstein-barr virus vaccines.* Clin Transl Immunology, 2015. **4**(1): p. e32.
132. McPherson, M.C., H.H. Cheng, and M.E. Delany, *Marek's disease herpesvirus vaccines integrate into chicken host chromosomes yet lack a virus-host phenotype associated with oncogenic transformation.* Vaccine, 2016. **34**(46): p. 5554-5561.
133. Zhang, Y., et al., *Recombinant Gallid herpesvirus 2 with interrupted meq genes confers safe and efficacious protection against virulent field strains.* Vaccine, 2017. **35**(36): p. 4695-4701.
134. Rispens, B.H., et al., *Control of Marek's disease in the Netherlands. II. Field trials on vaccination with an avirulent strain (CVI 988) of Marek's disease virus.* Avian Dis, 1972. **16**(1): p. 126-38.
135. Davison, F. and V. Nair, *Use of Marek's disease vaccines: could they be driving the virus to increasing virulence?* Expert Rev Vaccines, 2005. **4**(1): p. 77-88.
136. Cohen, J.I., et al., *The need and challenges for development of an Epstein-Barr virus vaccine.* Vaccine, 2013. **31 Suppl 2**: p. B194-6.
137. Epstein, M.A., et al., *Protection of cottontop tamarins against Epstein-Barr virus-induced malignant lymphoma by a prototype subunit vaccine.* Nature, 1985. **318**(6043): p. 287-9.
138. Morgan, A.J., et al., *Recombinant vaccinia virus expressing Epstein-Barr virus glycoprotein gp340 protects cottontop tamarins against EB virus-induced malignant lymphomas.* J Med Virol, 1988. **25**(2): p. 189-95.
139. Emini, E.A., et al., *Vero cell-expressed Epstein-Barr virus (EBV) gp350/220 protects marmosets from EBV challenge.* J Med Virol, 1989. **27**(2): p. 120-3.
140. Sashihara, J., et al., *Soluble rhesus lymphocryptovirus gp350 protects against infection and reduces viral loads in animals that become infected with virus after challenge.* PLoS Pathog, 2011. **7**(10): p. e1002308.
141. Shumilov, A., et al., *Epstein-Barr virus particles induce centrosome amplification and chromosomal instability.* Nat Commun, 2017. **8**: p. 14257.
142. Allday, M.J., Q. Bazot, and R.E. White, *The EBNA3 Family: Two Oncoproteins and a Tumour Suppressor that Are Central to the Biology of EBV in B Cells.* Curr Top Microbiol Immunol, 2015. **391**: p. 61-117.
143. Hoffman, G.J., S.G. Lazarowitz, and S.D. Hayward, *Monoclonal antibody against a 250,000-dalton glycoprotein of Epstein-Barr virus identifies a membrane antigen and a neutralizing antigen.* Proc Natl Acad Sci U S A, 1980. **77**(5): p. 2979-83.
144. Calarota, S.A., et al., *Detection of Epstein-Barr virus-specific memory CD4+ T cells using a peptide-based cultured enzyme-linked immunospot assay.* Immunology, 2013. **139**(4): p. 533-44.
145. Gurer, C., et al., *Targeting the nuclear antigen 1 of Epstein-Barr virus to the human endocytic receptor DEC-205 stimulates protective T-cell responses.* Blood, 2008. **112**(4): p. 1231-9.
146. Yu, X., et al., *Antigen-armed antibodies targeting B lymphoma cells effectively activate antigen-specific CD4+ T cells.* Blood, 2015. **125**(10): p. 1601-10.
147. Omiya, R., et al., *Inhibition of EBV-induced lymphoproliferation by CD4(+) T cells specific for an MHC class II promiscuous epitope.* J Immunol, 2002. **169**(4): p. 2172-9.
148. Nikiforow, S., et al., *Cytolytic CD4(+)-T-cell clones reactive to EBNA1 inhibit Epstein-Barr virus-induced B-cell proliferation.* J Virol, 2003. **77**(22): p. 12088-104.

149. Heller, K.N., C. Gurer, and C. Munz, *Virus-specific CD4+ T cells: ready for direct attack.* J Exp Med, 2006. **203**(4): p. 805-8.
150. Rubio, V., et al., *Ex vivo identification, isolation and analysis of tumor-cytolytic T cells.* Nat Med, 2003. **9**(11): p. 1377-82.
151. Grossman, W.J., et al., *Differential expression of granzymes A and B in human cytotoxic lymphocyte subsets and T regulatory cells.* Blood, 2004. **104**(9): p. 2840-8.
152. Neri, S., et al., *Calcein-acetyoxymethyl cytotoxicity assay: standardization of a method allowing additional analyses on recovered effector cells and supernatants.* Clin Diagn Lab Immunol, 2001. **8**(6): p. 1131-5.
153. Tsai, M.H., et al., *The biological properties of different Epstein-Barr virus strains explain their association with various types of cancers.* Oncotarget, 2017. **8**(6): p. 10238-10254.
154. Walsh, N.C., et al., *Humanized Mouse Models of Clinical Disease.* Annu Rev Pathol, 2017. **12**: p. 187-215.
155. Strowig, T., et al., *Priming of protective T cell responses against virus-induced tumors in mice with human immune system components.* J Exp Med, 2009. **206**(6): p. 1423-34.
156. Hutt-Fletcher, L.M., *Epstein-Barr virus replicating in epithelial cells.* Proc Natl Acad Sci U S A, 2014. **111**(46): p. 16242-3.
157. Goldberg, A.L., *Functions of the proteasome: from protein degradation and immune surveillance to cancer therapy.* Biochem Soc Trans, 2007. **35**(Pt 1): p. 12-7.
158. Cirac, A., et al., *Epstein-Barr virus strain heterogeneity impairs human T-cell immunity.* 2018.
159. Gottschalk, S. and C.M. Rooney, *Adoptive T-Cell Immunotherapy.* Curr Top Microbiol Immunol, 2015. **391**: p. 427-54.
160. Merlo, A., et al., *Immunotherapy for EBV-associated malignancies.* Int J Hematol, 2011. **93**(3): p. 281-293.
161. Munz, C., et al., *Human CD4(+) T lymphocytes consistently respond to the latent Epstein-Barr virus nuclear antigen EBNA1.* J Exp Med, 2000. **191**(10): p. 1649-60.
162. Bickham, K., et al., *EBNA1-specific CD4+ T cells in healthy carriers of Epstein-Barr virus are primarily Th1 in function.* J Clin Invest, 2001. **107**(1): p. 121-30.
163. Price, A.M. and M.A. Luftig, *Dynamic Epstein-Barr virus gene expression on the path to B-cell transformation.* Adv Virus Res, 2014. **88**: p. 279-313.
164. Elliott, S.L., et al., *Phase I trial of a CD8+ T-cell peptide epitope-based vaccine for infectious mononucleosis.* J Virol, 2008. **82**(3): p. 1448-57.
165. Rees, L., et al., *A phase I trial of epstein-barr virus gp350 vaccine for children with chronic kidney disease awaiting transplantation.* Transplantation, 2009. **88**(8): p. 1025-9.
166. Moutschen, M., et al., *Phase I/II studies to evaluate safety and immunogenicity of a recombinant gp350 Epstein-Barr virus vaccine in healthy adults.* Vaccine, 2007. **25**(24): p. 4697-705.
167. Gu, S.Y., et al., *First EBV vaccine trial in humans using recombinant vaccinia virus expressing the major membrane antigen.* Dev Biol Stand, 1995. **84**: p. 171-7.
168. Hutt-Fletcher, L.M., *Epstein-Barr virus entry.* J Virol, 2007. **81**(15): p. 7825-32.
169. Thorley-Lawson, D.A. and C.A. Poodry, *Identification and isolation of the main component (gp350-gp220) of Epstein-Barr virus responsible for generating neutralizing antibodies in vivo.* J Virol, 1982. **43**(2): p. 730-6.
170. Kanekiyo, M., et al., *Rational Design of an Epstein-Barr Virus Vaccine Targeting the Receptor-Binding Site.* Cell, 2015. **162**(5): p. 1090-100.

171. Ogembo, J.G., et al., *A chimeric EBV gp350/220-based VLP replicates the virion B-cell attachment mechanism and elicits long-lasting neutralizing antibodies in mice.* J Transl Med, 2015. **13**: p. 50.
172. Bachmann, M.F. and R.M. Zinkernagel, *Neutralizing antiviral B cell responses.* Annu Rev Immunol, 1997. **15**: p. 235-70.
173. Lopez-Sagaseta, J., et al., *Self-assembling protein nanoparticles in the design of vaccines.* Comput Struct Biotechnol J, 2016. **14**: p. 58-68.
174. Zhao, Q., et al., *Virus-like particle-based human vaccines: quality assessment based on structural and functional properties.* Trends Biotechnol, 2013. **31**(11): p. 654-63.
175. Liu, Z., et al., *Patterns of inter-individual variability in the antibody repertoire targeting proteins across the Epstein-Barr virus proteome.* J Infect Dis, 2018.
176. Hewetson, J.F., et al., *Neutralizing antibodies to Epstein-Barr virus in healthy populations and patients with infectious mononucleosis.* J Infect Dis, 1973. **128**(3): p. 283-9.
177. Miller, G., J.C. Niederman, and D.A. Stitt, *Infectious mononucleosis: appearance of neutralizing antibody to Epstein-Barr virus measured by inhibition of formation of lymphoblastoid cell lines.* J Infect Dis, 1972. **125**(4): p. 403-6.
178. Thorley-Lawson, D.A. and A. Gross, *Persistence of the Epstein-Barr virus and the origins of associated lymphomas.* N Engl J Med, 2004. **350**(13): p. 1328-37.
179. Arvin, A.M., et al., *Memory cytotoxic T cell responses to viral tegument and regulatory proteins encoded by open reading frames 4, 10, 29, and 62 of varicella-zoster virus.* Viral Immunol, 2002. **15**(3): p. 507-16.
180. Diaz, P.S., et al., *T lymphocyte cytotoxicity with natural varicella-zoster virus infection and after immunization with live attenuated varicella vaccine.* J Immunol, 1989. **142**(2): p. 636-41.
181. Sharp, M., et al., *Kinetics and viral protein specificity of the cytotoxic T lymphocyte response in healthy adults immunized with live attenuated varicella vaccine.* J Infect Dis, 1992. **165**(5): p. 852-8.
182. Weinberg, A. and M.J. Levin, *VZV T cell-mediated immunity.* Curr Top Microbiol Immunol, 2010. **342**: p. 341-57.
183. Lucchesi, W., et al., *Differential gene regulation by Epstein-Barr virus type 1 and type 2 EBNA2.* J Virol, 2008. **82**(15): p. 7456-66.
184. Feederle, R., et al., *Epstein-Barr Virus: From the Detection of Sequence Polymorphisms to the Recognition of Viral Types.* Curr Top Microbiol Immunol, 2015. **390**(Pt 1): p. 119-48.
185. Moosmann, A., et al., *Effective and long-term control of EBV PTLD after transfer of peptide-selected T cells.* Blood, 2010. **115**(14): p. 2960-70.
186. Bollard, C.M., et al., *Sustained complete responses in patients with lymphoma receiving autologous cytotoxic T lymphocytes targeting Epstein-Barr virus latent membrane proteins.* J Clin Oncol, 2014. **32**(8): p. 798-808.
187. Icheva, V., et al., *Adoptive transfer of epstein-barr virus (EBV) nuclear antigen 1-specific t cells as treatment for EBV reactivation and lymphoproliferative disorders after allogeneic stem-cell transplantation.* J Clin Oncol, 2013. **31**(1): p. 39-48.
188. Long, H.M., et al., *Cytotoxic CD4+ T cell responses to EBV contrast with CD8 responses in breadth of lytic cycle antigen choice and in lytic cycle recognition.* J Immunol, 2011. **187**(1): p. 92-101.
189. Durfee, T., et al., *The complete genome sequence of Escherichia coli DH10B: insights into the biology of a laboratory workhorse.* J Bacteriol, 2008. **190**(7): p. 2597-606.
190. Warming, S., et al., *Simple and highly efficient BAC recombineering using galK selection.* Nucleic Acids Res, 2005. **33**(4): p. e36.

191. Graham, F.L., et al., *Characteristics of a human cell line transformed by DNA from human adenovirus type 5.* J Gen Virol, 1977. **36**(1): p. 59-74.
192. Pulvertaft, J.V., *CYTOLOGY OF BURKITT'S TUMOUR (AFRICAN LYMPHOMA).* Lancet, 1964. **1**(7327): p. 238-40.
193. Neuhierl, B., et al., *Glycoprotein gp110 of Epstein-Barr virus determines viral tropism and efficiency of infection.* Proc Natl Acad Sci U S A, 2002. **99**(23): p. 15036-41.
194. Lin, X., et al., *The Epstein-Barr Virus BART miRNA Cluster of the M81 Strain Modulates Multiple Functions in Primary B Cells.* PLoS Pathog, 2015. **11**(12): p. e1005344.

7. List of Figures